Iron loading in rice endosperm controlled by cell-type specific over-expression of *OsNAS*

Bianca Anastasia Kyriacou

Flinders University of South Australia

Table of Contents

Abstract

Over 50 years after the attempt to combat worldwide famine with the Green Revolution and the expansion of agricultural practices, we face new and equally challenging battles of combating human micronutrient malnutrition. The prevalence of iron (Fe) deficiency anaemia is tightly associated with the proportion of people reliant on cheap nutrient poor rice diets, particularly women and children in Asia and Africa (Kraemer and Zimmermann, 2007). There is an amazing depth of knowledge available that demonstrates the uptake and transport of Fe in rice plants but little research has successfully resulted in biologically significant Fe enriched rice. This thesis attempts to address this problem with the development and investigation of cell type specific over expression of *OsNAS* genes in rice. The ultimate aim is to develop rice with enriched Fe in the endosperm - the most commonly consumed portion of the grain.

Iron uptake and translocation play a crucial role in the biochemistry of cell development in both animals and plants and as such, Fe must be tightly regulated. Plants acquire Fe via root transport of ferrous (Fe^{2+}) and ferric (Fe^{3+}) ions via transport mechanisms known as Strategy I (in dicots) and Strategy II (in monocots). An important factor in Fe accumulation in both dicots and monocots is the synthesis of nicotianamine (NA) molecules upon the activity of NA synthases. In Strategy I plants, NA is a well characterised Fe chelator, acting as a vehicle for Fe long distance transport. Strategy II plants, like rice, catalyse NA in the production of phytosiderophores, Fe^{3+} chelating molecules used to draw Fe in from the rhizosphere. There exist three NA synthase genes in rice; *OsNAS1*, *OsNAS2* and

OsNAS3. It is known that each gene is spatially controlled across the plant at differing periods of Fe homeostasis (Cheng et al., 2007, Inoue et al., 2003). What is not known is why this happens and whether these genes present any redundancy value or if they have highly specified roles in Fe acquisition in rice. Chapter Two of this thesis investigates the effect of Fe accumulation in rice (*Oryza sativa ssp. Japonica cv* Nipponbare) endosperm when manipulated using transgenic lines over-expressing the three rice NAS genes *OsNAS1*, *OsNAS2* and *OsNAS3*. The hypothesis states that a single *OsNAS* gene may lead to a more efficient Fe accumulator in the grain and that the cell type specific expression of this gene may influence this effect. In order to achieve cell type specific expression of these genes, GAL4 was used to control the enhancer trap system in root stele, root cortex and lodicules of developing grain, along with ovary of developing grain and leaf shoot tissues. Subsequent ICP-OES analysis of T1 grains indicated that Fe was enhanced up to two-fold in brown rice of root cortex-specific *OsNAS2* over-expression and developing grain lodicules-specific *OsNAS3* over-expression lines compared to the corresponding wild type. Furthermore, polished grains from transgenic plants retained up to 30% more Fe in the endosperm post-milling. In some cases 2-3 times more Fe was found in the grain of the transgenic than wildtype. We subsequently suggest there is not a redundancy between the three *OsNAS* genes, but that over-expression of *OsNAS2* may in fact trigger endogenous expression of *OsNAS1* and *OsNAS3*. This refers to the 'heterocot' nature of rice, where both strategies of Fe uptake (strategy I of dicots and strategy II of monocots) are utilised, enabling the NA to be produced for PS sequestration, Fe influx and Fe chelation and transport.

The exciting results from Chapter Two were further investigated in Chapter Three with the use of synchrotron radiation to visualise this increase in Fe accumulation in the grain. Traditionally, relatively little Fe is present in the endosperm, a fact worsened by the loss of 75-80% of Fe with the removal of the Fe rich bran and maternal tissue during milling (Briat et al., 1995). Levels of 14 μg g^{-1} Fe in the rice endosperm have been reported as the 'goal' for biofortified rice- over three times the typical concentration in consumed rice around the world. Grain developed in Chapter Two resulted in Fe concentrations of over 13 μg g^{-1} in the endosperm. It was therefore imperative to visualise the Fe distribution across the whole transgenic grain to ensure we had developed Fe enhanced rice that would provide increased nutritional benefit once milled. Interestingly, SXRF maps showed Fe was not limited to the aleurone and embryo but instead extended further into the sub aleurone and endosperm. Furthermore this increase in Fe was not co localised with P, a key indicator of the anti-nutrient phytate. This was further established with SXANES and nano-SIMS technology, highlighting the utility of multi-spectroscopic analysis of micronutrients in grain as well as suggesting a more bioavailable Fe enhanced rice grain.

Research into biofortified foods designed to combat human micronutrient deficiencies would be unrealistic if geographic considerations of rice production were ignored. Over 50% of the world's population consume rice, and the majority of this is grown in Asia. Due to anthropogenic contamination of crop soils with heavy metals such as cadmium (Cd), it is of no surprise that the greatest vehicle for Cd consumption and toxicity in humans is in fact rice. Chapter Four explores the potential for heavy metal accumulation in the transgenic grain, as NA is known to

bind several metals such as Zn, Mn and Ni. It was hypothesised that the root specific over-expression of *OsNAS2* would maintain enhanced levels of Fe in the grain when grown in Cd contaminated soils without increased the grain Cd concentrations. Interestingly, the converse of this was recorded, with Cd levels exceeding those allowed for human consumption in Australia and parts of Asia (Arao and Ae, 2003, Hseu et al., 2010) and Fe concentrations decreased from those found in previous generations. This demonstrates a relationship between NA and Cd - a relationship that has otherwise not been described in literature.

As we have shown in this thesis and other publications (Johnson et al., 2011), there is an increase in endosperm Fe in transgenic rice over expressing *OsNAS2*. The final chapter of this thesis challenges the source-sink relationship of Fe accumulation and loading in the grain. We ask whether an endosperm specific promoter controlling the over-expression of a vacuolar iron transporter (*OsVIT1*) in the background of the *OsNAS2* lines would result in further enhanced Fe loading than previously seen in the single transformant 35S *OsNAS2* lines (Johnson et al., 2011). It is expected that as there is already in increase Fe accumulation in *OsNAS2* grain, endosperm specific *OsVIT1* will further drive Fe into the grain, beyond the aleurone and into the centre of the endosperm. Preliminary results suggest we were able to produce a rice line with relatively higher grain Fe concentrations and this gives rise to a multitude of future research possibilities in the future.

Appendix One of this thesis contains the full manuscript of Johnson et al. (2011) as work from this thesis contributed to second authorship. The 35S *OsNAS* lines referred to in this thesis are further investigated in the manuscript of Appendix One. This work was published in PlosONE.

Declaration of Authenticity

I, Bianca Kyriacou, certify that this thesis does not incorporate without acknowledgment any material previously submitted for a degree or diploma in any university; and that to the best of my knowledge and belief it does not contain any material previously published or written by another person except where due reference is made in the text.

Bianca Kyriacou

Acknowledgements

There is always concern that presenting one's gratitude to a number of people will leave some with a feeling of contrite or un-heartfelt emotion. It is with great sincerity that I say this is not my intention.

Often as students we were told to enjoy the PhD journey and reflect on its ups and downs- 'they bring out the best in you as a scientist'. To be honest I feel the past few years have been too blurred and rushed. As I looked out from inside the cyclone, I wanted to click my heels three times and wake up from this thrilling and frightening dream. Now that I am awake and reviewing with the eyes of hind sight, I can confidently say I loved the whole rainbow this PhD presented me with.

The time spent during this PhD gathering data and performing the lab experiments were the best scientific years of my fledgling career. The environment in which I felt so comfortable allowed me develop my new skills, both lab and teaching related and this is due to great network of friends and colleagues. I have tremendous gratitude for my three supervisors, Scarecrow, Lion and Tin Man for helping develop my skills- and in no particular order or favour! (The three of you can decide which character you are!)

To James Stangoulis, for reading and ignoring half of my emails, believe it or not, I say thank you. Thank you for not disregarding the ultimate message, which was that I really wanted to finish this thesis. You knew what I was really trying to say amongst the virtual tear stained and frantic emails, ignored the rubbish and helped me calm down, and for that I'm grateful. I always enjoyed discussing my work with you. Even though you wandered off onto new tangents, diverted every conversation and most of the time we discussed the nuances of French cheese! You were always excited by blue sky thinking and I have learned how important this is in any scientific project development. Everything has a bigger picture.

To Alex Johnson who motivated me by ensuring I had the confidence to do what was necessary and to enjoy the science as it happened. Each time I presented data, you had an uncanny way of seeing the positive in each result and your enthusiasm helped me get through several 24 hour straight synchrotron sittings! You were always encouraging and engaging and this has shaped the way I travelled through my PhD journey greatly. I am grateful that you also presented yourself as a friend, an important gesture to a student from their supervisor.

Perhaps a total of 4,445,399 emails were sent to Mark Tester with an even mix of jubilation of having finished my first major presentation, excitement when my transformations worked and fear when my crops were crippled and destroyed. This resulted in 4,445,789 emails returned with words of wisdom, congratulations or comfort from a fantastic mentor, to whom I still send emails to just because the responses are hilarious enough to pull me out of a funk. I am grateful for the faith you had in me and my work and for inviting me to be a part of the Salt Group.

To all the Winkies (members of ACPFG) who helped me perform some of my most important experiments, Alison Hay, Margie Pallotta, Natasha Bazanova and Jan Nield. Your help and encouragement was very important in my success throughout this project. To Lorraine Carruthers for hilarious Lewis Carroll-esque emails, a pat on the back when I needed a hand up and for all the help in the glasshouse, with quarantine, in the lab and at every morning tea for three years! Your help shouldn't go unnoticed, and it never did with me.

To Boq (Enzo Lombi) who's wealth of knowledge, endless support, words of encouragement and determination got me through 48 hour straight synchrotron beam times – thank you so much. Your help was instrumental to the success of my PhD. I really appreciated all you did to get me there, even if you would take the occasional avuncular jibe at my music tastes! Your skills are extraordinary and your passion for science is incredible. I wouldn't have an entire chapter in this thesis if it weren't for your help.

My husband needs a 'man-of-the-past-five-years' award for all the support and encouragement he's given me. He really was the Great Wizard. He'd know when to leave me alone to sook or cry or throw my lab books around the study. He was still there for me when I would eventually walk out of the study a few hours later smiling and feeling happy again. When Foreigner wailed that they wanted to know what love is- they hadn't met Nick Warnock. Support, love, laughter, and a dry t-shirt ready to let me cry on. What more can I say other than I love you more than apples.

Of course I hate to say it but I'm glad my bubble-bound-Glinda-Mum screwed up her face when I said 'Ma I'm gonna be a star- I'm going to the Broad-way!" Her simple reply in that ever-so-blunt Bugeja family way of "You can't sing or dance, haven't you noticed you're good at science?" helped me more than it might sound! She let me explain the intricate details of modern biotechnology over dinner and would then sit with me during every episode of Darling Buds of May when I couldn't bear to do science for another second. My

sister Ozma Michaela gave me a realistic ear, telling me to stop fretting, suck it up and keep going. Holding hands as children, she never let her grip weaken then nor now and it helped me all this time. I have immense gratitude for my Dad, King Rinkitink, who has now read and proof read every single assignment I have ever had to submit during my primary, secondary, tertiary, higher degree and post graduate education. Most of the time these experiences ended in tears but I needed your help and I love that you offered it unconditionally. Λυπάμαι που ποτέ δεν έμαθα τη γλώσσα σου. Σου ευχαριστω που έμαθες τη γλώσσα μου.

My Munchikins Simona Carbone, Maxine Delangas, Mahima Krishnan, Jingwen Tiong, Emma deCourcy Ireland, Melissa Gregory, Patrick Laffy, Georgia Guild, UB, Yann Tiersen, The Plant Cell Wallies, Walt Disney, Aretha Franklin for putting on a show in New York just for me and not dying before I submit, The United Realm of Warnock and all my other Munchikin friends and family who answered emails, rewrote emails (Natalie Kibble!), read drafts, poured me cups of tea, baked me cakes to cheer me up and found me when I was lost on the yellow brick road: T-H-A-N-K Y-O-U! In the same way that thanking everyone personally would take days, I can't thank every person in print. So if you're reading this thesis and come upon these acknowledgements without seeing your name, do the following:

Thank you to (insert name here) for all your love, support, guidance, help and wisdom.

Bianca Kyriacou

Abbreviations List

[x]	Concentration of element
°C	Degrees Celcius
$^{56}Fe^{16}O^{-}$	Radiolabelled iron oxide
AA	Ascorbic acid
AAS	Atomic absorption spectroscopy
AQC	6-aminoquinolyl-n-hydroxysuccinimidyl carbamate
ACPFG	Australian centre for plant functional genomics
AQIS	Australian quarantine inspection services
At	*Arabidopsis thaliana*
B	Boron
BO_3	Borate
Ca	Calcium
Caco-2	Immortalised human colonic epithelial cells
CCC1	Cation ca^{2+}-sensitive cross-complementer
Cd	Cadmium
CdCS	Cadmium contaminated soils
cDNA	Complementary deoxyribonucleic acid
CER	Controlled environment growth rooms
CGIAR	Consultative group on international agricultural research
Cs	Caesium
Cu	Copper
DAB	Diaminobenzidine
DF	Developing flower
DF:L	Lodicules of developing flowers
DF:O ; LC	Ovary of developing flower; and leaf collar
DF:VB ; LC	Vascular bundle of developing flower; and leaf collar
DMA	Deoxymugenic acid/s
DNA	Deoxyribonucleic acid
EDTA	Ethylenediaminetetraacetic acid
EDX	Energy dispersive x-ray microanalysis
eV	Electron volts
FAO	Food and agriculture organisation of the United Nations
FDRL	Ferric reductase defective-like
Fe	Iron
Fe^{2+}	Ferrous ions
Fe^{3+}	Ferric ions
$FeCl_2$	Ferrous chloride
$FeNO_3$	Ferric nitrate

FRO	Ferric reductases/oxidases
gDNA	Genomic DNA
Ge	Germanium
GFP	Green fluorescent protein
HCl	Hydrochloric acid
ICP-OES	Inductively coupled plasma optical emission spectroscopy
IRRI	International rice research institute
IRT	Iron-regulated transporters
K	Potassium
keV	Kilo electron volts
KOH	Potassium hydroxide
L, ml	Litre, millilitre
LC	Liquid chromatography
µ	Micro
M, mM	Molar, millimolar
MA	Mugenic acid/s
µg g^{-1}	Micrograms per gram
Mn	Manganese
MS	Mass spectroscopy
NA	Nicotianamine
Na	Sodium dodecyl sulfate
NAAT	Nicotianamine aminotransferase
NAS	Nicotianamine synthase
NCdS	Non-(cadmium) contaminated soils
Ni	Nickel
nmol	Nanomole/s
NPTII	Neomycin phosphotransferase selective marker
NRAMP	Natural resistance associated macrophage protein/s
Os	*Oryza sativa L.*
OsIRO2	*Oryza sativa iron regulated transporter 2*
OsNAS	*Oryza sativa* nicotianamine synthase gene
OsNAS	*Oryza sativa* nicotianamine synthase protein
OsNAS1	*Oryza sativa* nicotianamine synthase gene 1
OsNAS2	*Oryza sativa* nicotianamine synthase gene 2
OsNAS3	*Oryza sativa* nicotianamine synthase gene 3
P	Phosphorous
pA	Pico Amperes (pico Amps)
PCR	Polymerase chain reaction
pmol	Picomole/s
PPB	Perl's Prussian blue stain
PS	Phytosiderophore/s

PSV	Protein storage vacuole
qPCR	Real time PCR
R:C	Root cortex
R:S	Root stele
RO	reverse osmosis
RNA	Ribonucleic acid
RNAi	Interference ribonucleic acid
S	Sulfur
SAM	S-adenosylmethionine
SARDI	South australian research and development institute
Sc	*Saccharomyces cerevisiae*
SDS	Sodium dodecyl sulfate
SE	Secondary electron
SEM	Scanning electron microscopy
SR	Synchrotron radiation
SXANES	Synchrotron radiation x-ray absorption near edge spectroscopy
SXRF	Synchrotron radiation x-ray fluorescence microscopy
T0, T1, T2	Transgenic material from original transformation, T1 is progeny of T0…
TAE	Tris-acetate EDTA
TEM	Transmission electron microscopy
UAS	Upstream activation sequence
UC Davis	University of California, Davis campus
UK	United Kingdom
UNICEF	United Nations children's fund
US	United States of America
USDA	United States department of agriculture
v/v	Volume per volume
VIT1	Vacuolar iron transporter 1
w/v	Weight per volume
w/w	Weight per weight
WAS	Waite analytical service
XFM	X-ray fluorescence microprobe
YS1	Yellow stripe 1
YSL	Yellow stripe-like
Zn	Zinc

Chapter One: Introduction

1.1 Human malnutrition

In many developing countries, the 'Green Revolution' of the 1960s led to the dedication of agricultural farming land to an increased production of high yielding, semi-dwarf cereal crops such as rice (Conway, 1997). This was undertaken in an effort to increase food production and while less expensive and calorie-rich, the reliance on rice has decreased dietary diversity and resulted in a reduced intake of essential micronutrients and vitamins, thereby leading to an increased incidence of micronutrient malnutrition in many under-developed nations (Welch and Graham, 2000).

Approximately 30% of the world's population suffer from iron (Fe) deficiency, with women and children over-represented in this group (Kraemer and Zimmermann, 2007). Extreme lack of micronutrients such as Fe and zinc (Zn) causes health disorders including stunted growth, poor cognitive function, and increased susceptibility to diseases including malaria (Dallman, 1986, Asobayire et al., 2001). Often, these disorders are not attributed to the causative lack of essential micronutrients and are referred to as 'hidden hunger', resulting in severely deleterious effects for both the individual and society on the whole.

Studies conducted in several Asian countries by UNICEF and the Asian Development Bank have shown that Fe deficiency anaemia contributed to productivity losses of up to 5% (Hunt, 2002). The need to combat micronutrient deficiencies has never been more urgent.

1.2 Non-biological approaches to combat 'Hidden Hunger'

1.2.1 Community education

Education is vital for the prevention of micronutrient deficiencies as nutrition education programmes convey the importance of including more nutrient-rich food varieties in diets. Such programmes promote simple strategies to encourage communities to increase food diversification to enhance nutrient intake. Research carried out in the Philippines shows that diets incorporating brown rice together with meats and leafy greens increase Fe absorption when compared with diets of brown rice alone (Juliano, 2000, Welch and Graham, 2004). However, obvious impediments to the adoption of this strategy include the expense related to diversified diets as well as availability of and access to a variety of food types.

The education and provision of information to communities requires significant funding from governments and aid organisations. Such external costs are often out-weighed by the internal costs of acquiring the tools necessary to apply this new-found knowledge, such as obtaining seeds and animals to maintain small farms, as such education alone is not a practical means to reduce human nutrient deficiencies.

1.2.2 Supplements

Supplements such as Fe or Zn capsules offer communities a small, convenient means of delivering nutrients otherwise lacking in a typical diet. National immunisation days are common in several African and sub-Saharan communities and could potentially enable widespread distribution of vaccines and dietary supplements (Campos-Bowers and Wittenmyer, 2007). However, a lack of participation in these

programmes is a key obstacle and limits the extent to which such treatment can be provided (Smith, 2000).

Community support is imperative for the success of supplementation programmes. One such example is the successful reduction of Vitamin A deficiencies (xeropthalmia) in Indonesia (Campos-Bowers and Wittenmyer, 2007, Sherwin et al., 2012), where positive public responses to treatment were attributed to community and government-driven efforts to support the programmes. However, it has been noted that any changes in social or political climate are likely to decrease the distribution and use of supplements. This suggests that supplementation is unlikely to be a sustainable long-term approach to combating micronutrient malnutrition, particularly in those countries where political and civil unrest are common (Campos-Bowers and Wittenmyer, 2007).

1.2.3 Food fortification

The fortification of foodstuffs with nutrients and essential vitamins has proved to be successful in lowering the incidence of micronutrient malnutrition in many Chinese communities. Nutrient enrichment of foods can be achieved in a number of ways, including soaking wheat or rice grains in nutrient-rich solutions, adding vitamins to sugar, or iodine to salt. These methods enable vast quantities of fortified foods to be prepared and distributed. Despite the relative simplicity of this procedure, it is not viable in communities without access to established commercial food industries. Consequently, the distribution of enriched foods on a mass scale is not feasible in the areas most in need (Campos-Bowers and Wittenmyer, 2007).

Gaining access to education, supplements and fortification tools is often difficult due to the challenges of location or cost. These difficulties have directed attention towards biotechnology and the potential of cereal crop biofortification as a long-term solution to the problem.

1.3 Cereal biofortification

Biofortification is an alternative tool to increase the micronutrient density in the edible part of crop plants. This is a self-sustaining system which does not usually involve mechanical processes or human participation. Biofortification can be achieved through plant breeding or genetic modification to generate micronutrient fortified or enhanced cereals such as rice. Cereals that are inexpensive, relatively easy to maintain and nutrient-enriched will provide communities en masse with increased nutrients at an ongoing cost which is less than that of supplements or traditional fortification (Bouis et al., 2003). This is particularly important in relation to rice, which is a major food staple around the world.

1.3.1 Costs and benefits

Nutrient supplement and fortification programmes rely heavily on constant funding for stability and success and the finance required to sustain community health is simply not attainable by those countries which are most in need (as discussed in sections 1.2.2 and 1.2.3 above). According to the Food and Agriculture Organisation of the United Nations (FAO), Fe-fortified foodstuffs (such as flour) in India costs the country US$40 million per year (Chhuneja et al., 2006). It has been suggested that investment in plant breeding research would cost far less. In fact, according to the

Consultative Group on International Agricultural Research (CGIAR), the investment of US$2 million in a five year development plan could be effective in facilitating the research and distribution of Fe-enriched rice crops (Bouis et al., 2000). Communities would then have access to those crops already common in their diet but now nutritionally-enhanced, ultimately increasing the micronutrient intake and reducing the incidence of nutrient malnutrition.

1.3.2 Plant mechanism studies

As well as improving human health, biotechnological research can also improve our knowledge of mechanisms associated with nutrient uptake and translocation in plants. This leads to improved understanding of metal ion hyper-accumulation, including limitations of metal uptake and ion toxicity. Additionally, genetic manipulation allows direct genetic changes to the plant providing better investigation of gene pathways. Elucidation of these pathways will have application not only to human nutrition and agricultural development, but also to the study of phytoremediation (Callahan et al., 2007, Clemens et al., 2002). For example, hyper-accumulation of heavy metals by plants may contribute to the amelioration of soil toxicity (Arao and Ae, 2003, Li et al., 2008). This is discussed in greater detail in Chapter Four of this thesis.

1.3.3 Past, present and future

Recently, there have been many positive outcomes from worldwide collaborations in the effort to develop biofortified crops for nutritional benefit following recent advances in human nutrition studies. These efforts are further strengthened by the

inception of agricultural development foundations and research centres. For example, CGIAR supports many multidisciplinary institutions including the International Rice Research Institute (IRRI) and HarvestPlus. Currently, IRRI is supporting cultivation of rice enhanced with provitamin A (Golden Rice) in field trials in Asia; and HarvestPlus is supporting the development of iron-enriched varieties of rice and wheat. Such collaborations have facilitated the development of rice, maize and wheat crops fortified with micronutrients such as vitamin A, Fe and Zn. The testing of many of these cereal crops worldwide for nutrient benefits has yielded positive results (Haas 2005, Tang 2009). For example, IRRI has reported that *'iron from high-iron rice lines is absorbed by iron-deficient women'* (Chhuneja et al., 2006, Normile, 2008). This indicates that such an approach could represent a successful treatment for Fe deficiency.

At present, a lot of research is being carried out for the biofortification of various cereal crops with a number of different essential metal ions such as Fe and Zn. The focus of this literature review will be on the application of biotechnology and biofortification of rice with Fe.

1.4 Iron

1.4.1 Biological importance

Iron is the fourth most abundant element on earth, representing 5% of the composition of soil. One of the 49 essential nutrients in plant, animal and human life (Guerinot, 2001, Welch and Graham, 2004), Fe is critical for electron transfer during photosynthesis, respiration, nitrogen fixation and DNA synthesis. Therefore, because

Fe uptake and translocation plays a crucial role in the biochemistry of cell development, Fe must be tightly regulated in plants. Iron readily donates and accepts electrons and consequently is predominantly found in complexed ionic ferrous (Fe^{2+}) or ferric (Fe^{3+}) forms within plant. From this point onwards "Fe" will refer to the total ionic iron, ie Fe = $\Sigma(Fe^{2+} + Fe^{3+})$ unless otherwise stated. A substantial decrease in Fe available to a plant will result in reduced chlorophyll content, leading to stunting and chlorosis. Conversely, excessive levels of cellular Fe (e.g. greater than 100 μg g^{-1} in rice plants) can result in the generation of free radicals, resulting in toxicity (Foy et al., 1978). A state of homeostasis is maintained as Fe complexes with cellular organic compounds, reducing the potential for toxicity and increasing the solubility of Fe^{3+} (Brinch-Pedersen et al., 2007, Curie and Briat, 2003, Busch et al., 2008, Curie et al., 2001).

Living organisms require micronutrients to be soluble in order to utilise these essential elements. In soils of neutral pH, Fe exists predominantly as Fe^{3+}, which is insoluble and not readily absorbed by the plant. Before Fe^{3+} can be taken up, the ions must either be reduced to Fe^{2+} or chelated to form a soluble complex (see Chapter Two, section 2.1.1 for more details). After uptake, storage of Fe is vital to prevent formation of free radicals whilst at the same time maintaining sufficient Fe levels essential for processes of cell development. Unlike other cereal crops, such as wheat or barley, the mechanisms of Fe translocation in rice are yet to be fully elucidated.

1.4.2 Iron uptake and transport in rice plants

Plants are sessile and depend on highly evolved systems of nutrient acquisition in order to cope with abiotic environmental stresses. Dicots such as *Arabidopsis*

thaliana use a series of mechanisms referred to as 'Strategy I', which involve the reduction of rhizospheric Fe^{3+} to soluble Fe^{2+}. Iron transporters then mobilise the soluble Fe^{2+} directly from the roots to the shoots. Graminaceous monocots such as rice employ 'Strategy II' mechanisms whereby phytosiderophores (PS) are synthesised under Fe deficient conditions and secreted into the rhizosphere. Here they bind Fe^{3+} and directly transport the chelated ions into the plant through complex-specific transporters. A major component of the Strategy II system is nicotianamine.

1.4.3 Nicotianamine

Nicotianamine (NA) is formed as a condensation product of three S-adenosylmethionine (SAM) molecules, a reaction catalysed by nicotianamine synthase (NAS). NA is ubiquitous in the plant kingdom and a strong metal chelator (Bughio et al., 2002) capable of binding Mn, Zn, Cu, and Fe. Chelation by NA is crucial in maintaining control over Fe homeostasis by optimising the distribution of Fe and preventing Fe toxicity. Nicotianamine also plays an important role in maintaining Fe homeostasis during Fe deficiency in plants that employ the Strategy II mechanism. An increase in NA levels in the plant elevates Fe uptake, which in turn leads to the catalysis of NA to initially produce and subsequently sequester phytosiderophores (PS) such as mugenic acids (MA) and deoxymugenic acids (DMA). Figure 1 illustrates the pathway of NA production in both Strategy I and II plants as well as the reduction of NA in Strategy II plants during Fe homeostasis in plants. Chelation of PS with Fe^{3+} (PS: Fe^{3+}) and subsequent solubilisation allows more Fe to enter the plant via PS: Fe^{3+} specific transporters present on the plasma

membrane of the root (Colangelo and Guerinot, 2004, Curie and Briat, 2003, Curie et al., 2001).

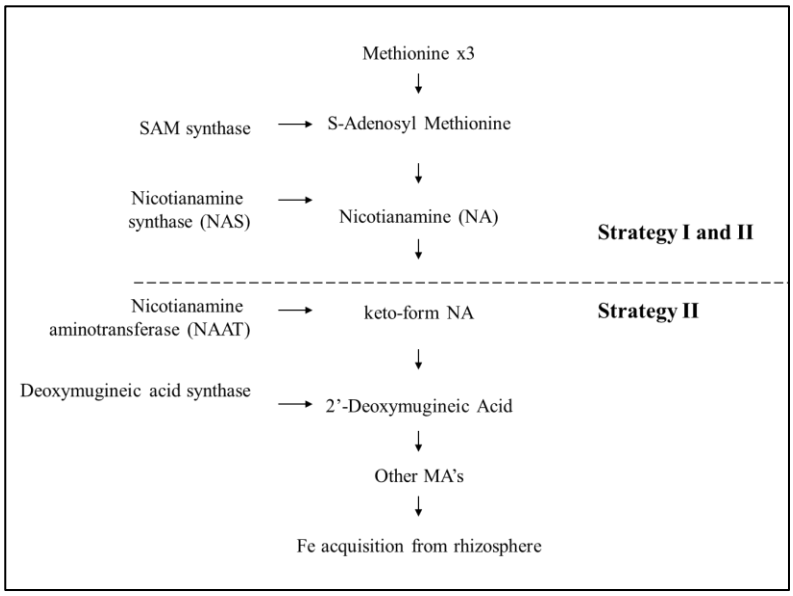

Figure 1: The metabolic pathway of phytosiderophore synthesis

1.4.4 Nicotianamine in long distance transport of iron

The role of NA as a long distance phloem metal transport molecule was first demonstrated in the tomato *chlornova* mutant where a loss of function of the *NAS* gene significantly reduced NA production and led to reduced Fe accumulation in tomatoes (Ling et al., 1999). In tobacco transgenic lines overexpressing nicotianamine aminotransferase (NAAT) (Takahashi et al., 2003), NA concentrations were reduced due to the increased consumption of NA during MA production. Both the *chlornova* mutant and tobacco lines showed significant build-up of Fe in vascular bundles of young tissue, and the plants also displayed chlorotic leaves, stunted growth and sterility, all of which are symptoms of Fe deficiency. This is likely caused by the plants' diminished capability to distribute Fe uniformly *in planta* due

to the lack of NA:Fe complexes through the phloem network. This hypothesis has since been supported by the work of Pich et al. (1997), where NA: Fe complexes have been extracted from stelar vacuolar cells of wild-type tomato roots tips (Liu et al., 1998). Collections of phloem exudate have also been shown to contain NA: Fe^{2+} complexes (von Wiren et al., 1999). The presence of NA: Fe complexes have also been investigated in roots of the metal hyperacummulator *Thlaspi* (Mari et al., 2006).

Recent studies show that NA has a strong affinity for both Fe^{2+} and Fe^{3+} ion complexes. Although most research reports a greater presence in plant tissue of NA: Fe^{2+} (especially in phloem sap), there is evidence of NA binding to Fe^{3+} (von Wiren et al., 1999). In fact, *in vitro* studies show that the affinity of NA for Fe^{3+} is 10^8 times greater than that for Fe^{2+} (von Wiren et al., 1999). This work revealed that whilst the NA: Fe^{2+} interaction has a K value of $10^{12.8}$, the kinetic stability of this chelate in phloem sap is higher than that of NA: Fe^{3+}. Despite the ability of NA to bind both Fe^{3+} and Fe^{2+}, it is not understood why NA is selective in predominantly binding to Fe^{2+} in phloem. An improved appreciation of the function of Fe transport proteins may help decipher the Fe^{2+} specificity of NA.

1.4.5 The molecular basis of iron transport

IRT

The sedentary nature of plants has resulted in the development of intricate long distance transport mechanisms to obtain and distribute macro nutrients and micronutrients such as Fe from roots to shoots and reproductive tissue. Dicots such as *Arabidopsis* use the Strategy I uptake system whereby sequestration of ferric

reductases/oxidases (FRO) from roots increases the concentration of Fe^{2+}. Iron-regulated transporters (IRT1 and IRT2) then transport the rhizospheric Fe^{2+} directly into roots (Eide et al., 1996). Strategy II plants (monocots) generally do not rely on *FRO* and the *IRT* genes. However, rice is unique amongst its monocot relatives in that it is capable of up-regulating expression of *IRT1* during Fe deficiency to allow Fe^{2+} ions to enter the plant (as do Strategy I plants). The cultivation of rice in paddy systems results in acidic conditions in which the concentration of Fe^{2+} ions is greater than in drier soils. Interestingly, rice plants will also up-regulate expression of the Yellow stripe-like (*OsYSL18*) gene to increase transport of rhizospheric Fe^{3+} directly into the plant (Ishimaru et al., 2006), an action of Strategy II plants.

YSL

Yellow stripe 1 (YS1) is a MA: Fe^{3+} transporter identified in maize (Bernards et al., 2002). Yellow stripe-like (*YSL*) homologues have been characterised in *Arabidopsis*, rice and barley (Murata et al., 2006). The function of YSL as a NA: Fe^{2+} transporter involved in long distance transport from root phloem to shoot and grain has been demonstrated in several homologues, with 18 *YSL* homologues identified in rice. Whilst it is known that *OsYSL2* is a NA: Fe^{2+} transporter, *OsYSL18* (Aoyama et al., 2009) and *OsYSL15* (Inoue et al., 2009) are both described as DMA: Fe^{3+}-specific transporters. The expression of *OsYSL15* is up-regulated during Fe deficiency in root epidermis, exodermis and phloem cells, demonstrating its importance in rhizospheric uptake of Fe^{3+} as a homeostasis control. Expression of *OsYSL18* is not up-regulated in roots during Fe deficiency but has been detected at 'basal' levels in shoots and leaf tissue, as well as pollen tubes during reproduction (Aoyama et al., 2009). It has been

reported that DMA also exists in developing and mature rice grains (Takahashi et al., 2006), suggesting that *OsYSL18* could be important as a DMA:Fe^{3+} transporter during grain development, however this has not been officially published (Aoyama et al., 2009).

Specifically expressed in phloem tissue, *OsYSL2* can transport NA: Fe^{2+} and NA: Mn^{2+} but not DMA: Fe^{3+} complexes. Expression of *OsYSL2* is Fe-deficient inducible, particularly in leaf and grain tissue, thus indicating a role in long distance transport (Koike et al., 2004)What was initially considered a redundancy in *OsYSL* expression may, in fact, be an example of a long distance cation transporter family involved in Fe requisition, transport and loading in rice grains (Briat et al., 2007). The *OsYSL* gene family may act as a signalling transport system whereby Fe^{3+} is mobilised from soils through *OsYSL18* transporters at the root, and then translocated into root phloem through *OsYSL2* where a more stable chelation of NA: Fe^{2+} can occur (Aoyama et al., 2009, von Wiren et al., 1999). Expression of *OsYSL2*, *OsYSL15* and *OsYSL18* and *OsFRDL1* exists in shoots and seeds and so it is possible that Fe may move from the phloem to the xylem either as Fe^{2+} through *OsYSL2* (Hell and Stephan, 2003), or as Fe^{3+} through the citrate: Fe^{3+} specific transporter *OsFRDL1* (Yokosho et al., 2009). Remobilisation may occur as *OsYSL18* translocates DMA: Fe^{3+} to shoot and leaf phloem where *OsYSL2* transports NA: Fe^{2+} to the grain, or else *OsYSL15* transports DMA: Fe^{3+} to grain (Aoyama et al., 2009, Curie et al., 2001, Inoue et al., 2009).

1.5 Iron storage in rice seed

Iron is typically found in highest concentrations in the scutellum and aleurone layers of rice grains with very little Fe detected in the endosperm. This preferential allocation of Fe thus results in approximately 75-80% of total Fe loss during the polishing process, which removes the outer bran layers of the rice grain (Briat et al., 1995). Traditionally the grain is polished to remove the oily bran layers that would render the product rancid if not stored correctly. More relevant to the research topic, this preservation technique renders the cereal lower in nutritional value, especially that of Fe, for human consumption.

Present predominantly as Fe^{3+} in the plant, 90% of cellular Fe is stored or compartmentalised in vacuoles, chloroplasts and mitochondria (Clark, 1983, Taiz and Zeiger, 2002). Within grains, the protein storage vacuole (PSV) of the embryo and aleurone is an efficient depository compartment for Fe. The PSV is important for seed germination as it contains the required nutrients and enzymes. Wada and Lott (1997)found that phytate-containing globoids were present in embryo tissue, and Zn complexes were also identified in the scutellum and in the provascular tissues of the rice grain (Yoshida et al., 1999).

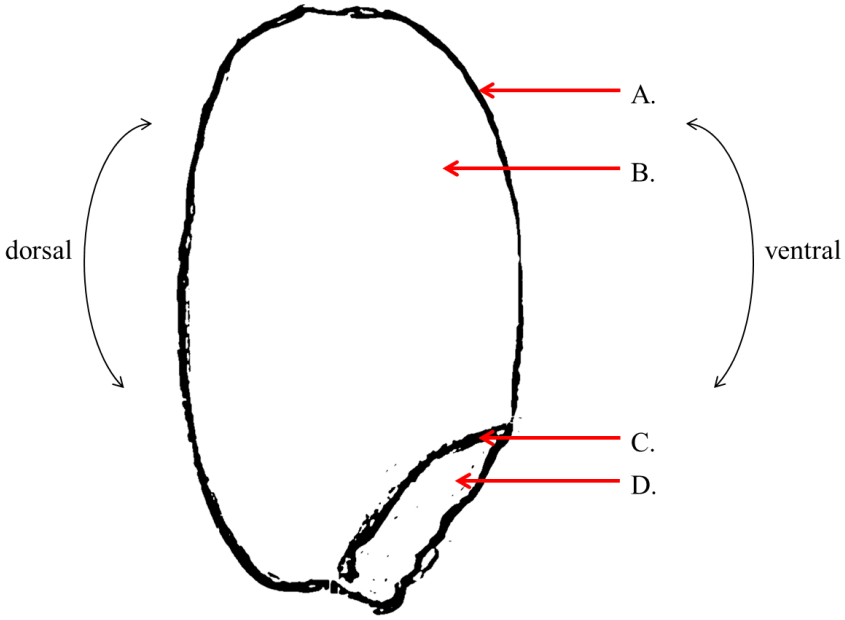

Figure 2: A simplified transverse section of a brown rice grain.

The entire rice grain is enclosed by pericarp tissue and a single cell layer of aleurone tissue (A). Directly interior to the aleurone is the starch filled parenchyma of the endosperm (B), with the scutellum (C) and embryo (D) on the lower right of the grain.

Image was modified developed from (Ogawa et al., 2002) and (Hoshikawa, 1989)

Ferritin, an Fe binding protein in plants and animals, binds hydrous Fe^{3+} oxide phosphate in plant chloroplasts or plastids. Capable of storing 4500 Fe^{3+} atoms, this ferritin complex is found in plastid stroma, and is also present in the mitochondria of xylem phloem and seeds (Briat et al., 2007, Briat et al., 1995, Clark, 1983, Busch et al., 2008). Ferritin, therefore, has become an interesting candidate tool in biotechnological research into Fe enrichment. Unlike pea models, cereals such as rice do not naturally sequester Fe via ferritin (Brinch-Pedersen et al., 2007). Expression of soybean ferritin cDNA in wheat and rice resulted in increased leaf Fe but no increase in grain Fe was noted (Drakakaki et al., 2000). Therefore, it was suggested that excess ferritin resulted in increased Fe sequestering in leaves, which consequently resulted in a reduced amount of Fe reaching the grain and ultimately causing chlorosis at the site of Fe overload. This work complemented research by Goto et al. (1999) in which rice grains were developed to over-express the soybean ferritin gene under an endosperm specific promoter. This work resulted in increased ferritin and Fe concentrations in the grain, and thus it was determined that endosperm-specific targeted approaches are potential techniques to successfully enrich Fe in the grain. The difficulty with this approach is that the effect of increasing Fe levels into the grain results in exhausting Fe in the leaves, resulting in severe chlorotic symptoms during grain development (Brinch-Pedersen et al., 2007, Yoshihara et al., 2005).

The influx and efflux mechanisms of minerals into the protein storage vacuole have been further explored in *Arabidopsis*. In addition to IRT, a protein family important in Fe transport includes natural resistance associated macrophage proteins (NRAMP). Known as *Arabidopsis* membrane efflux pumps, NRAMP were first

identified as having the ability to enhance bacterial resistance by reducing metal availability (Gunshin et al., 1997). Several *AtNRAMP* genes have since been found to encode metal transporters (Curie and Briat, 2003), and show inducible expression in response to Fe deficiency. Important for Fe distribution rather than uptake, *NRAMP* is known to reduce Fe toxicity by transporting the ions away from the point of accumulation. Interestingly, *NRAMP* homologues have been found to be present in all eukaryotes (Bereczky et al., 2003). Two transporters, *AtNRAMP3* and *AtNRAMP4*, are able to retrieve Fe from the vacuolar globoids of germinating seeds. However, in lines with point mutations in the two genes, Fe was stored properly but could not be retrieved (Lanquar et al., 2005).

The vacuolar iron transporter (*VIT1*) has been identified in *Arabidopsis* protein storage vacuoles (Kim et al., 2006). A plant homologue of the yeast *CCC1*, *VIT1* transports cytosolic Fe into the vacuole (Li et al., 2001) and conversely, the knockdown of *VIT1* function results in the diffusion of Fe distribution across the seed (Kim et al., 2006).

1.6 Bioavailability of consumed Fe

Increasing Fe uptake or loading in crop plants is important in biotechnological research. Equally important is the need to increase Fe bioavailability. A major inhibitor of Fe bioavailability in rice is the existence of 'antinutrients' in the plant. Compounds such as tannins and phytates serve as mineral storage bodies, and yet they are capable of reducing the absorptive capacity of Fe in humans and animals by forming strong complexes which pass through the digestive system without releasing the ion. Rice grains typically store phytate globoids in the aleurone layer, a

membrane of high Fe density. Studies have shown that phytases and phosphotase isozymes are continuously degrading these globoid formations, releasing the minerals or phosphates required during grain maturation.

Preventing phytate activity or increasing phytase activity has been targeted by many researchers in recent years to increase the bioavailability of micronutrients in cereal grains. Although phytases have been over-expressed in rice lines, the increased phytases did not remain stable once the rice grain was cooked (Bajaj and Mohanty, 2005, Lucca et al., 2002) and thus most the consumed Fe will still be bound to phytate. Therefore, this method of indirect targeting of Fe bioavailability may not be the most suitable approach to Fe enrichment in rice. Alternatively, the targeted enrichment of Fe directly within the endosperm of grain could be effective in increasing Fe bioavailability. Although many of the ongoing researches focusing on Fe enrichment has resulted in high levels of Fe in the plant, there is little evidence showing increased levels of Fe in the endosperm.

1.7 Concerns of heavy metal accumulation in biofortified rice grains

It is possible that in the effort to increase the uptake of Fe, the uptake of other cations may inadvertently occur. Such cations may include heavy metals such as cadmium (Cd), which pose a serious threat to the health of plants and animals, including humans when consumed. In plants, Cd reduces photosynthesis and water and nutrient uptake (Sanita di Toppi and Gabbrielli, 1999), and inhibits enzyme activities and cellular transport (Clemens, 2001). In humans Cd accumulates predominately in the kidneys with a half-life of 10-33 years (Kawada and Suzuki, 1998) and contributes to reproductive dysfunction, increased risk of cancer and reduced endocrine activity

(Fechner et al., 2011, Jarup and Akesson, 2009, Satarug and Moore, 2004). Levels of Cd in rice grain that are toxic to humans may not be toxic to the plant, however, and hence there may be no sign of phenotypic or phytotoxic symptoms which could warn humans against consumption of the plant.

Rice is the second most frequently consumed cereal worldwide after wheat (Hseu et al., 2010) with over 135 million ha of land being dedicated to the production of rice in Asia alone. Of the 20 million ha of cultivated land in China that is contaminated with heavy metals, 0.28 million ha is farmland contaminated with Cd (Li et al., 2008). Therefore, the consumption of rice poses a serious risk of dietary Cd intake(Arao and Ae, 2003).

Soil contamination is all too often a result of human pollution. Anthropogenic sources of Cd contamination in soils often result from illegal or inappropriately managed industrial practises (Hamon et al., 1998). For example, wastewater discharged from plastics or chemical plants and agricultural industries has contaminated 40% of rivers in Taiwan with heavy metals (Taiwan, 2009), with recorded Cd accumulation in soils and rice grains above their respective threshold levels (Chen, 1992, Hseu et al., 2010). Each country has independent standards on environmental protection. Countries such as Australia and Taiwan state that soils containing more than 3 $\mu g\ g^{-1}$ Cd are deemed contaminated (Satarug et al., 2003).

The Food and Agriculture Organization of the United Nations (FAO) and the World Health Organisation (WHO) have worked together since 1963 to develop standards with regards to safe food practices; known as the CODEX Alimentarius Commission. According to Commission and Commission (2011), polished rice must

have less than 0.43 μg g^{-1} Cd in the grain to be permissible for human consumption. However due to such variation in Cd concentrations in soils, much of the rice grown in Asia is rendered contaminated and not suitable for consumption. Efforts to remove or reduce Cd in soils, which could prevent or minimise Cd accumulation in rice grains, include flooding soils (Hseu et al., 2010), soil dressing (He et al., 2006), chemical stabilisation (Meers et al., 2007), and phytoextraction or phytoremediation (Arao and Ae, 2003). Previous studies have demonstrated that there is genotypic variation in rice for grain Cd accumulation (Arao and Ae, 2003). This knowledge can help in the selection of cultivars that accumulate less Cd in the grain

Interestingly, of the 135 million ha of land used in Asia for rice cultivation, 90% of that is dedicated to *Japonica* varieties. This is not only due to public taste preference but also an increased awareness that *Indica* varieties accumulate greater levels of Cd in the grain than *Japonica* (Arao and Ae, 2003). Furthermore, the Nipponbare cultivar of rice (*Oryza sativa ssp. Japonica* cv Nipponbare) appears to be a low accumulator of Cd in the grain (Arao and Ae, 2003, Hseu et al., 2010) with *Indica* varieties accumulating up to 1.5 times more Cd. As a result, *Indica* has become a model for phytoextraction of Cd from soils (Ibaraki et al., 2009).

1.8 Project aims and objectives

This project has several aims in relation to increasing Fe loading into rice grains. Chapter Two challenges current spectroscopic analysis of micronutrients in cereals by proposing that multi-spectroscopic analysis is required to confidently establish elemental distribution, speciation and chelation within grains. This chapter examines

non-transgenic rice grains with the intention of illustrating the need for such composite technical analysis in future transgenic investigations.

Chapter Three outlines the investigation of the over-expression of the three *OsNAS1*, *2* and *3* genes under cell type specific promoters (root cortex, root stele, developing flower (ovary, lodicule and vascular tissue) and leaf shoots). This work aims to establish which of the *NAS* genes, driven by which cell type specific promoter, will induce the greatest amount of Fe loading into the rice endosperm. In order to address this question, several tools are used to establish the true level of biofortification of the transgenic rice grains, namely nicotianamine quantification, synchrotron analysis and bioavailability analysis. A small scale Cd trial was also set up to establish whether or not the increased potential for NA to load more Fe into the grain may in fact increase the potential for Cd accumulation in the endosperm as Cd is a cation with similar properties to Fe and Zn. It is hypothesised that a specific combination of the *NAS* gene and cell-type specific expression will yield a plant with an Fe-enriched grain but without the concomitant undesirable loading of Cd. The ultimate aim of this section is to address the potential for such a biofortified transgenic line as a tool to combat human micronutrient deficiencies.

The fourth and final chapter outlines the investigation of the potential for a rice line, already transformed to over-express *OsNAS2* and demonstrating high levels of Fe in the endosperm, to load a greater amount of Fe into the endosperm using the rice vacuolar iron transporter gene (*OsVIT1*) under an endosperm specific promoter. This co-expression may highlight important source/sink relationships pertaining to Fe transport in the grain.

Chapter Two: Cell Type Specific Over-Expression of *OsNAS1, OsNAS2, and OsNAS3*

2.1 Introduction

Biofortification of rice as a means to increase human dietary Fe offers a promising vehicle to improve human health. Biofortification is the nutritional enhancement of staple food crops, using the plant's natural nutrient uptake mechanisms (Nestel et al., 2006). For example, biofortification is the act of enabling plants to increase Fe uptake via native uptake pathways, instead of anthropogenically adding supplementary nutrients during food preparation. Classic breeding or biotechnological tools are often implemented in such practises.

Iron is vital for plant and human nutrition; however the concentrations of Fe within both organisms must be tightly regulated. A significant decrease in Fe results in stunted growth and chlorosis in plants or anaemia in humans, and yet an excess of cellular Fe will result in the generation of free radicals and toxicity as Fe undergoes the Fenton Reaction (Foy et al., 1978). Cellular chelation of Fe by organic compounds or storage proteins reduces the toxic potential of ferric ions (Fe^{3+}) (Brinch-Pedersen et al., 2007, Curie and Briat, 2003).

Typically, the greatest accumulation of Fe in rice occurs in the embryonic scutellum and aleurone layers of grain, with relatively little Fe detected in the endosperm (Wada and Lott, 1997). Approximately 75-80% of total Fe is lost during the polishing process which removes the outer bran layers of the rice grain (Briat et al., 2007). This imposes a barrier to the delivery of increased dietary Fe via a food staple, as polished rice is the most preferred form of the grain by consumers around the world. The challenge is to increase Fe in the endosperm, in a stable, bioavailable

state. To achieve this, long distance transport of Fe from the roots to the grain must be enhanced.

Iron uptake varies depending on plant species. In dicots, solubilisation of rhizospheric Fe must occur prior to Fe uptake. Solubilisation occurs with the secretion of H^+ and the release of reductants or chelators from the root plasma membrane (Yi and Guerinot, 1996). This acidification of the rhizosphere releases Fe^{3+} from the soil colloid, followed by chelation of the Fe^{3+} by citrates, phenolics and various amino acids. These complexes are then reduced at the plasma membrane by the action of the ferric reductase/oxidases. One such example is FRO2 on the root surface of *Arabidopsis*, which reduces Fe^{3+} to Fe^{2+} (Curie and Briat, 2003), thus enabling Fe to be transported into the plant via Iron Regulated Transporters (IRT1 and IRT2) (Eide et al., 1996). Whilst most plants are capable of this ferric reductase activity, the mechanism is specific to non-graminacious monocots in what is termed the Strategy I uptake model (as Discussed in section 1.4.3).

Monocots like wheat and barley are Strategy II plants and do not rely on *FRO* and the *IRT* genes. Instead they secrete PS into the rhizosphere upon onset of Fe deficiency in the plant. Ferric ions (Fe^{3+}) bind to these chelators and enter the plant via complex-specific transporters (Curie and Briat, 2003, Curie et al., 2001). Rice, however, is a unique monocot and is capable of transporting Fe via both Strategy I and strategy II mechanisms with the capability of both *OsIRT1* expression and PS production.

Nicotianamine (NA) is a well-documented metal chelator (Bughio et al., 2002) ubiquitous in the plant kingdom and critically important for the transport of the

newly acquired Fe in both Strategy I and II plants. NA is the condensation product of three S-adenosylmethionine (SAM) molecules and is catalysed by nicotianamine synthase (NAS) (Figure 1 of Section 1.4.3), and is present in multiple forms in rice: *OsNAS 1, 2* and *3*. Each gene is spatially controlled across the plant (Cheng et al., 2007, Inoue et al., 2003) and this cell-type specific expression of the *OsNAS* genes is of particular importance in this work, which aims to specifically increase Fe in the endosperm. Cheng et al. (2007) investigated the expression of *OsNAS* and illustrated the expression of the three *OsNAS* genes occurring in different regions of the plant and also varying under different conditions. These studies identified that *OsNAS1* and *OsNAS2* were constitutively expressed in roots but not in shoots during Fe-sufficient conditions. However, this pattern changed significantly during Fe deficiency where *OsNAS1* and *OsNAS2* were expressed in shoot tissue and up-regulated in roots (Figure 1). *OsNAS3* also showed altered expression under different levels of Fe, with *OsNAS3* expressed in the shoots only during Fe sufficient conditions but in Fe deficiency, *OsNAS3* being present only in the roots. It is interesting to note not only the change in expression patterns of the three genes, but also the changes in spatial control during Fe homeostasis (Figure 1). The ultimate aim of this chapter is to investigate the individual roles of *OsNAS1*, *OsNAS2* and *OsNAS3* on Fe uptake and endosperm accumulation when controlled by cell type specific promoters.

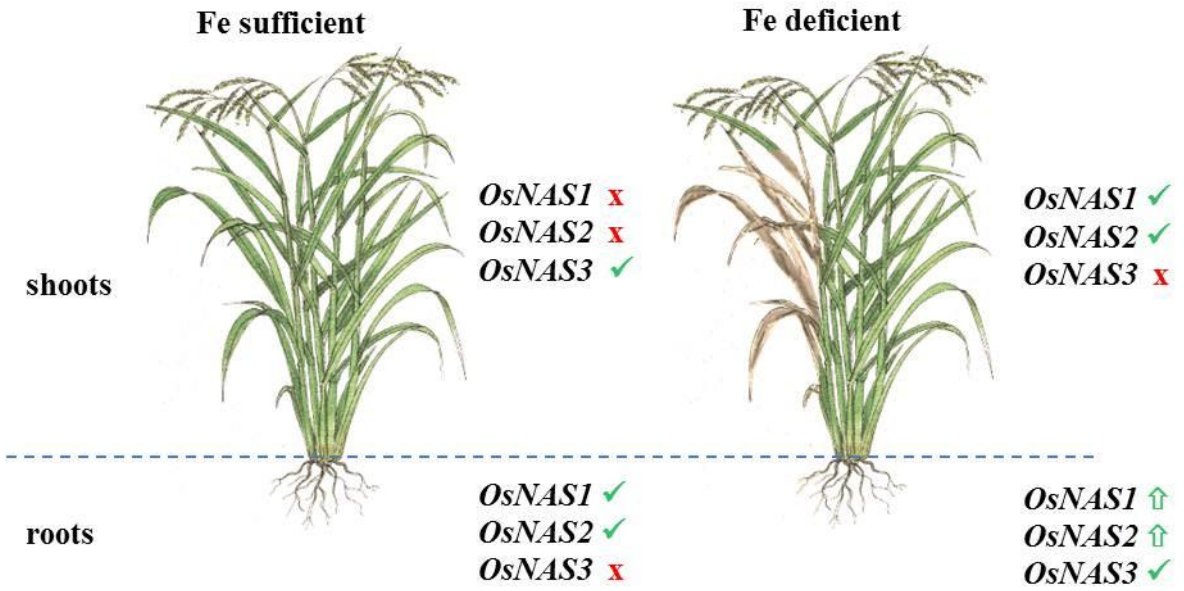

Figure 1: Spatial regulation of *OsNAS* genes during Fe homeostasis.

During Fe sufficient periods, *OsNAS1* and *2* are expressed in roots but both genes are not up regulated in the shoots. The contrary can be said for *OsNAS3* where the gene is expressed in shoots and not roots. Low Fe levels signals the up regulation of *OsNAS1* and *2* in shoots and down regulates *OsNAS3*. All three *NAS* genes are up regulated in the roots. This spatially controlled expression of the three *NAS* genes in rice may be important in the development of Fe rich rice grains, via the over-expression of one of the *OsNAS* genes in particular cell-types within the plant. Exactly which of the cell type/ gene combinations will achieve this goal is yet to be defined and is therefore the principle aim of this thesis. ✓ gene expressed (activity detected) **x** gene not expressed ⇧ gene expression up-regulated

Image modified from (Hoshikawa, 1989, Inoue et al., 2003, Cheng et al., 2007)

2.1.1 Project development

The hypothesis for the research presented here is that the over-expression of any *OsNAS* gene, under the control of a native cell-type specific promoter, will result in increased NA production in the plant. This is expected to have a two-fold action in the plant; the first will see an increase in PS secretion from roots resulting in increased Fe transport from the rhizosphere into the plant. Secondly, it is proposed that not all NA will be converted into PS production and therefore will result in an increase in NA available to transport the newly acquired Fe from the roots up to the grain. Additionally, whilst in a single transformant *OsNAS1* (for example) that may be over-expressed, there will still be endogenous levels of *OsNAS2* and *OsNAS3* expression in the plant. Therefore these may have increased activity simply due to the increased presence of Fe in the plant, signalling the need to transport the Fe to maintain homeostasis. Overall, it is proposed that there will be increased Fe loading into the grain which would typically accumulate in the embryonic and pericarp tissues. The major hypothesis of this study states that a substantial increase in NA production, as a result of over-expressing *OsNAS1*, *OsNAS2* or *OsNAS3* under cell type specific promoters in rice, will lead to enhanced levels of Fe in rice endosperm.

2.1.2 Cell-type specific control of *OsNAS*

In this study, cell type specific over-expression of each of the three *OsNAS* genes is driven using the GAL4-GFP enhancer trap system developed by Johnson et al. (2005). A simplified schematic of the enhancer trap system is provided in Figure 2A. Essentially, this process involves two independent transformation events in the plant.

The first event results in the insertion of the transcription activator *GAL4* (derived from yeast) into the plant genome. This activator can then be driven by a native promoter up-stream of the GAL4 gene, for example in root cortical cells. The Gal4 protein binds to and activates the upstream activation sequence element (UAS) (downstream to GAL4) in turn activating the green fluorescent protein (GFP) gene (downstream to UAS), eliciting a green fluorescence in the cells specific to the native promoter. This process is of a random nature and a library of plants screened for GFP expression must be established to ascertain cell-type specific expression of the insert. It is then expected that screened plants may be selected for a desired cell-type and can undergo a second transformation event (Figure 2B), whereby the expression of the second gene of interest (ie *OsNAS2*) is spatially controlled by the GAL4 enhancer trap under the native promoter, localised to the site of GFP expression (therefore at root cortex, in this example).

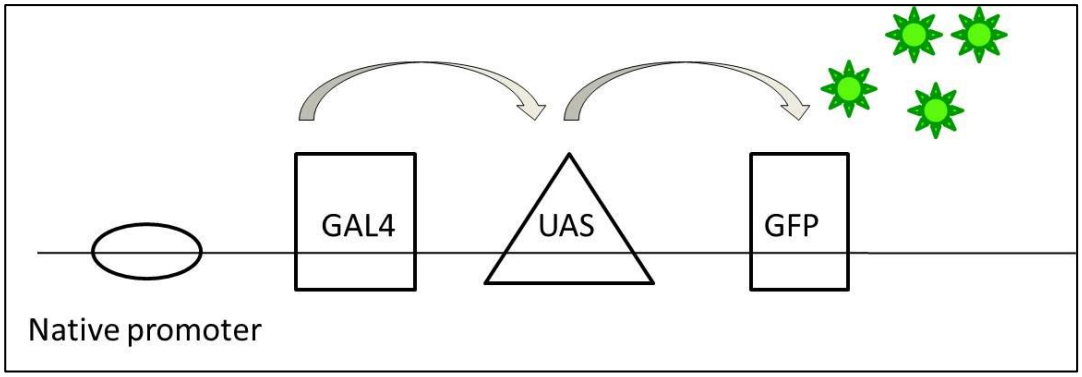

Figure 2A: First transformation event incorporating the GAL4-GFP enhancer trap cassette downstream from plant's native promoter (Random insertion, detected by GFP expression).

Expression of each element is controlled by each up-stream insert; native promoter activates the *GAL4* transcription activator. The expressed gal4 protein then binds to UAS resulting in the activation of the *GFP* (localised at site of native promoter expression, ie root cortex).

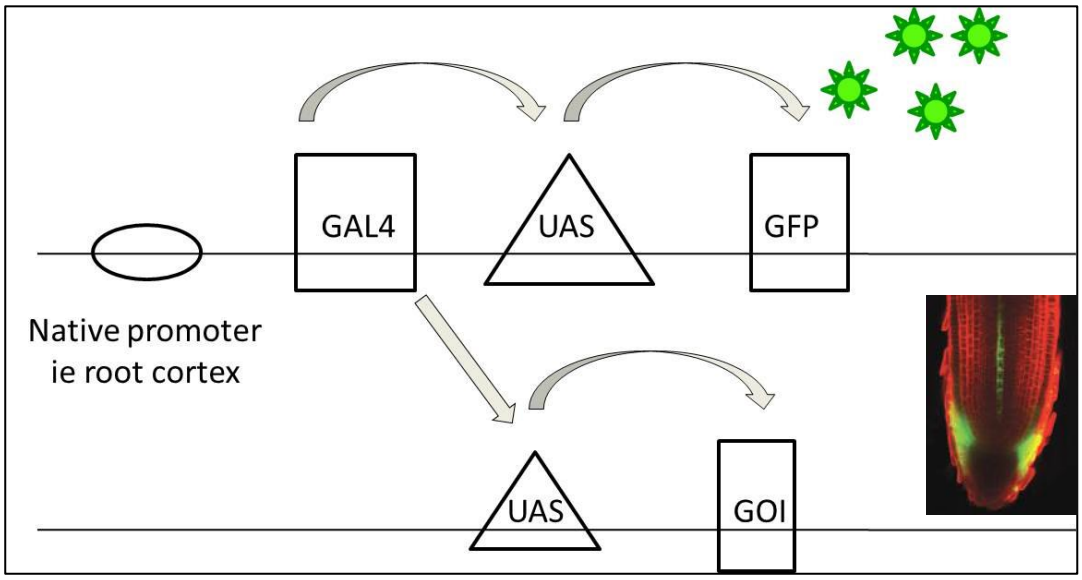

Figure 2B: Second transformation event incorporating gene of interest GOI (ie *OsNAS2*)

Expected that insertion occurs in close proximity to GAL4-GFP enhancer trap cassette and is therefore controlled by GAL4, with localisation determined by GFP, under native promoter (ie root cortex) as per coloured inset of root cortex in root expressed as a result of the GAL4-GFP enhancer trap insert (Figures 2A and B modified image from (Johnson et al., 2005)

2.2 Materials and methods

Generation of genetic material

2.2.1 cDNA synthesis

Complimentary DNA (cDNA) was synthesised from 2 ul RNA from two week old seedlings of rice (*Oryza sativa* s*sp. Japonica cv.* Nipponbare). Both RNA and cDNA samples were obtained courtesy of Dr Olivier Cotsafstis and Dr Alex Johnson. The full-length cDNA of each *OsNAS* gene was PCR amplified with Phusion Taq polymerase (Finzymes) using primers described in Appendix Two and parameters outlined in Table 1A/B below.

Table 1A: PCR-Phusion Taq reaction mix

Order	Reagent	Concentration	Final concentration	Volume (µl)
1	Water			7
2	Phusion High Fidelity 2× Master mix with HF buffer	2×	1×	10
3	Forward primer	10µM	0.5µM	1
4	Reverse Primer	10µM	0.5µM	1
5	Template DNA	2ng/µl		1
				20
6	DMSO		3%	0.6

Table 1B: PCR Cycling parameters

Temp	Time	Cycles
98°C	30sec	1×
98°C	10sec	35×
Annealing temperature dependent on primer pair	30sec	
72°C	(30s/kb)	
72°C	10’	1×
15°C	Hold	∞

2.2.2 Gateway vector cloning

The PCR fragments were cloned, separately, into the Invitrogen Gateway Entry vector pCR8H/GW/TOPOH according to manufacturer's instructions as outlined by Invitrogen.

2.2.3 pMDC100 cloning

Error free sequences were recombined into a modified pMDC100 vector according to methods outlined by Curtis and Grossniklaus (2003) that placed the *OsNAS* coding sequences under the control of a dual CaMV 35S promoter (Figure 1).

2.2.4 Calli transformation

Cell type specific *OsNAS* lines were generated from those previously transformed and screened for GFP expression in tissue, from which a cell type library was established. This work was detailed by Johnson et al. (2005). Embryogenic nodular units arising from scutellum-derived callus were inoculated with supervirulent *Agrobacterium tumefaciens* strain AGL1 (carrying the *OsNAS* over-expression vectors) and geneticin-resistant shoots were regenerated after nine weeks using established protocols (Sallaud et al., 2003). Rooted T0 plantlets were transferred to the growth room in Jiffy® peat pots, and moved to soil after 15 days. The same methods were applied to the generation of constitutive expression lines of the three *OsNAS* genes, as well as *35S* constitutive expression of the three *OsNAS* genes.

Characterisation of transgenic material

In this chapter, cell type specific over-expression of *OsNAS1*, *OsNAS2* and *OsNAS3* was investigated at cell type specific regions, which produced 15 genotypic varieties (see Table 2 below)

Table 2: Assigned labels for transgenic material

Assigned label	Genotypic possibility
Root : Cortex	RC *OsNAS1/ 2/ 3*
Root : Stele	RS *OsNAS1/ 2/ 3*
Developing Flower : Lodicule	DF : L *OsNAS1/ 2/ 3*
Developing Flower : Vascular Bundle ; Leaf Collar	DF : VB ; LC *OsNAS1/ 2/ 3*
Developing Flower : Ovary ; Leaf Collar	DF : O ; LC *OsNAS1/ 2/ 3*

2.2.5 Seed germination and plant maintenance

Oryza sativa ssp. Japonica cv. Nipponbare seeds were soaked in 70% ethanol for 5 minutes, washed with 30% bleach (v/v) and 1% Tween 20 (v/v) and agitated for 30 minutes at 25°C. Seeds were then washed with reverse osmosis (RO) water 3 times, with 10 minutes between washes and subsequently placed on Petri dishes lined with Whatman filter paper Number 1 and 5 ml RO water. Plates were sealed with parafilm and incubated at 28 ºC with 24 hours of light for one week. The germinated seedlings were planted in the greenhouse in UC Davis soil mix (Hoagland and Arnon, 1950) in pots placed on large trays of water ensuring pots were not fully submerged. Plants were cultivated (12 day light hours, 28 ºC day temperature, 24 ºC night temperature, 70% humidity) in greenhouse or controlled environment growth rooms (CER). After the plants were two weeks old, Manutec Acidic Plant Food fertiliser was applied weekly, according to manufacturer's instructions. Plants were grown until maturity

(post seed filling) after which point watering was ceased to allow plants to desiccate, following which grain was harvested and further dried in a 37 ºC oven for 3 days.

2.2.6 Visualisation of GFP expression in transgenic material

Visualisation of GFP was performed as per Johnson et al. (2005). In brief, spikelets of plants expected to express GFP at developing flower specific tissue (lodicule, ovary, vascular bundle) were harvested two months after sowing. Only spikelets between anthesis and grain development phases were used. Leaf tissue was also collected for assessment of GFP expression in the leaf collar. Flowers or leaf tissue were inspected under a Leica MZ FLIII fluorescence stereomicroscope (Leica Microscopie Systemes SA, Heerbrugg, Switzerland) with a GFP+ fluorescence filter [GFP2, 480 nm excitation filter (bandwidth of 40 nm) and 510 nm barrier filter] and images collected using a Leica DC 300F digital camera.

2.2.7 High-throughput DNA extractions of rice plant tissue

Youngest emerged leaf blades (YEB) were harvested for each plant and freeze dried overnight. Samples were ground to a fine powder in a Retsch Mill at 650 Hz for 2 minutes with two 4 mm stainless steel ball bearings. Samples were then incubated at 65°C for 30 minutes with 600 µL extraction buffer (0.1M Tris-HCl pH 7.5; 0.05M EDTA pH 8.0; 1.25% SDS (w/v)), followed by incubation at 4°C for 15 minutes with 300 µL 6 M ammonium acetate. Samples were subsequently centrifuged at 6100 rpm for 15 minutes followed by the addition of 600 µL of supernatant to 360 µL isopropanol. After incubation at room temperature for 15 minutes, samples were centrifuged at 4000 rpm for a further 15 minutes. Supernatant was discarded and

pellets washed three times with 70 % ethanol. Pellets of genomic DNA (gDNA) were finally resuspended with RO water and stored at -80°C until required.

2.2.8 Amplification of *OsNAS* from gDNA

Genotyping reaction mixtures were prepared as per conditions below, using NPTII primers (GeneWorks) to identify the presence of the selective marker (indicative of the second transformation event) within gDNA. Samples were amplified via PCR with Platinum Taq polymerase (Invitrogen) (Table 3A/B below) and analysed by agarose gel electrophoresis.

Table 3A: PCR – Platinum Taq reaction mix

Components	Final Concentration	Volume (μL)
10 X PCR buffer, minus Mg	1 X	1.25
1.25mM dNTP mixture	0.2 mM each	2
50mM MgCl2	1.5 mM	0.375
Primer mix (10uM each)	0.2 μM each	0.25
Template DNA prepared 1 in 50 dilution of gDNA	as required	0.25
Platinum Taq DNA polymerase	1.0 unit	0.05
DMSO	5 % of total volume	0.625
autoclaved, RO water	to complete a 12.5 μl reaction mixture	7.7

Table 3B: PCR cycle conditions

PCR Cycle Conditions	Temperature (°C)	Time	Cycles
Initial Denaturation For Hot Start Reaction	94	2 min	-
Denature	94	30 sec	25-35
Anneal	56	30 sec	
Extend	72	1 min per KB	
End/Store	15	∞	-

2.2.9 Agarose gel electrophoresis

Genomic DNA or PCR products were analysed via agarose gel electrophoresis using a 1% agarose (w/v) and 1x TAE buffer (0.04 M Tris acetate and 0.001 M EDTA) solution. Syber Safe DNA Gel Stain (Invitrogen) added as per manufacturer's instructions, prior to solidifying to enable the DNA products/ fragments to be imaged under UV light. Samples were loaded after 1:1 dilution with 0.15% Orange G loading buffer (Sigma-Aldrich) and the gel was run at 130V for approximately 1 hour. Images were acquired under Gel Doc-It 310 imaging system (Ultra Violet Productions Cambridge, England).

2.2.10 Establishing milling conditions

Using a commercial bench-top miller (Kett Electrical Laboratory, Tokyo, Japan), modified to prevent metal contamination (Stangoulis, 2010), 50 brown non-transgenic *Oryza sativa ssp. Japonica cv. Nipponbare* seed grains were milled for 30 seconds. This was repeated with brown grains for the mill periods of 60, 90, 120, 150 and 180, seconds. The milled grain was then incubated in 1:3 solution of 100% ethanol and 2% aqueous potassium hydroxide (KOH) for 15 min to stain remaining aleurone yellow. In order to replicate commercial practice, any samples with more than 20% breakage or greater than 15% aleurone remaining were deemed too broken or unmilled, respectively, and not considered for further experiments. The optimum milling times, resulting in the least broken grains and highest aleurone removed was 150 seconds and was employed for all further milling.

2.2.11 Quantification of elemental concentrations in transgenic grain

Concentrations of Fe, Zn, P and S were studied for T0, T1 and T2 generations of the transgenic lines. Brown grain was obtained by manually threshing hulls off 25 randomly selected grains from individual plants. An additional 75 grains were randomly selected and milled (as per section 2.2.10 above) to obtain polished grain. Inductively coupled plasma optical emission spectroscopy (ICP-OES) was used to determine elemental concentrations in both brown and white grains. Methods used for ICP-OES are described by Wheal et al. (2011).

2.2.12 Determination of nicotianamine levels in rice grain

Analysis of nicotianamine content analysis was performed by LC- triple-quad -MS according to the method published by Callahan et al. (2007). Briefly, brown or white grains were ground to a fine powder and 200 µL of 5 mM EDTA solution was added to the flour. From this, 10 µL of supernatant was added to 70 µL borate (0.2 M Na_3BO_3; pH 8.8) and 10 µL of 6-aminoquinolyl-N-hydroxysuccinimidyl carbamate (AQC) solution (10 mM in dry acetonitrile) and incubated at 55°C for 10 minutes. Chromatograms and mass spectra obtained via LC-triple-quad-MS and evaluated using the MassHunter Quantitative analysis program (Agilent). An external calibration curve was developed using standards in the concentration range of 2.75 - 100 pmol.µL^{-1}. Samples were prepared and analysed in triplicate.

2.2.13 Visualisation of iron deposition via Perl's Prussian blue staining

Brown rice grains were glued, dorsal side down, onto a small piece of Perspex using Araldite epoxy (Huntsman Advanced Materials). Once dried, grains were shaved open with a small drill bit attached to an orbital sander, to expose the endosperm and embryo of the grain (see Figure 1). The Perspex plate was incubated in Perl's Prussian Blue stain (PPB) using methods published by Choi et al. (2007). Briefly the reaction required the plate of grains to be submerged in 142 mM potassium hexanocyanoferrate (Sigma Aldrich) in 4% HCl for 8 minutes, and air-dried for a further 30 minutes. Photos of grain were taken using a Leica microscope (model MZ16) with DFC280 camera attachment and supporting software (Leica Application Suite v3.6.0 (Leica Microscopie Systemes SA, Heerbrugg, Switzerland)).

2.2.14 Bioavailability of iron to human model

In order to determine Fe availability with Caco-2 cell lines, grains were first polished for 150 seconds with a modified commercial bench-top miller (Kett Electrical Laboratory, Tokyo, Japan). The polished grain was then ground to a fine homogenous powder with a Retsch mill MM300 with 10 mm agate ball. Samples were introduced to the Caco-2 model system (human epithelial colorectal adenocarcinoma cells) as per Glahn et al. (1996) (see Figure 3 for details).

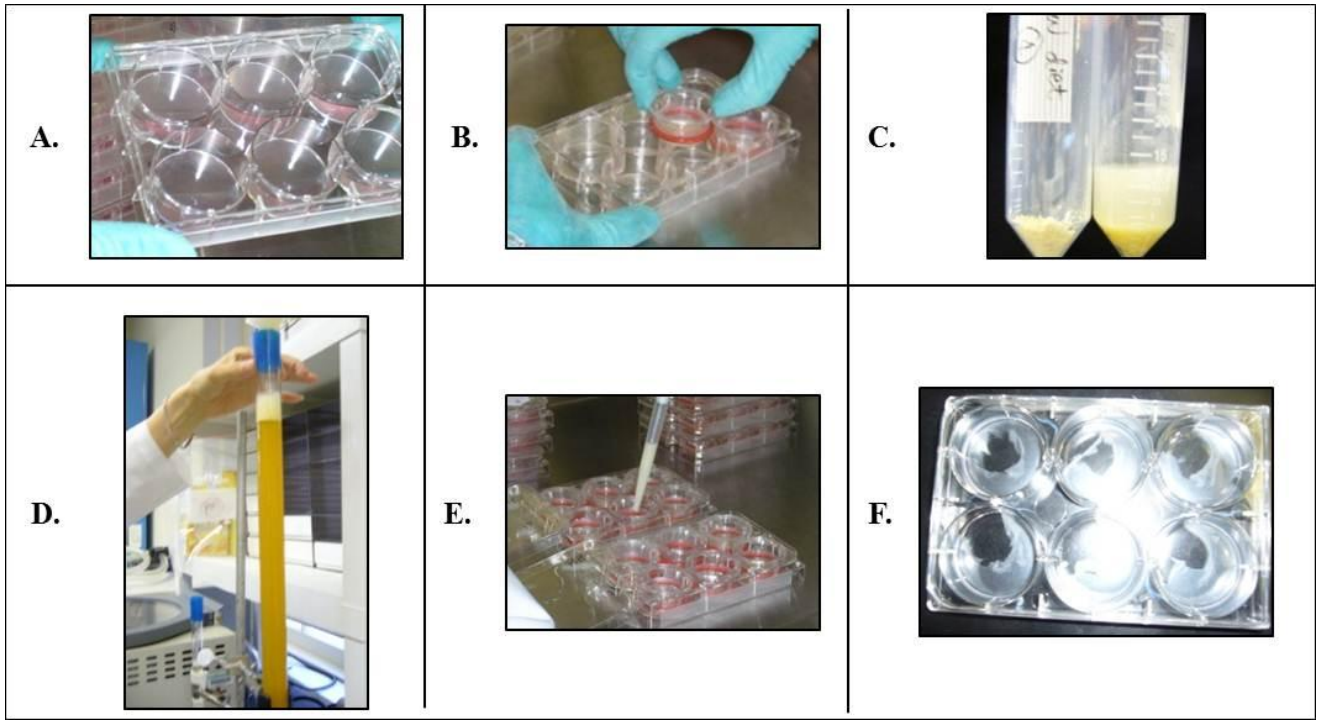

Figure 3: In vitro digestion of OX *OsNAS* rice and Caco-2 uptake procedures.

A. Caco-2 cell monolayer seeded in 6 well plates (seeding method as per Glahn et al 1996 (Glahn et al., 1996)). **B.** insert ring with cellulose dialysis membrane placed over monolayer. **C.** Rice grains milled for 150 seconds in modified Kett Mill, powders were introduced to pepsin (pH 2) and digested for 1h at 37°C. **D.** Pepsin digested rice samples introduced to pancreatin-bile colum, pH 7 and digested for 2h at 37°C. **E.** Sample introduced to Caco-2 culture well to allow diffusion of soluble Fe. **F.** Caco-2 cells harvested and radioimmunoassayed for ferritin levels. Images: personal files.

2.3 Results

2.3.1 T0 *OsNAS* transformants

Rice plants (*Oryza sativa* s*sp. Japonica cv*. Nipponbare) generated for this project were originally transformed to over-express the GAL4 enhancer trap developed by Johnson et al. (2005). Five lines showing GFP expression in root stele were selected to be transformed a second time (dubbed maternal lines, listed in Table 4 below). The aim was to generate plants over-expressing *OsNAS 1*, *2* and *3*, under the control of these cell-type specific GAL4 enhancer traps. Lines referred to as 35S *OsNAS1*, *2* or *3* are described further in Appendix One (Johnson et al., 2011).

Over 280 transgenic lines were generated from this second transformation event with genotypes and cell-type specific expression summarised in Appendix Three. These transformants are henceforth referred to as "T0 transgenics" with grain harvested from these plants called "T1 grain". Plants to be used for further propagation and analysis were selected based on cell-type specific GFP expression and high Fe content in the grain.

Table 4: Nomenclature assigned to T0 transgenic rice plants.

Labels have been assigned depending on cell-type specific expression of the gene of interest and site of expression in the plant tissue. Five final lines were selected for further analysis. Several lines have a combination of cell type specific expression, ie VB and LC etc.

Specific Cell Type	Plant Tissue	Assigned Label	Selected Line
Cortex (C)	Roots (R)	Root : Cortex	R : C
Stele (S)	Roots (R)	Root : Stele	R : S
Lodicule (L)	Developing Flowers (DF)	Developing Flower : Lodicule	DF : L
vascular bundle (VB)	Developing Flowers (DF)	Developing Flower : Vascular Bundle ; Leaf Collar	DF : VB ; LC
Ovary (O)	Developing Flowers (DF)	Developing Flower : Ovary ; Leaf Collar	DF : O ; LC
leaf collar (LC)	Leaves	no lines selected with expression solely at this cell type	

2.3.2 GFP expression in T0 transgenics

Using a fluorescence stereomicroscope, GFP expression was identified in rice plants expressing *OsNAS*1, 2 or 3 in developing flowers (lodicules, vascular bundles or ovaries) and leaf tissue (collar). This identification confirmed the expected GFP expression location based on original data obtained from the maternal line library (Johnson et al., 2005 and personal communication). The expression of GFP was difficult to visualise in root cortical and stellar tissue of T0 transgenics and due to time constraints, was not further investigated. Each of the maternal lines had been positively identified as expressing GFP in the root cortex and stele (Johnson et al., 2005) prior to the generation of T0 transgenics within this project. Images of a negative GFP expression line is shown in Figure 4A and is further compared to three positive GFP expression lines in Figure 4B-D.

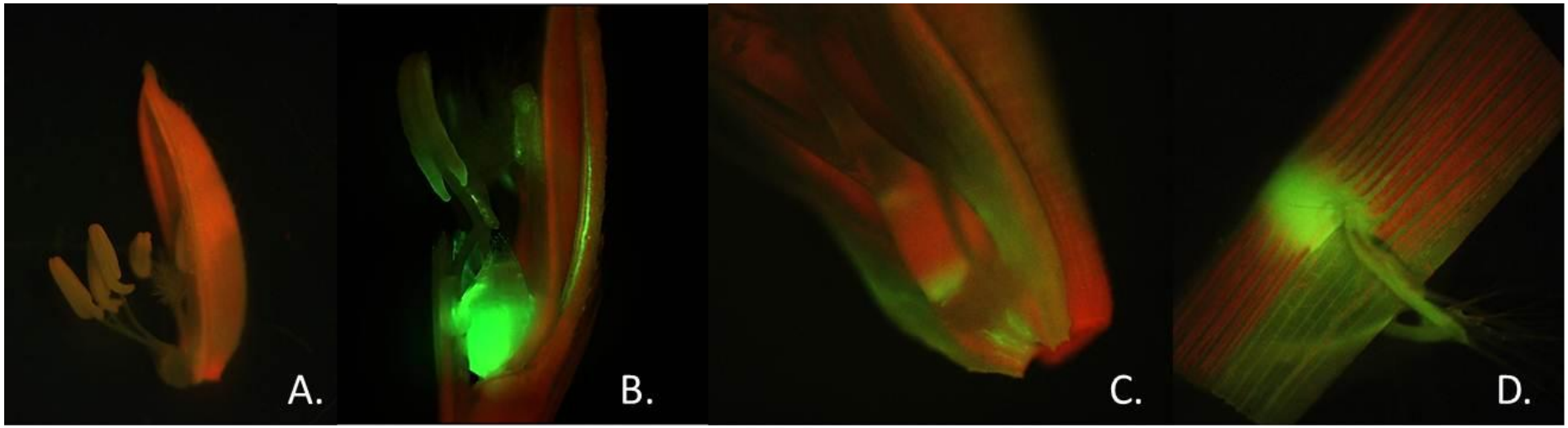

Figure 4 (A-D): GFP localised to three cell type specific regions within the transgenic *OsNAS* rice plants.

A. Negative GFP expression in developing rice flower. Palea, lodicule, stamens, anthers and stigma visible. **B.** Positive GFP expression in lodicule and the vascular bundle on the palea. Glow on anthers is reflection of lodicule only. **C.** Positive GFP expression in ovary of developing rice flower. **D.** Positive GFP expression at the site of the leaf collar. Cell type specific expression of GFP in root cortex and root stele were not personally identified in these lines

.

2.3.3 Crude elemental distribution: ICP-OES

Grains milled for various times were analysed for aleurone retention using KOH stains which produces a yellow- brown colouring when in contact with aleurone strands. The KOH method is a standard method used by IRRI to visualize retention of aleurone and to optimise milling degree. This method has not been published, however KOH is commonly used in the extraction of phenolics and polysaccharides from cell walls (Ingold et al., 1988), specific to the aleurone layer of cereal grains (Bacic and Stone, 1981). We believe the stain occurs due to the release of fluorescing ferulic acid within the aleurone layer, a result of KOH hydrolysis (Fulcher et al., 1972). Further analysis of this would be interesting to confirm the derivation of this apparent oxidation reaction. From the images in Figure 5, it can be seen that a longer milling period reduces the yellow/brown colouring, thus showing almost complete removal of the aleurone layers. 150 seconds was eventually chosen as the best milling time as it removed the majority of the aleurone layer.

Commercially, samples with more than 20% breakage and 15% aleurone attached were deemed unsuitable for distribution, and therefore these samples are not considered for further experiments. The 150 seconds milling time resulted in the least grain broken and most aleurone removed, thus was used throughout the rest of this chapter and thesis.

Figure 5: KOH stained rice grains post-milling.

Rice grains were milled in a Kett Mill for A: 30 seconds, B: 2 minutes, C: 3 minutes and then stained with KOH, D: unstained grain milled for 150 seconds. Red arrows demonstrate scutellum to denote missing embryo and therefore polished grain.

Elemental concentrations of brown and polished grains varied widely with over 70% of the Mn, P and Fe lost after 150 seconds of milling (see Table 5). The Zn concentration post-milling is not significantly different from the brown grain suggesting the majority of the Zn is present in the endosperm rather than the outer layers. It is also interesting to note that the majority of sulphur (S) accumulation is endosperm bound with up to 70% retained post milling. This was repeated in triplicate, as shown in Table 5, but it is recommended that these methods should be repeated to generate strong statistical relevance.

2.3.3 ICP-OES of Brown and White Rice Grains from T0 plants

Grain was analysed for elemental concentrations using ICP-OES for both brown and white T1 grain (from T0 plants). As per Table 5A/B, ICP-OES data was collated for several elements including Fe and Zn. Elements such as calcium (Ca), Mn and copper (Cu) were also analysed, however there were no significant differences between wild-type and transgenics for these elements (data not shown). Phosphorous (P) and sulfur (S) concentrations are also shown below in Table 5A/B to demonstrate potential changes in phytate (referring to P) concentrations and protein bodies (referring to S), which could indicate changes in bioavailability of Fe or inhibition of uptake, respectively.

Table 5A : Elemental composition in brown grain of T0 transformants as determined by ICP-OES.

Samples of 25 brown grains were randomly selected from each plant sample and analysed for Fe, Zn, P and S concentrations via ICP-OES (courtesy of Waite Analytical Services). NOTE ICP-OES analysis of 35S *OsNAS* lines are presented in Johnson et al. (2011) available in Appendix One.

		Gene	Fe µg g^{-1}		Zn µg g^{-1}		P µg g^{-1}		S µg g^{-1}	
			ave ± stdev	range	ave ± stdev	range	ave ± stdev	range	ave ± stdev	range
Brown Grains	**wildtype**		19 ± 3	(16-24)	29 ± 6.	(24-42)	4317 ± 299	(3800-4600)	1473 ± 164	(1210-1670)
	root: stele	*OsNAS1*	30 ± 7	(22-37)	45 ± 9	(35-56)	4633 ± 528	(4100-5500)	1288 ± 101	(1100-1360)
		OsNAS2	32 ± 4	(27-37)	46 ± 7	(40-56)	4480 ± 377	(4100-5100)	1204 ± 85	(1120-1340)
		OsNAS3	38 ± 7	(27-49)	53 ± 7	(42-62)	4750 ± 797	(3700-5600)	1228 ± 148	(1020-1390)
	root: cortex	*OsNAS1*	37 ± 6	(31-45)	51 ± 5	(43-57)	5033 ± 186	(4900-5400)	1373 ± 55	(1300-1460)
		OsNAS2	42 ± 12	(34-66)	58 ± 13	(44-83)	5367 ± 207	(5100-5600)	1425 ± 97	(1340-1610)
		OsNAS3	37 ± 8	(25-46)	48 ± 10	(35-59)	5150 ± 509	(4300-5800)	1325 ± 85	(1220-1420)
	developing flower: lodicule	*OsNAS1*	32 ± 7	(21-40)	47 ± 6	(38-53)	4483 ± 279	(4200-4900)	1208 ± 73	(1110-1290)
		OsNAS2	40 ± 5	(34-47)	55 ± 5	(47-60)	5050 ± 207	(4700-5200)	1280 ± 73	(1210-1410)
		OsNAS3	37 ± 11	(22-50)	51 ± 10	(35-61)	4500 ± 283	(4200-5000)	1215 ± 57	(1160-1290)
	developing flower: vascular bundle & leaf: collar	*OsNAS1*	32 ± 4	(28-35)	53 ± 10	(43-63)	4867 ± 611	(4200-5400)	1287 ± 104	(1170-1370)
		OsNAS2	36 ± 5	(30-40)	53 ± 9	(42-60)	4967 ± 252	(4700-5200)	1387 ± 32	(1350-1410)
		OsNAS3	28 ± 6	(21-33)	43 ± 9	(33-48)	4500 ± 520	(4200-5100)	1263 ± 101	(1200-1380)
	developing flower: ovary & leaf: collar	*OsNAS1*	35 ± 7	(27-41)	48 ± 7	(42-46)	4933 ± 58	(4900-5000)	1360 ± 55	(1300-1410)
		OsNAS2	31 ± 16	(21-50)	45 ± 20	(32-68)	4567 ± 666	(4000-5300)	1270 ± 175	(1090-1440)
		OsNAS3	40 ± 6	(34-47)	54 ± 8	(45-60)	4600 ± 346	(4400-5000)	1287 ± 98	(1230-1400)
	constitutive 35S expression	*OsNAS1*	42 ± 6	(36-47)	60 ± 4	(56-63)	5467 ± 306	(5200-5800)	1450 ± 89	(1400-1520)
		OsNAS2	66 ± 14	(54-81)	85 ± 15	(68-95)	5833 ± 58	(4700-5900)	1447 ± 81	(1320-1540)
		OsNAS3	51	-	65	-	4700	-	1320	-

Table 5B: Elemental composition in white grain of T0 transformants as determined by ICP-OES.

Samples of particular genotypes were milled 150 seconds in a modified Kett Mill to obtain white grains for ICP analysis. NOTE ICP-OES analysis of 35S *OsNAS* lines are presented in Johnson et al. (2011) available in Appendix One.

		Gene	Fe µg g^{-1}		Zn µg g^{-1}		P µg g^{-1}		S µg g^{-1}	
			ave ± stdev	range	ave ± stdev	range	ave ± stdev	range	ave ± stdev	range
White Grains	**wildtype**		4 ± 1	(4-5)	30 ± 4	(26-34)	1287 ± 71	(1210-1350)	1110 ± 164	(930-1250)
	developing flower: lodicule	*OsNAS1*	5 ± 1	(4-7)	37 ± 5	(32-41)	1427 ± 280	(1140-1700)	1097 ± 67	(1040-1170)
		OsNAS2	7 ± 1	(6-7)	43 ± 4	(40-48)	1560 ± 114	(1480-1690)	1110 ± 78	(1060-1200)
		OsNAS3	7 ± 1	(6-8)	44 ± 5	(39-49)	1320 ± 56	(1260-1370)	1000 ± 17	(980-1010)
	root: cortex	*OsNAS1*	9 ± 3	(6-12)	45 ± 3	(42-48)	1680 ± 250	(1400-1880)	1253 ± 75	(1210-1340)
		OsNAS2	10 ± 2	(9-13)	53 ± 12	(45-67)	1847 ± 40	(1870-1800)	1257 ± 97	(1150-1340)
		OsNAS3	7 ± 2	(5-9)	36 ± 10	(26-45)	1693 ± 220	(1470-1910)	1203 ± 103	(1090-1290)

From the ICP-OES analysis it is evident that there is a marked increase in Fe concentration in transgenics compared to wildtype samples, with Fe concentrations ranging from 28-66 μg g^{-1} in brown grains of the constitutive and cell-type specific *OsNAS* genotypes compared to approximately 19 μg g^{-1} Fe of wildtype. The highest Fe concentration is recorded in the grains of 35S *OsNAS1*, *2* and *3* lines and corresponds to more than a two-fold increase in Fe of brown grain. The differences in elemental grain concentrations are further illustrated in Figure 6 A-E where it can be seen that the median value for each transgenic gene and cell type combination is consistently higher than that of the wildtype. Interestingly, the Fe concentrations in the 35S *OsNAS2* line had an average of 66 μg g^{-1} and a maximum of 81 μg g^{-1} in a single line. Zinc also peaked at 95 μg g^{-1} compared to 29 μg g^{-1} in wildtype (Table 5A). This strong trend in consistently elevated micronutrient levels can be seen in Figure 6 A-E, with the minimum, maximum and 25^{th} and 75^{th} percentiles for each of the elements well above that for the wildtype. The 35S *OsNAS2* lines appear to be the most efficient Fe and Zn accumulator in brown grain when compared to wildtype and constitutive and cell-type specific expression lines. The 35S *OsNAS3* lines are not represented on the box-and-whisker plots as the data obtained was from a single plant and could not be included with a group of sibling transgenics (n=1).

Additional positive trends are evident within several cell-type specific over-expression lines in relation to Fe and Zn grain content when compared to wildtype. In particular, the DF:L *OsNAS*3, DF:O;LC *OsNAS2* and RC *OsNAS2* lines present the highest increase in Fe (50, 50 and 66 μg g^{-1} respectively). From this two-fold increase in brown grain Fe content, there appears to be a trend for higher Fe accumulation when *OsNAS2* and *OsNAS3* are over expressed in developing flowers and root tissue.

From these genotypes, he root cortex (RC) *OsNAS2* genotype is the most interesting, in that it showed a 2.3-fold increase in Fe concentration compared to wildtype with a single sibling having 66 μg g^{-1} and 13 μg g^{-1} Fe in brown and white grain, respectively. This genotype also shows the highest increase in Zn and P concentrations in both brown and white grain compared not only to the other transgenic lines but also with the wildtype.

Concentrations of S appear to decrease in brown and white grain in all transgenics compared to wildtype, except for a single plant from the RC *OsNAS2* transgenics with S concentration of 1610 μg g^{-1}. In white grain the S concentration does not vary greatly between the majority of the transgenics and the wildtype. Contrary to this pattern is the stand-out RC *OsNAS2* line with 1340 μg g^{-1} S in white grain which is greater than that of the wildtype with S concentration ranging from 930-1250 μg g^{-1}.

Figure 6 (A-F) (continued): Elemental composition of wildtype rice and transgenic T1 rice over-expressing Os*NAS1*, *OsNAS2* and *OsNAS3* under cell type specific promoters, as determined via ICP-OES.

(A): Fe concentrations from brown grains. (B): Zn concentrations from brown grains. (C): P concentrations in brown grains. (D): S concentrations from brown grains. (E): Fe and Zn concentrations of wildtype and *OsNAS* over-expression lines under DF:L and RC cell type promoters, in white grains.

Root stele (RS), root cortex (RC), developing flower; lodicule (DF;L), developing flower; vascular bundle:leaf collar (DF;V;L), developing flower; ovary and lodicule (DF;O;L) and 35S constitutive expression lines. ICP-OES concentrations are in µg g^{-1}. All figures are compiled from data in triplicate and therefore contain error bars.

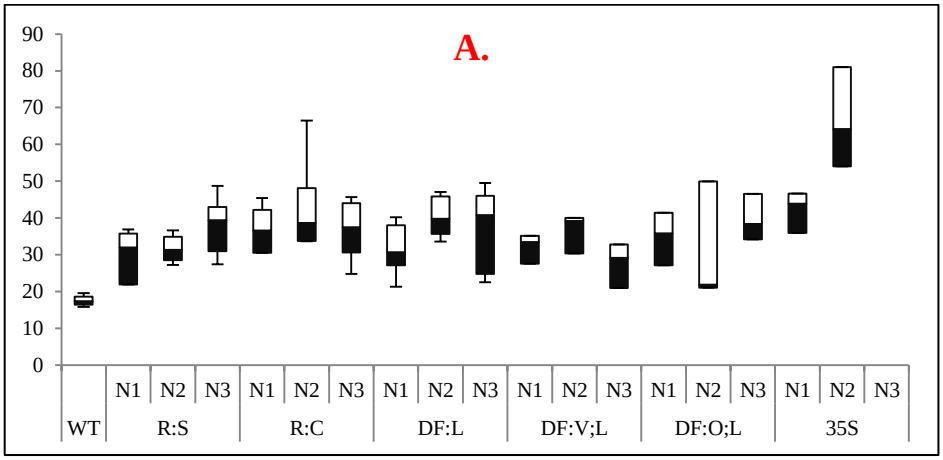

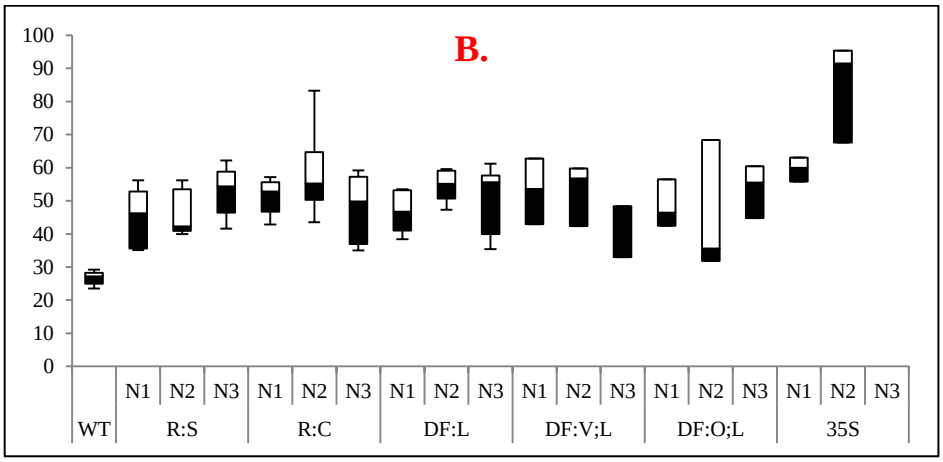

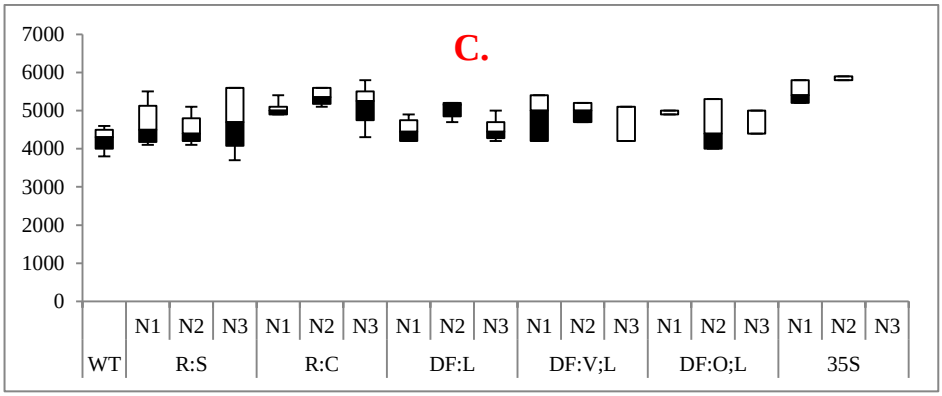
C.
7000
6000
5000
4000
3000
2000
1000
0
N1 N2 N3 N1 N2 N3 N1 N2 N3 N1 N2 N3 N1 N2 N3 N1 N2 N3
WT
R:S
R:C
DF:L
DF:V;L
DF:O;L
35S

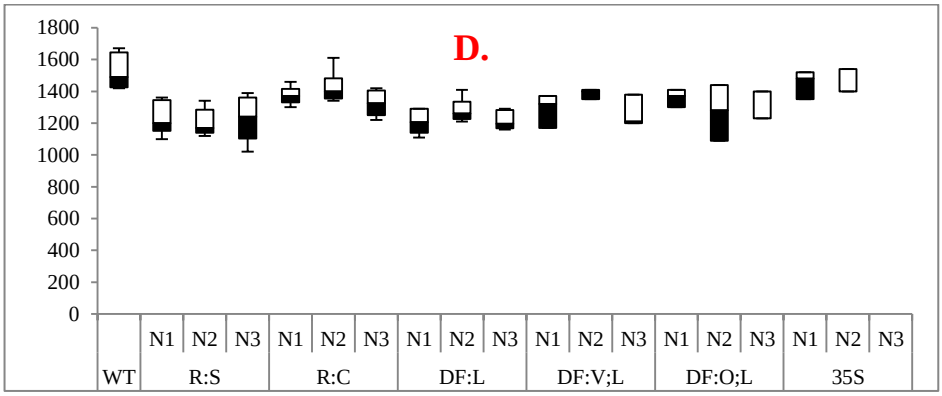
D.
1800
1600
1400
1200
1000
800
600
400
200
0
N1 N2 N3 N1 N2 N3 N1 N2 N3 N1 N2 N3 N1 N2 N3 N1 N2 N3
WT
R:S
R:C
DF:L
DF:V;L
DF:O;L
35S

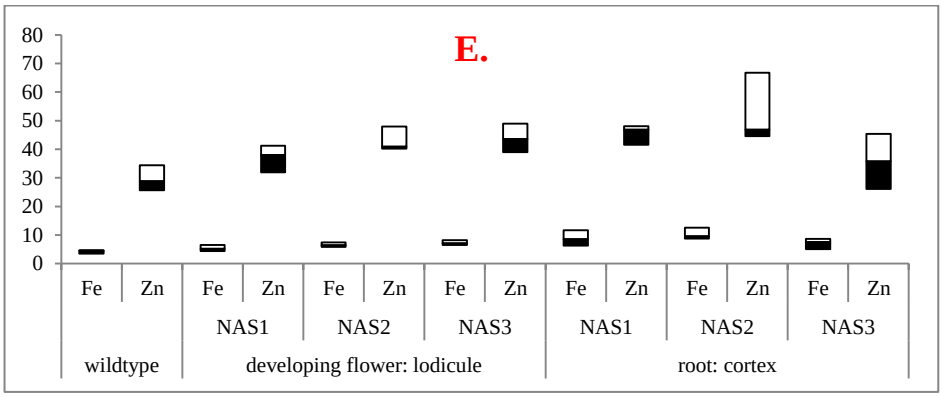
E.
80
70
60
50
40
30
20
10
0
Fe Zn Fe Zn Fe Zn Fe Zn Fe Zn Fe Zn Fe Zn
NAS1
NAS2
NAS3
NAS1
NAS2
NAS3
wildtype
developing flower: lodicule
root: cortex

2.3.4 Nicotianamine concentration in T1 white grains

Nicotianamine (NA) concentrations were quantified from 6 rice lines using LC-QqQ-MS as a means to establish a true increase in NA as a result of the over-expression of the *OsNAS* genes. The two T1 transgenic GAL4 *OsNAS* lines used to examine NA concentration were a developing flower: lodicule *OsNAS3* line and a root: cortex *OsNAS2* line, each presenting the highest Fe concentrations amongst all the transgenic cell-type expression lines (see section 2.3.3). Nicotianamine was quantified in both brown and white grains but solely white grains for the motherline control (contains GAL4 enhancer trap only). The two transgenic lines had a 77-78% increase in NA accumulation in brown grain compared to the control (average of 9 $\mu g.g^{-1}$ grain NA in control). The DF:L *OsNAS3* grain that was milled showed a 4% enrichment in NA in the endosperm compared to the brown grain. This difference in content between brown and milled samples is evident in the RC *OsNAS2* line also, with a 16% higher concentration of NA between white and brown grain. Furthermore, Figure 8 suggest that the increasing stain correlates well with the increasing Fe concentrations and may support a positive correlation between NA accumulation and Fe concentrations in brown grain. Such derivations can only be confirmed with more rigorous sample analysis. Data from both Figure 7 and Figure 8 strongly suggest that the cell-type specific expression of *OsNAS2* and *3* elicits high transport of Fe into the endosperm, likely bound to the increased NA.

Data represented in Figure 7 demonstrates that the over-expression of *OsNAS2* and *3* in two transgenic lines increases NA levels over five-fold, in both brown and white grains when compared to controls. This analysis of a small subset of samples

provides positive evidence that the over-expression of *OsNAS2* and *3* is responsible for the increased NA in brown and white grains. Additionally, the significant increase in NA compared to controls ($P = 0.003$, student t-test) and the increase in Fe in the brown grain of the transgenics (Figure 8) indicates a strong correlation between increased NA and Fe accumulation. This supports the hypothesis that an increase in *OsNAS* under cell type specific promoters will lead to an increase in NA which could lead to increased Fe loading in the endosperm.

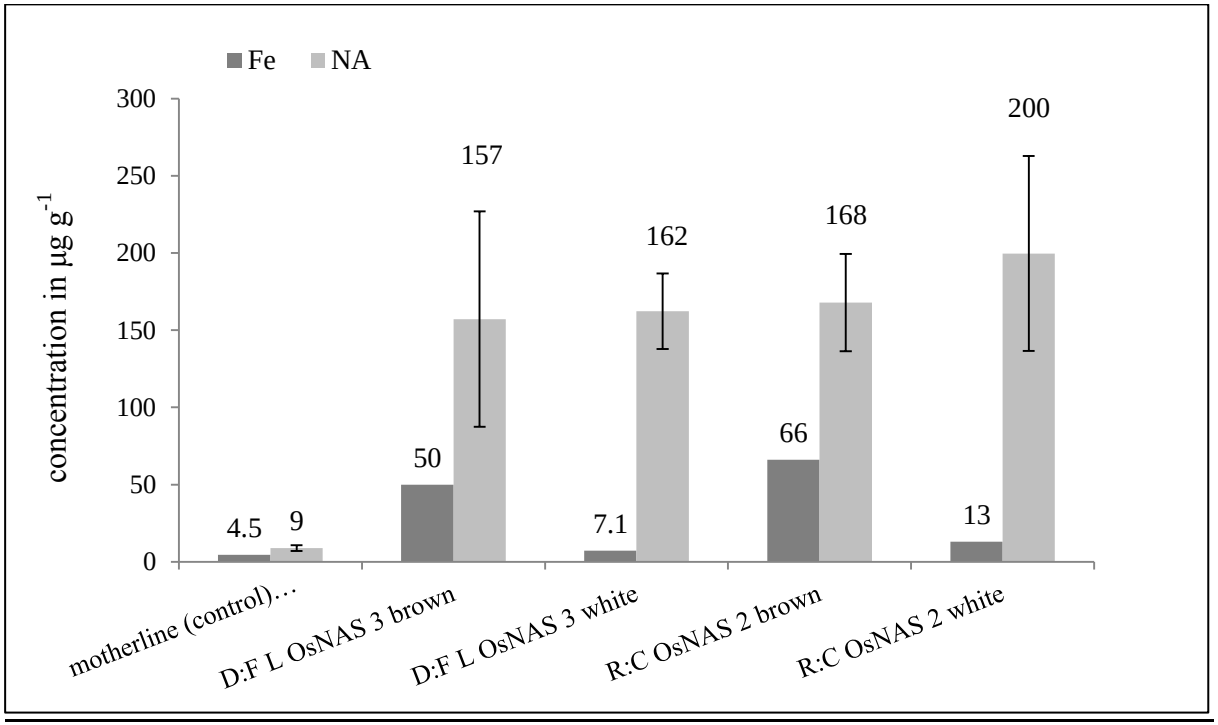

Figure 7: Nicotianamine content in brown and white grains compared to corresponding Fe concentration data.

Grains of control (white grains) and transgenic T0 Developing Flower: Lodicule (DF:L) *OsNAS3* and Root: Cortex (RC) *OsNAS2* were ground in triplicate and used for nicotianamine analysis. Data shown on figure includes Fe concentrations (µg g^{-1}) as determined via ICP-OES (n=1), and nicotianamine levels (µg g^{-1} DW) as determined via LC-MS (n=3). Note ICP-OES not performed in triplicate

2.3.5 Visualisation of Iron deposition via Perl's Prussian Blue Staining

In order to visualise Fe distribution and the increase in Fe concentration in the transgenic T1 rice grains (compared to controls), Perl's Prussion Blue (PPB) stains was used on shaved grain. In the presence of potassium hexanocyanoferrate in an acidic environment, ferric ions are reduced to Fe^{3+} and this creates a blue colour on the surface of the grain (Prom-u-thai et al., 2008). As per Figure 8, controls are brown wildtype grains and the transgenic T1 were a mix of 35S *OsNAS1*, *2* and *3* lines. It is clear that intensity of blue colour increases in transgenic lines when compared to controls. This is expected as there is an increase in Fe concentration from 20 to 64 μg g^{-1} (controls to transgenics respectively). Also, as expected, the majority of the blue stain resides in the embryo, scutellum and aleurone. Interestingly, the two grains at the far right of Figure 8 had two-fold higher Fe concentrations when compared to controls, and yet the depth of blue stain does not seem to be considerably different.

ICP-OES data for white grains shows an increase in Fe concentration compared to wildtype (Table 5B), and yet it was unexpected to find that very little Fe deposition (distinguished with blue staining) was visible in the endosperm of these samples in Figure 8. In Figure 9, blue stains can be seen on the endosperm of a transverse section of a brown transgenic grain. Whilst this appears to represent Fe deposition in the grain, it became apparent that the forceps used to control the grain samples were in fact contributing to the stain and was not indicative of Fe concentration in the grain. Furthermore it was found that grains left to air dry for more than 30 minutes would appear to have more of a blue stain, with distribution evident from aleurone

through to the centre of the grain. It was at this point that PPB was determined to be too subjective as an analytical tool and would not yield quantifiable data and therefore was abandoned as a method.

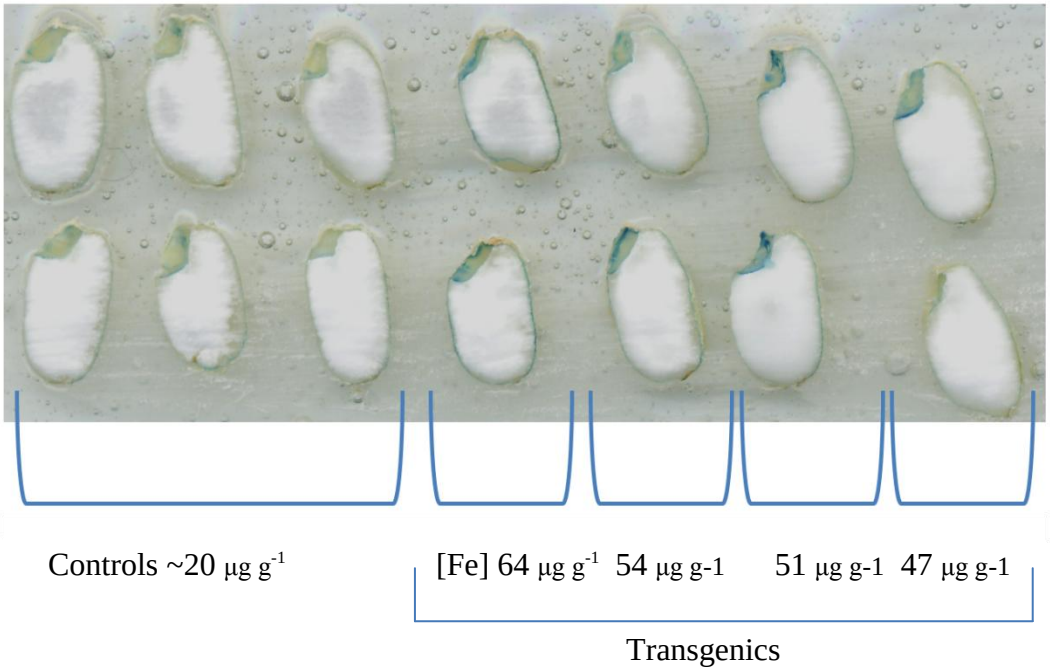

Figure 8: PPB stains demonstrate Fe deposition in aleurone and embryonic tissue of exposed rice grains.

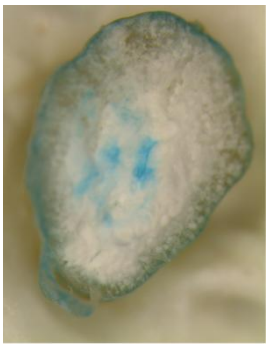

Figure 9: PPB stains presenting false positive information regarding Fe distribution.

2.3.6 Bioavailability

Human colonic cancer cells (Caco-2) were used to model the human intestinal epithelial lining to ascertain whether the transgenic *OsNAS* over-expression lines offers grains with more bioavailable Fe relative to wildtype rice. This study used a small subset of samples to investigate any increase in ferritin production in the mammalian cells directly correlative to the amount of Fe absorbed by the membranous tissue. This dictates whether or not this analysis is viable for this project. A null transgenic line (similar to those used in NA analysis, 35S *OsNAS1* (Johnson et al., 2011)) was used as a control as this represented the low Fe in brown and white grain (27 μg g^{-1} and 4 μg g^{-1} respectively, see Figure 10). All samples were polished in a Kett Mill for 150s and ground in a Retsch mill to a fine powder. Samples were prepared in enzymatic conditions similar to those in the human digestive system prior to introduction to the Caco-2 monolayer system. Figure 10 below illustrates the ICP-OES data for brown and white grains for the null control and three sibling transgenics of the Developing Flower Lodicule (DF: L) *OsNAS3* over-expression line (Fe concentration ranges 45-50 μg g^{-1} brown and 6.5-8.2 μg g^{-1} white grains, see Figure 10).

It is apparent in Figure 10 that the DF: L *OsNAS3* over-expression line has two-fold more Fe in the brown and white grain, compared to the null segregate. ICP-OES data shows 27 μg g^{-1} versus up to 50 μg g^{-1} in brown grain and 4 μg g^{-1} versus 8.2 μg g^{-1} in white grain, in wildtype and transgenics respectively. The exciting information gathered from this analysis is the significant increase in ferritin production (measured

over total protein in the Caco-2 harvests) for the *OsNAS3* transgenics compared to the null control.

There exists an approximate 13-fold increase in ferritin production in the DF:L *OsNAS3* white grains (24-31 ng ferritin / mg protein) compared to the controls (2 ng ferritin / mg protein). This significant increase ($p = 0.002$) is again seen after the addition of ascorbic acid (AA) to the digestion of the rice grains ($p = 0.003$). The molecule AA is a known promoter of Fe bioavailability (Hurrell, 2003) and has significantly increased ferritin production in the control from 2 ng ferritin/mg protein without AA, to 10 ng ferritin/mg protein, after incubation with AA. Furthermore, the ferritin production with DF: L *OsNAS3* white grains increases approximately four-fold with the addition of AA compared to those without. The increased ferritin production of DF:L *OsNAS3* samples compared to controls complements data showing a 18-fold increase in NA accumulation in white transgenic grain compared to null segregant controls (see Figure 7).

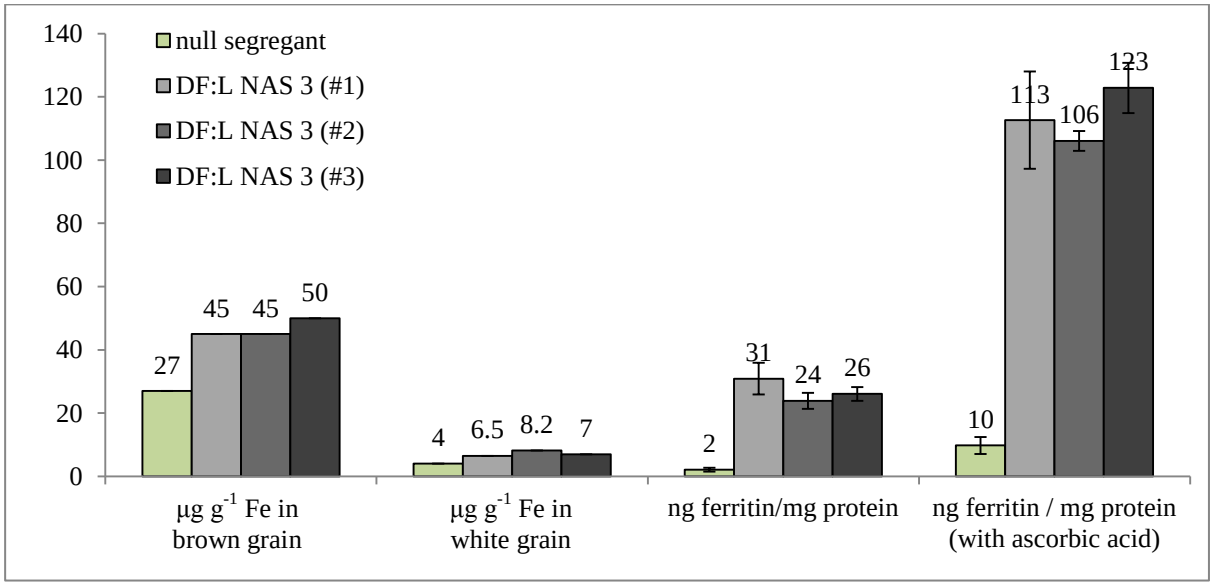

Figure 10: Bioavailability of Fe has been increased in transgenic lines compared to null segregant control as determined by the increase in ferritin production in Caco-2 cell lines.

There is a clear increase in ferritin production as a result of incubating transgenic white rice grains with caco-2 cell lines, compared to white grains of a null segregant. Furthermore, incubation with ascorbic acid (AA) has greater production of ferritin and therefore suggests greater Fe bioavailability to the cells than those without AA.

2.3.7 Expanding progeny to T2 and T3 seed

The results described in this chapter indicated that RC *OsNAS2* and DF:L *OsNAS3* are efficiently loading more bioavailable Fe into the grain as a result of increased NA. However, only a small subset of grain was originally analysed from T1 grain; the sample selection was expanded for genotypic and phenotypic profiling. Cell-type specific over-expression *OsNAS1, 2, 3* lines were selected based on positive GFP expression and/or high Fe (above 45 μg g^{-1}). Table 6 demonstrates the major lines selected for subsequent plantings to generate extended and detailed phenotypic and genotypic information about the progeny. The aim for this stage of the project was to generate T1 plants to obtain genotypic and phenotypic profiling analysis of T2 grain. Plants with a positive *OsNAS* genotype were to be separated from negative genotyped plants to establish a set of transformant controls, as well as wildtype Nipponbare controls. All genotypes were to be grown in triplicate (three siblings per genotype). Tissue specific to *OsNAS* over-expression (ie root cortex) was to be harvested for qPCR analysis to determine expression of *OsNAS* in T1 plants. Plant biomass and grain yield would also be recorded. This information would be compiled with new ICP-OES and NA analysis data to generate an extensive genotypic, molecular and phenotypic profile of the T1 plants, with the aim of growing grain that would be used for expanded Caco-2 analysis for Fe bioavailability.

During grain development, several plants belonging to another researcher, growing in the same glasshouse became infected with *Sarocladium oryzae*, or sheath rot. Whilst efforts were made not to cross contaminate infected plants or related matter with the T1 *OsNAS* plants all transgenic cell-type specific lines did eventually

become infected with the pathogen. Photographs of grain from infected plants can be seen in Figure 11, with brown spotting on husk and blackened poorly filled, sterile grains.

Table 6: Fe concentrations of T1 and T2 rice grains grown in glasshouse conditions, showing decrease in [Fe] between generations. Values represent µg g^{-1}

Plant Genotype		T1		T2	
control		21	n/a	21[a] ± 2.5[b]	(18-24)[c]
root: stele	NAS3	40	n/a	35 ± 9	(24-46)
developing flower: lodicule	NAS2	46 ± 1.4	(45-47)	30 ± 10.8	(21-41)
	NAS3	47± 2.9	(45-50)	39 ± 12.8	(18-47)
root: cortex	NAS1	41 ± 3.5	(38-45)	29 ± 6.4	(22-36)
	NAS2	50 ± 14.2	(41-66)	32 ± 8.2	(23-47)
	NAS3	43 ± 2.1	(42-46)	32 ± 6.5	(21-40)

a = mean, b = standard deviation, c = range of data

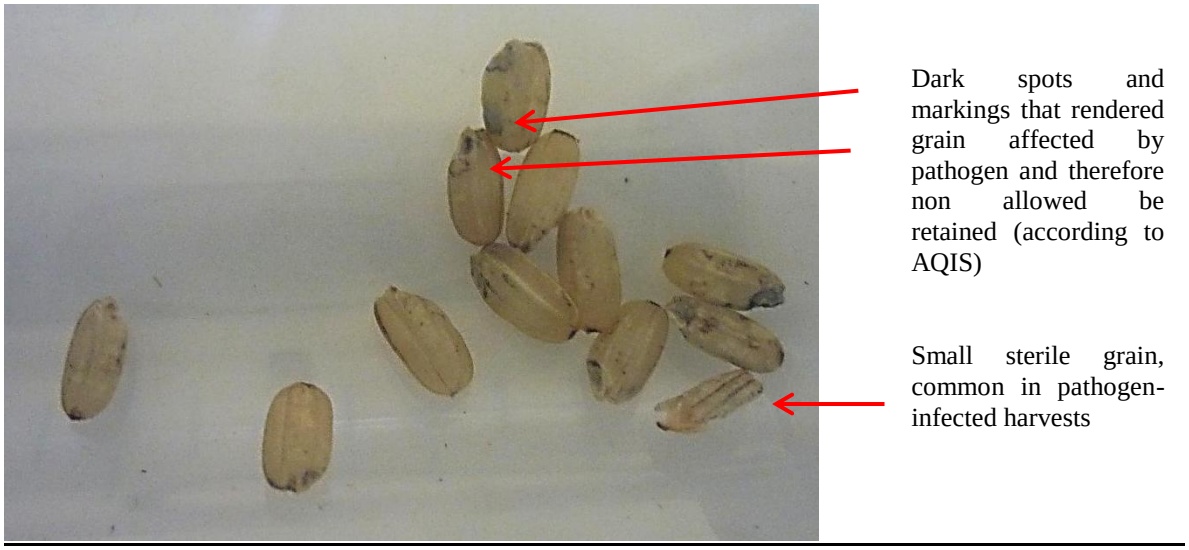

Figure 11: Rice grains from *Sarocladium oryzae* infected T2 plants of cell type specific *OsNAS* transformants

As plants weakened, they became further susceptible to aphid infestation. According to Australian Quarantine Inspection Services (AQIS) all plants growing in the implicated glasshouse were ordered to be destroyed by autoclave treatment, regardless of pathogen infection. Any T2 seed that did not appear to have brown or black marks was collected and permitted to be grown for T2 plants, once the glasshouse reached acceptable improvements outlined by AQIS.

Prior to destruction, T1 plants were genotyped (for the NPTII gene identifying the presence of the selective antibiotic resistance marker used in the second transformation event). Elemental analysis via ICP-OES of T2 brown grain was used, along with genotypic information, to select lines which would be planted for T2 plant and T3 grain analysis (see Table 6). Interestingly, the Fe concentration in T2 grains saw a strong decrease compared to that of the T1 grains.

There appears to be no decrease in Fe concentrations between T1 (21 μg g^{-1}) and T2 (18-24 μg g^{-1}) grains (Table 6) of controls. It could be said that the average Fe concentration for the cell-type specific lines decreased as much as 5 μg g^{-1} in each line (T1 versus T2 grain). However, these lines are still segregating and what is seen here is an increased variance in genotype and sample range. Many samples still produced T2 grain with similar Fe concentrations to T1 grain, for example DF:L *OsNAS3* (50 μg g^{-1} T1 and 47 μg g^{-1} T2). The greatest decrease is noted in the RC *OsNAS2* line. This standout line in T1 with 66 μg g^{-1} Fe has only reached a maximum of 47 μg g^{-1} Fe in T2 grain. Without Southern analysis, it is not possible to determine if T1 grain is from a plant with single *OsNAS2* transgene inserts. T2 grain may have then come from a segregating line and may therefore have positive

OsNAS2 over-expression but reduced expression levels compared to a multiple copy number progenitor in T1. Thus there may be reduced NA and therefore reduced Fe loading in the grain. It is without doubt that future analysis will require genotypic studies including Southern analysis and q-PCR to confirm the presence of copy number and activity of the transgene.

The decrease in Fe accumulation in T2 grain may also be attributed to the parasitic nature of the *Sarocladium oryzae* pathogen. Furthermore the plants were additionally stressed by the presence of aphids during grain filling. This may explain the loss of nutrients. This concern led to the decision to plant T2 grain and use T2 plants and T3 grain to generate the desired profiling data. T2 grain was then planted with the intention of 'cleaning' the grain and removing the possibility of any pathogen-related phenotypes to affect this research.

2.4 Discussion

2.4.1 Over-expression of *OsNAS2* is the most efficient genotype in regards to increased NA and Fe loading in rice grains.

This proof-of-concept project was designed to develop Fe enhanced rice to prevent human micronutrient deficiencies, such as Fe anaemia, by directly targeting the human diet. The preliminary data established in this project have shown that over-expression of *OsNAS2* is a clear candidate for further research. Twice transformed constitutive over-expression of *OsNAS2* produced the highest Fe accumulating grain compared with 35S *OsNAS3* and *1*. A single 35S *OsNAS2* sibling line peaked at 81 μg g^{-1} and 19 μg g^{-1} Fe in brown and white grain, respectively. This is in agreement with extensive investigations of 35S *OsNAS* over-expression in rice, where it was again seen that the constitutive 35S over-expression of *OsNAS2* produced up to 19 μg g^{-1} Fe in white grain (Johnson et al., 2011).

2.4.2 Root cortex-driven over-expression of *OsNAS2* is the most efficient cell-type specific Fe and NA accumulator in rice grains.

The development of the original *OsNAS* lines was undertaken to identify the strongest change in iron loading in response to over-expression in various tissues. This variation was important as it is known that the three *OsNAS* genes are spatially controlled within the plant. The exact location of expression within these lines was yet to be determined and thus formed a major focus of this work. The variation in expression sites was randomly controlled by the GAL4/GFP insert controlling the *OsNAS* over-expression. In what can be considered a reverse genetics approach, we

were able to identify cell-type specific over-expression of *OsNAS* patterns that enhanced iron loading in the rice grain.

With a 2.3-fold increase of Fe in the endosperm of the grain, compared to non-transformed rice, RC *OsNAS2* dominated the positive trends seen in ICP-OES data for Fe and Zn. The majority of samples analysed within this genotype produced grain with Fe concentrations similar to the constitutive 35S expression of *OsNAS1*, *2* or *3*. The 13 μg g^{-1} Fe seen in the white grains of the RC *OsNAS2* line is a positive result for cell-type specific over-expression. Importantly, the targeted Fe concentration in the endosperm (14.5 μg g^{-1}) (Hotz and McClafferty, 2007) has almost been reached, making this line a true candidate for the generation of biofortified rice to reduce human micronutrient deficiencies.

The over-expression of the *OsNAS2* gene has also led to the grain having the highest level of NA present in brown and white grains (Figure 7) compared to *OsNAS3* expressed in developing flower tissue and wildtype samples. The NA concentration calculated for control brown grain was 32-45 μg.g^{-1} DW. This data agrees with recently published work by Johnson et al. (2011) where similar concentrations were detected in brown rice from non-transformed plants. Additionally, it can be said that the NA concentrations found in constitutive over-expression of *OsNAS2* and *3* brown grains (as published by Johnson et al., 2011) are similar to those found in cell type specific grain of this project.

It is known that NA-bound Fe complexes have been found in the phloem of rice plants (von Wiren et al., 1999). A possible mode of transport may involve the dissociation of the NA:Fe complex allowing free Fe^{2+} to enter the grain via the

embryo. An accumulation of Fe in the embryo and endosperm may also trigger the production of NA. Production of NA and DMA was identified by Nozoye et al. (2007) in both embryo and endosperm. This suggests the increased concentration of Fe entering the grain may be triggering the conversion of SAM to NA to stabilise Fe levels, thus providing more S-containing molecules into the grain, as seen in the RC *OsNAS2* line. Additionally, there is the possibility that there is an increased deposition of Fe in ferritin bodies, therefore accounting for increased S, a marker for protein bodies (Levi-Setti, 1988).

From this work it is clear that root cortex driven over-expression of *OsNAS2* enhances Fe and NA in both brown and white grain. It is not clear however, why the root cortex driven *OsNAS2* over-expression is a more efficient Fe accumulating genotype than *OsNAS1*, considering the two genes share 87% homology. Cheng et al. (2007) has previously described the endogenous levels of *OsNAS2* expression in rice roots during Fe sufficiency is up regulated when the plant is Fe deficient. Additionally *OsNAS2* is activated in shoots during Fe deficiency, converse to Fe sufficient conditions (see Figure 1). Based on this information and the preliminary findings in this project, it is believed that root-driven *OsNAS2* over-expression triggers a 'pseudo-Fe deficient' stress response in the plant, eliciting the production of rhizospheric PS secretion and increased Fe uptake (see Figure 12 below).

Several reports have suggested the action of NA to be involved in sensing Fe levels within the plant (Bereczky et al., 2003, Douchkov et al., 2005, Le Jean et al., 2005, Mari et al., 2006) From this understanding, the results in this study suggest that the elevated Fe entering the roots causes the plant to signal NA production in attempt to maintain homeostasis, as seen in Fe deficient graminaceous plants (Higuchi et al.,

1995, Pich et al., 1997). Therefore, the plant up-regulates endogenous *OsNAS2* expression in shoots, producing more NA to transport the newly acquired Fe across the plant. Additionally, more Fe entering the grain may elicit a greater production of NA in the endosperm. This hypothesis is supported by the NA quantification data for the RC *OsNAS2* line where both brown and white grains show higher NA concentration than the DF:L and wildtype samples (Figure 7), and where Fe accumulation is highest in the RC *OsNAS2* line, compared to other transgenics and controls.

Again this data suggests *OsNAS2* is the most efficient gene target for Fe accumulation, but also promotes the hypothesis that cell-type specific expression is a more efficient and direct approach to biofortifying rice grains. This finding strongly supports the hypothesis that a cell-type specific over-expression of *OsNAS* will lead to increased Fe loading into the endosperm.

Figure 12: Proposed Schematic of the triggering of false state of Fe deficiency in rice due to OsNAS2 over-expression in root cortex.

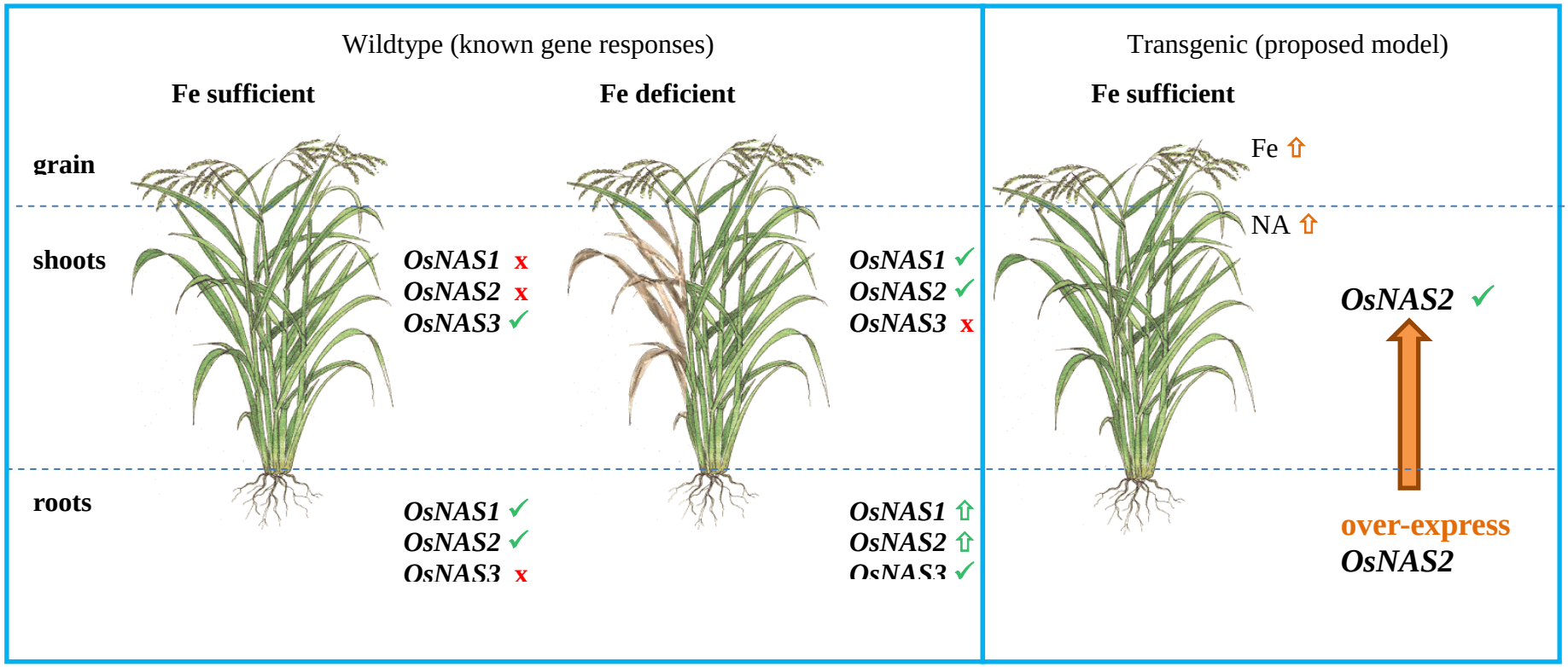

2.4.3 Developing Flower : Lodicule –driven over-expression of *OsNAS3* produced a strong bioavailable Fe accumulator as demonstrated by Caco-2 studies.

Similar to the transgenic RC *OsNAS2* rice line, the over-expression of *OsNAS3* under the control of native lodicule promoters active in developing flowers (DF:L) proved to be a strong Fe accumulator in both brown and white rice grains. A single sibling reached 50 μg g^{-1} Fe in brown grain and 8 μg g^{-1} Fe in white grains. Additionally, the NA concentration in both brown and white grains greatly exceeded that of the control line. Again like RC *OsNAS2*, DF: L *OsNAS3* appeared to have more NA in the white grains than brown, suggesting NA resides predominately in the endosperm of the rice grain.

There is strong evidence to suggest this positive trend in Fe and Zn accumulation in the transgenic grains is a result of increased production of the metal chelator and transporter, NA, due to the over-expression of the three *OsNAS* genes. Johnson et al. (2011) demonstrated that constitutive over-expression of the three *OsNAS* genes significantly increased the Fe and Zn concentrations in the rice endosperm compared to wildtype rice. Furthermore, the increase in NA was substantially higher in transgenic brown and white rice grains compared to wildtype. The strong correlation that Johnson and colleagues found, between NA and Fe or Zn accumulation in the grain is also seen in the findings of this project where the over-expression of *OsNAS2* under the control of root cortex and developing flower (lodicule) promoters has elicited a strong increase in NA compared to the null segregant control.

The substantial increases in Fe and NA in the transgenic rice grains were detected easily in brown and white grain using ICP-OES and LC-MS respectively, however the visualisation of the Fe distribution in the grain proved difficult. Perl's Prussian Blue Stain (PPB) is still commonly used to demonstrate Fe localisation in rice grains and combinations of diaminobenzidine (DAB) and PPB stains has recently been used to identify distribution of both ferric and ferrous ions (Roschzttardtz et al., 2010). However, in this project it was determined that PPB alone was too subjective, and dependant on personal interpretation. Whilst (Choi et al., 2007) had developed semi-qualitative methods to measure Fe, it was found to be non-quantifiable and therefore PPB was rejected as a means to visually compare increased Fe loading in the transgenic rice grains compared to wildtype.

Bioavailability of Fe in the transgenic rice grains was determined using the Caco-2 model system. These human colon carcinoma cell lines undergo spontaneous differentiation in cell culture to form a polarized epithelial cell monolayer with many characteristics of enterocytes, thus mimicking the human digestive system. The introduction of foods like rice, allows any free nutrients to permeate through the cell membrane. In the case of Fe, any free ions (bioavailable Fe) pass through the membrane, resulting in ferritin production which is directly proportional to the amount of Fe uptake by the Caco-2 cell monolayer (Glahn et al., 1996). The presence of milled rice flour from DF:L *OsNAS*3 lines has demonstrated a 13-fold increase in ferritin production compared to controls with an additional 12-fold increase with the addition of AA. These are extremely promising results in regards to the generation of rice that has been enhanced with bioavailable Fe and NA as a result of the cell-type specific over-expression of *OsNAS3*, further supporting the hypothesis that the cell

type specific expression of *OsNAS* will result in a rice product potentially purposed as a tool to reduce human micronutrient deficiencies.

Conclusions drawn in this chapter raise several interesting questions. Chapter Three pursues the localisation of the abundant Fe to determine whether the Fe is indeed endosperm distributed. Synchrotron radiation is utilised to visualise the elemental fingerprint within the grain. Synchrotron radiation is also employed to investigate the Fe speciation to compliment the important bioavailable data available for these transgenic lines. It is accepted that NA chelates several divalent metals other than Fe, therefore Chapter Four assays the effects of heavy metal accumulation within this transgenic lines. And finally, Chapter Five questions whether it is possible to exploit the role of NAS in Fe accumulation and drag this Fe further into the endosperm by increasing the source/sink relationship.

Chapter Three: Multi-spectroscopic investigation of Fe and Zn distribution and speciation in rice grains

3.1 Introduction

3.1.1 Fe accumulation in the seed

Polished rice is the second most consumed cereal in the world after wheat (Hseu et al., 2010) and is a major source of nutrition for many of the world's poor. In the future, rice may be used as a major vehicle to supply more micronutrients through biofortification strategies. For Zn biofortification, it is likely that sufficient genotypic variation exists for a conventional plant breeding strategy, while for Fe, the lack of significant genotypic variation amongst commercial varieties may require a transgenic approach to enhancing Fe nutrition in human diets. Furthermore, due to the demand for polished rice, the distribution of Fe is an important consideration. Iron in rice grain is typically concentrated in the embryonic scutellum and aleurone layers (Wada and Lott 1997), which are removed during the polishing process and results in a loss of approximately 75-80% of total Fe (Briat et al., 1995, Hansen et al., 2012).

Biofortification of Fe in rice has resulted in an increased Fe uptake in women (Haas et al., 2005) however Hotz and McClafferty (2007) argue that greater quantities of Fe are required within the endosperm to ensure a significant biological impact. To obtain the desired 14.5 μg g^{-1} Fe in rice endosperm proposed by Hotz and McClafferty (2007), and supported by HarvestPlus, it is imperative that measures are taken to truly appreciate where Fe is distributed across the whole grain. Additionally, with highly specific analyses, we may identify molecules that bind to Fe within the

grain. This could provide information for the breeding or engineering of new cereal crops with higher concentrations of these molecules in the grain. This chapter investigates the distribution and speciation of Fe across the rice grain to complement the research discussed in Chapter Two. The development of transgenic rice overexpressing *OsNAS* genes has resulted in a significant increase in bioavailable Fe in the endosperm. It is believed that the investigation of the elemental speciation of Fe in the grain may help us have a greater understanding of the bioavailable nature of the Fe present in the grain.

3.1.2 Analytical tools in Fe characterisation in rice

Staining

Histochemical analyses such as Perl's Prussian blue stain (PPB) and diaminobenzidine (DAB) are commonly used to investigate *in situ* elemental localisation in rice grains. Free ions on the surface of the sample hybridise to immunochemical, colorimetric or fluorescent probes emitting quantifiable chemical signals, allowing visualisation of elemental deposition (Choi et al., 2007, Ozturk et al., 2006, Prom-U-Thai et al., 2003). Due to the specificity and oxidative or reductive nature of PPB and DAB, only one species of the element can be identified (Fe^{3+} and Fe^{2+} respectively). Only recently did Roschzttardtz et al. (2009), (2010) show simultaneous staining of ferrous and ferric ions *in situ* in *Arabidopsis* leaves using a combination of the PPB and DAB stains. Whilst this enhances the value of histochemical techniques, the stains are still limited by the fact that only ions free to interact with the chemical agents will be visualised. Only ions strongly chelated to

the chemical agent will be accounted for, therefore those bound in strong endogenous complexes such as Fe bound to phytate would not be identified. This makes these techniques qualitative and subjective. Furthermore semi-quantitative colourimetric stains fail to differentiate cellular specificity, leading to an incomplete understanding of Fe distribution.

Microscopy

Electron microscopic techniques such as transmission and scanning electron microscopy (TEM and SEM, respectively) have been important tools for imaging of rice grain ultrastructures (Bechtel and Juliano, 1980, Bechtel and Pomeranz, 1977, Harris and Juliano, 1977, Tanaka et al., 1973). These methods provide detailed images of the grain surface but are unable to determine molecular or element specific data in their own right. However, these techniques can be complemented with elemental analysis systems such as energy dispersive X-ray microanalysis (EDX) to further investigate elements of interest within the sample (Ockenden et al., 2004). However, SEM/TEM-EDX techniques are limited by relatively high detection limits (Lombi et al., 2011) which preclude the possibility to obtain detailed micronutrient distribution maps.

Synchrotron X-ray fluorescence

Synchrotron radiation in recent years has provided researchers with extremely sensitive detection limits for elemental profiling and can be used to obtain detailed elemental and speciation maps, *in situ*, of even greater sensitivity than particle induced x-ray emission (PIXE) (Meharg et al., 2008). Synchrotron X-ray

fluorescence microscopy (SXRF) is a particularly useful tool which detects fluorescence emissions from atoms that have been excited with ionising energies from a synchrotron photon beam to generate an elemental map. SXRF can detect transition metals at sub μg g^{-1} limits with lateral resolution of 100 nm (Johnson et al., 2011, Punshon et al., 2009). Relative metal concentrations can be determined using the fluorescence data obtained from SXRF, but this is not a trivial exercise as sample thickness and availability of appropriate standards are essential (Punshon et al., 2009). Mapping Fe location in rice endosperm is best achieved with multiple spectroscopic *in-situ* techniques. Combinations of synchrotron radiation such as XRF and x-ray absorption near edge spectroscopy (XANES) spectra have successfully imaged Se distribution in *Astralagus bisulcatus* (Pickering et al., 2003). Whilst highly specific, spatial resolution of images generated with synchrotron technologies depends on surface volume of the sample. Analysis is generally specific to the first atomic monolayer of the grain surface and spectra generated are fast proving synchrotron radiation to be the best for fine mapping of grain.

SIMS

High resolution nanosecondary ion mass spectrometry (nano-SIMS) is emerging as an important technique for the localisation of trace elements in biological samples at cellular and subcellular scales. The NanoSIMS 50 (CAMECA, France) is a recent development in SIMS instrumentation and has been designed specifically for simultaneous high lateral resolution, mass resolution and sensitivity analysis and can detect five ions from the same sputtered volume (sputtered volume referring to the atoms removed from the samples surface by the bombardment of high energy atoms

thus allowing ionic spectroscopy). The SIMS technique also offers many other advantages such as molecular imaging, detection of all elements and isotopes and three-dimensional imaging is also possible. Three-dimensional imaging is a destructive application and may not be desirable in all circumstances (future analysis, repeat analysis etc). Recent examples of biological Nano-SIMS analysis include localisation of As and Se in cereal grains (Moore et al., 2010), high-resolution imaging of nickel (Ni) distribution in leaf tissue of the Ni hyperaccumulator *Alyssum lesbiacum* (Smart et al., 2010), in situ mapping of nitrogen uptake in the rhizosphere (Clode et al., 2009) and localisation of As and Si in rice roots (Moore et al., 2011). Additionally, Moore et al. (2011) successfully teamed synchrotron radiation analysis with nanoSIMS technology to investigate the As distribution in rice, confirming the need for multi-spectroscopic analysis of Fe distribution and speciation in the grain.

3.1.3 Multi-spectroscopic analysis of transgenic rice

Like so many scientific investigations, often the best analysis and characterisation of matter is derived from a collective of analytical operations and applications. It is surprising then to see very little multi-spectroscopic techniques used to fine map the Fe distribution and speciation across the interior of the rice grain. This project combines synchrotron radiation and SIMS technologies to elucidate the Fe nature in rice, including an investigation of transgenic cell type specific *OsNAS2* grains, as discussed in Chapter Two of this thesis. It is believed that we will generate extremely fine detailed maps of the grain surface and further characterise Fe chelators in wildtype and transgenic grain.

3.2 Materials and methods

In this thesis the term brown grains/ rice is synonymous with unpolished grains/ rice (palea and lemma of husk removed (threshed). The term white grains/ rice have been milled to remove the outer layers and therefore synonymous with polished grains/ rice.

3.2.1 Plant material generation

Oryza sativa ssp. Japonica cv Nipponbare grains were harvested from greenhouse-grown plants in 12 day light hours, 28/24 ºC day/night temperature, 70% humidity. Temperatures were controlled within 10 ºC of the outside environment and as plants were grown in the summer months, no additional supplementary lighting was required. Cultivated in a mixture of UC Davis soil (Hoagland and Arnon, 1950), plants were fertilised weekly with Manutec Acidic Plant Food according to manufacturer's instructions. Grain development was recorded two and a half months post planting. Plants were left to reach maturity for a further three months. After harvest, the grains were dried in a 37 ºC oven for 3 days.

All details pertaining to development of the transgenic cell type specific line RC *OsNAS2*, including genotypic and phenotypic analysis is available in Chapter Two of this thesis. Elemental composition of brown and polished grains is also explained, along with PPB results.

3.2.2 Grain milling

Using modified commercial bench-top miller (Kett Electrical Laboratory, Tokyo, Japan), 50 brown non-transgenic *Oryza sativa ssp. Japonica cv. Nipponbare* seeds grains were milled for 150 seconds according to published milling conditions. Note that the Kett Mill had previously been modified to prevent metal contamination of the grain (Stangoulis, 2010).

3.2.3 Elemental composition of grains

For determination of total elemental concentrations in grains, 75 grains (25 brown grains and 50 polished grains were analysed for elemental composition by inductively coupled plasma optical emission spectroscopy (ICP-OES) (Wheal et al., 2011).

3.2.4 Synchrotron radiation analysis- SXRF

For SXRF analysis, brown grains were prepared following the method described by Lombi et al. (2009). Briefly, grains were first glued to a plastic platform "dorsal side down" and 60 µm ventral longitudinal sections were then prepared using a Leica 1200 Vibratome, so that each section of approximately 5.5 x 2.2 mm contained both the embryo and endosperm. Sections were mounted on plastic windows with Kapton tape which were then mounted onto a motorized sample stage at the x-ray fluorescence microprobe (XFM) beamline at the Australian Synchrotron. Synchrotron XRF maps were collected using a 7.5 keV beam using either a 96-element prototype Maia detector (for whole grain imaging) or a Vortex detector (to

collect S and P maps). Whole grain maps were generated by scanning the samples on the fly in the horizontal direction at a speed of 2 mm.s^{-1}, which translated in a transit time of approximately 0.6 ms.$pixel^{-1}$ (2 µm). Full fluorescence spectra were collected and analysed using GeoPIXE software (Ryan, 2000, Ryan and Jamieson, 1993). The whole grain maps obtained using the Maia detector (with area of 160 x 40 µm at 2 µm lateral resolution) were mapped from the exterior of the aleurone layer, progressing into the grain, using a Vortex detector and a dwell time of 1 s.$pixel^{-1}$. This enabled collection of elemental maps for P and S as the Maia detector is unable to analyse elements lighter than potassium (K). The fluorescence spectra obtained using the Vortex detector were refined using the MAPS package (Vogt, 2003).

3.2.5 Synchrotron radiation analysis - SXANES

For SXANES, 75 grains were randomly selected, dehulled and polished as explained above. Seed aleurone and pericarp (bran) was collected and the milled grains (representing endosperm) were then ground in a mortar and pestle and then further ground in a Fritcsh mill for 10 s to gain a homogenous fine powder. Powder samples of bran or endosperm were then mounted onto Kapton tape-covered plastic windows, plunged in liquid nitrogen and then mounted into a cryostat sample holder operating at approximately 15 K at the XAS beamline at the Australian Synchrotron. Spectra from SXANES analysis were collected in fluorescence mode using a 100-element solid state Ge detector. The beam size was adjusted to ca. 1.2 x 0.7 mm. Five replicate SXANES spectra were collected (from different areas of the samples), at the Fe K-edge (7112 eV). A Fe metal foil spectrum was collected congruently with each sample scan in transmission mode. Standards of 2 mM NA: Fe^{3+}, NA: Fe^{2+},

phytate: Fe^{3+} and phytate: Fe^{2+} were prepared as liquid in degassed high purity water (prepared by reverse osmosis) and 30% glycerol. Samples of 4 mM $FeNO_3$ and 4 mM $FeCl_2$ were used to prepare the NA standards, with solutions adjusted to pH 5.5.

3.2.6 NanoSIMS analysis

Rice grains were desiccated in a vacuum of approximately 10^{-2} mbar for 1 week to remove any moisture absorbed during seed storage and prevent seed shrinkage in the ultra-high vacuum of the NanoSIMS. Whole grains were then mounted in London Resin (LR) White (London Resin Company, Basingstoke, UK) in 10 mm steel rings which fit into the NanoSIMS holders. The LR White did not penetrate the grain; it was simply used to mount the rice grain in the ring. The rice grain was positioned so that it could be transversely sectioned with half of the grain left protruding from the top of the ring. The grain was sectioned using a zirconia ceramic knife to create a flat surface for analysis and ensure the grain was level with the top of the holder. As Fe was the element of interest in this study, a razor blade was not used as this may result in Fe contamination on the surface, and care was taken to ensure the steel ring was not scratched during cutting, which could have also caused contamination. Flat regions of the grain were identified by conventional light microscopy before the whole sample was coated with 10 nm platinum to prevent charging during SIMS analysis.

3.2.7 NanoSIMS Analytical Methods

A CAMECA NanoSIMS 50 (CAMECA, France) was used to perform high-resolution SIMS analysis. Flat areas of the grain identified with light microscopy

were first selected using the optical camera on the NanoSIMS and then regions of interest were chosen more precisely using the secondary electron (SE) image which is generated by scanning the primary ion beam. A finely focused 16 keV Cs^+ primary ion beam with a current of 2 – 2.5 pA was raster scanned over the surface of the sample and the negative secondary ions were collected and analysed using a double focusing mass spectrometer. As a compromise between good lateral resolution and sensitivity, the primary aperture was inserted (D1=2) which gave a lateral resolution of around 100 nm yet still maintained sufficient sensitivity to detect the low concentration of Fe. Images were acquired with a dwell time of 60 ms at a resolution of 256 x 256 pixels taking approximately 1 h per image. To improve the counts of $^{56}Fe^{16}O^-$, several sequential images from the same area were acquired, corrected for drift using ImageJ (Harvard) and summed. There are two sources on the NanoSIMS, O^- and Cs^+ however the highest lateral resolution can be obtained using the Cs^+ beam, meaning that Fe was detected as the $^{56}Fe^{16}O^-$ ion. As the bulk concentration of Fe in these samples was low, it was important to carefully tune the spectrometer on an appropriate standard to avoid potential mass interferences. High resolution mass spectra around m/z = 72 were acquired from a polished steel sample and compared with the mass spectra from the sample to ensure the correct positioning for $^{56}Fe^{16}O^-$. NanoSIMS maps are presented in an arbitrary linear colour scale (unless specified), with red and yellow regions indicating higher concentration and blue and black indicating lower concentration.

3.3 Results

3.3.2 Elemental composition and distribution: SXRF

In order to determine the distribution of micronutrients in the rice grain, unpolished, brown rice grains were cut in ventral longitudinal sections to expose each significant tissue across the grain (Figure 1A). Synchrotron XRF data were converted to three dimensional elemental maps which are reported in Figure 1B-E. The distribution of Zn in Figure 1B illustrates this element is abundant in the endosperm and confirms the results reported in Table 1 of Chapter Two and previous work reported by Lombi et al. (2009). An enlargement of an area of the whole grain map (Figure 1C) illustrate that Mn accumulates in the outermost part of the grain, more so than Fe and Zn. There is a co-localisation of both Mn and Fe (yellow in Figure 1C), and extending into the endosperm, Fe appears to dominate the signal. As expected both Zn and Fe are abundant in the scutellum.

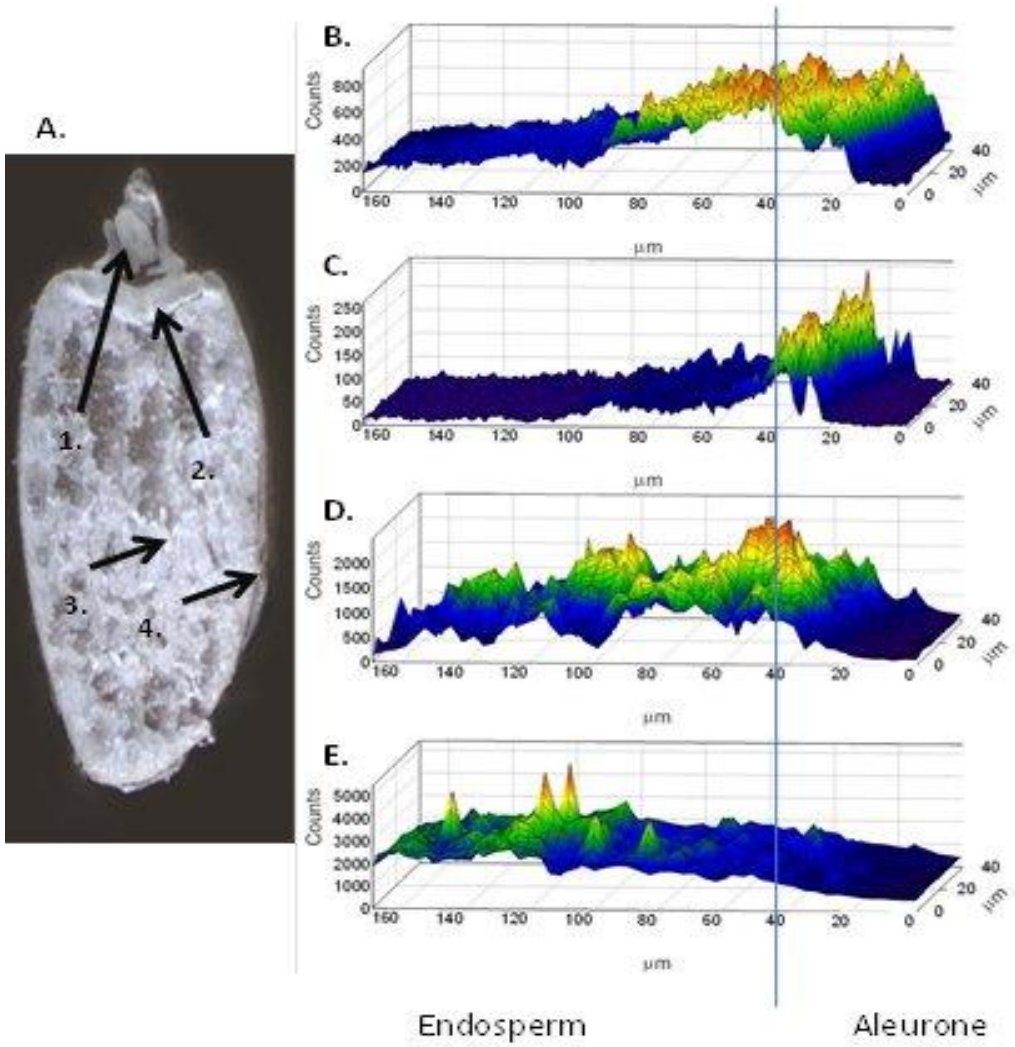
A.
1.
2.
3.
4.
B.
C.
D.
E.
Counts
µm
Endosperm
Aleurone

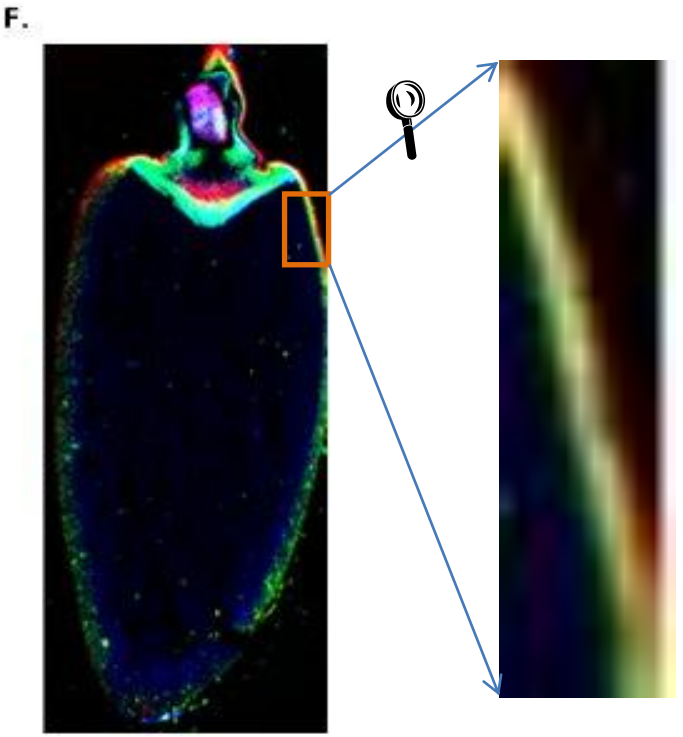
F.

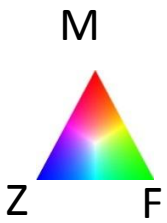
G.
M
Z
F

<u>Figure 1:</u> SXRF elemental map of *Oryza sativa* ssp. *Japonica cv.* Nipponbare brown rice grain.

Light microscopy image of ventral longitudinal sections of brown grain (A). Numbers indicating the location of embryo (1), scutellum (2) endosperm (3) and outer edge of grain (4). Outer edge (4) also indicates 100 μm region spanning aleurone outer edge to endosperm, from which 3D 100 μm line scans in B-F were collected using the Vortex detector; (B): Mn, (C): P, (D): Fe, (E): Zn. (F) is the 3-colour (red, green and blue) multielement comoposite image of Mn, Fe and Zn generated using the Maia detector, (G) elemental colour intensity.

Elemental maps, or spectra, collected on a small area on the margin of the grain with the Vortex detector, allows for a comparison of metal distribution in conjunction with P localisation (Figure 1B-E). Manganese distribution clearly also extends into the aleurone and sub-aleurone region (Figure 1B), which is supported in the literature (Tanaka et al., 1973). The aleurone layer can be clearly identified with the narrow distribution of P over an area of approximately 20 μm (between 20 and 40 μm in Figure 1C) which is consistent with published results and possibly indicative of phytate globoids (Tanaka et al., 1973).

It is evident from Figures 1C and 1D that Fe is partially co-localised with P in the external part of the grain. However, Fe also appears to penetrate further into the grain and is localised in the sub-aleurone layer of the endosperm. In fact, Fe is localised further into the grain than Mn by approximately 50 μm, as seen in the line scans in Figure 1B and D, respectively. This distribution if confirmed with the whole grain maps collected with the Maia detector (Figures 1F and 1G). This confirms the suggestion that while Fe is present in high concentrations in the aleurone, it is not limited to this region and does indeed extend into the sub-aleurone region (Johnson et al., 2011).

3.3.3 Elemental speciation: SXANES

The data collated from SXRF (Figure 1) clearly demonstrate the localisation of P and Fe are not limited to the aleurone and both extend into the endosperm. However, whilst the localisation of these elements is useful, this does not extend our knowledge regarding metal speciation and chelators which is particularly useful

when attempting to determine the bioavailability of Fe and elucidate the metal transport into the grain. In order to garner more information on these points, SXANES was utilised. Grain bran and flour is compared to phytate and nicotianamine standards to determine how the Fe is chelated within the various regions of the grain. The resulting SXANES energy fingerprints are illustrated in Fig 2. In each of these figures it is evident there is a different energy pattern when comparing bran and flour.

Synchrotron XANES technology was used to elucidate any relationship between Fe and P and the presence of potential Fe and phytate complexes. The 'fingerprints' generated from SXANES for bran and flour, as per Figures 2A and 2B, show very different energy patterns with flour presenting a lower energy compared to bran, with an initial rise at 7120 eV. Bran also presented two noticeable peaks at 7128 and 7135 eV, both of which are not evident in flour scan. When comparing the flour with standard spectra it is clear that flour is closely matched with Fe^{2+} bound phytate. There is no doubt that the bran and Fe^{3+} bound phytate have extremely similar energy values, but with relatively similar patterns to Fe^{2+}:phytate, it can be defined that the majority of bran is comprised of ferric and not ferrous bound phytate.

In Figure 2B the most striking similarity lies within the SXANES spectra for flour compared to NA:Fe^{3+}. The energy for NA:Fe^{2+} is quite dissimilar to those of flour and bran. Additionally NA: Fe^{3+} bears no resemblance to the energy of bran. This clearly suggests the majority of NA in flour is bound to Fe^{3+}. It is also important to note that the Goodness fit chi-squared values show a stronger relationship of Fe^{3+} bound to phytate than when bound to NA in bran (84% and 16% respectively).

Conversely, the detection of Fe^{3+} bound to NA is much stronger than when bound to phytate in flour (77% and 27% respectively). From SXANES analysis of bran and flour it can be summarily suggested that Fe^{3+} is the dominant species of Fe in the grain, being bound to phytate in bran and NA in flour.

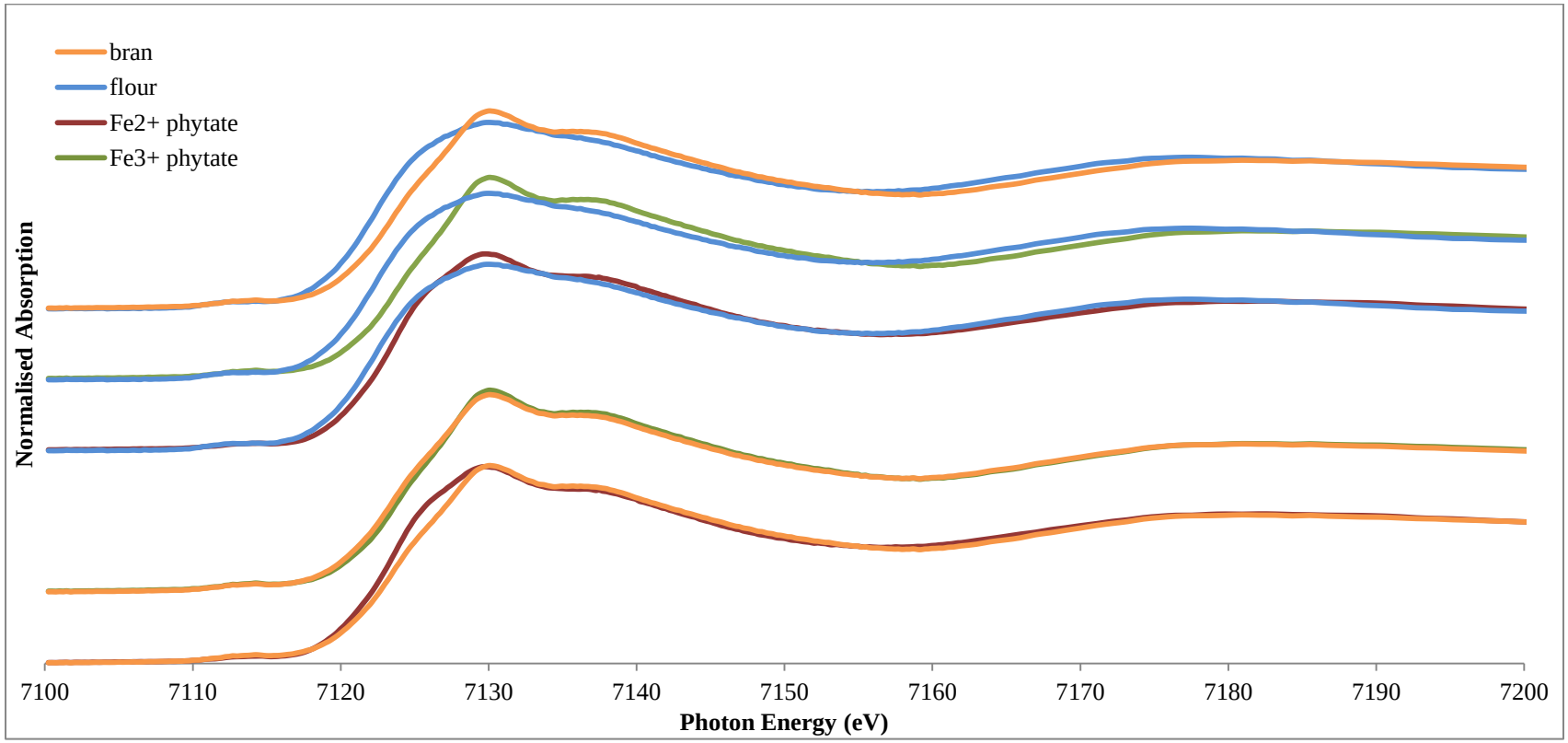

Figure 2A: SXANES of ligand-bound Fe species in flour or bran of *Oryza sativa ssp. Japonica cv.* Nipponbare compared to phytate bound Fe.

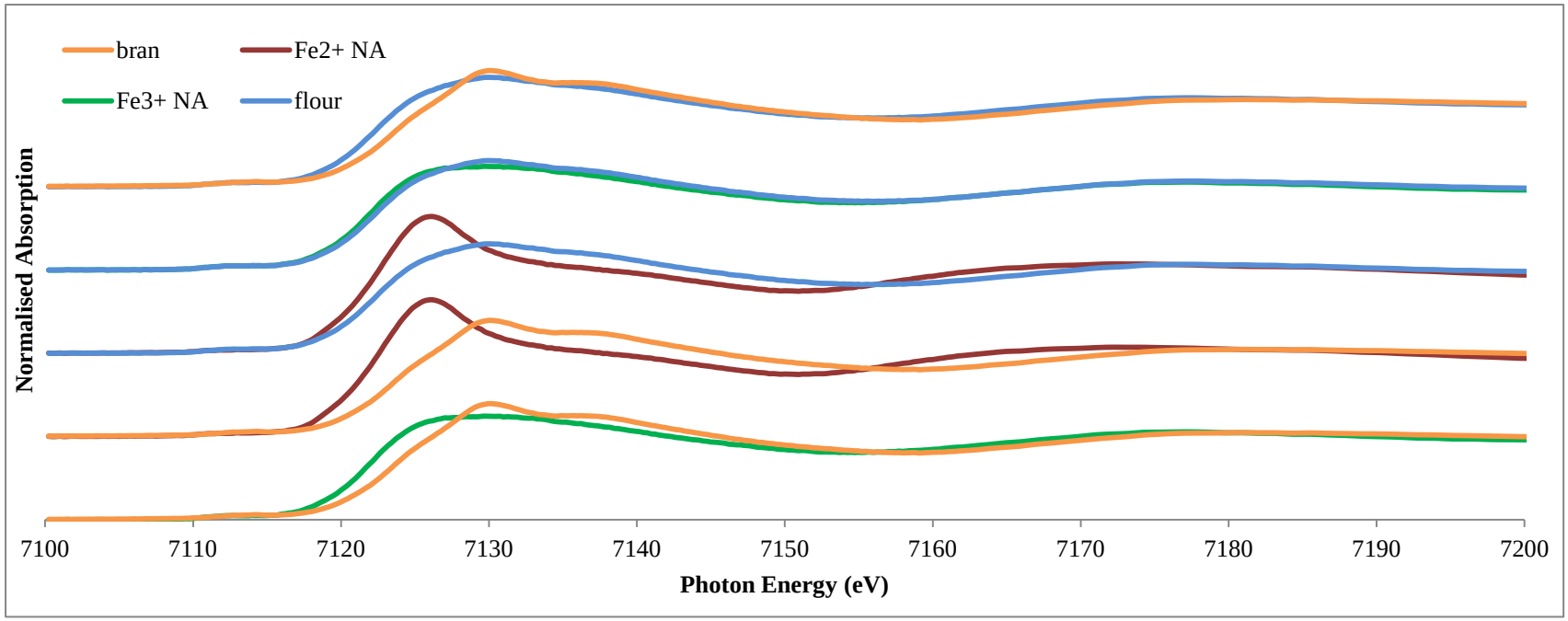

Figure 2B: SXANES of ligand-bound Fe species in flour or bran of *Oryza sativa ssp. Japonica cv.* Nipponbare compared to NA bound Fe.

3.3.4 Elemental chelation: nanoSIMs

Presented in Figure 3 are NanoSIMS ion maps of the outside edge of a transversely sectioned rice grain showing three aleurone cells at the top and the sub-aleurone region towards the bottom of the image. The $^{12}C^{14}N^-$ image is commonly used in biological SIMS analysis as a marker for proteins (Levi-Setti, 1988), along with the $^{32}S^-$ image indicates the location of the proteins. There is a much higher concentration of protein in the protein matrix of the sub-aleurone region surrounding the starch grains as has been demonstrated previously for wheat grain (Tosi et al., 2009). A lower concentration of protein is observed in the aleurone layer. The $^{31}P^{16}O^-$ image clearly indicates the position of the phytate granules within the aleurone cells. The phytate granules appear as bright rings in the $^{31}P^{16}O^-$ image yet appear as dark holes in the $^{12}C^{14}N^-$, $^{32}S^-$ and SE images. This has been observed previously during SIMS analysis of cereal grain (Heard et al., 2002, Moore et al., 2010).

The $^{56}Fe^{16}O^-$ image shows two distinctly different regions of Fe localisation. A low concentration of Fe is observed in the aleurone cells, which appears to be co-localised with the phytate granules. The shape of the aleurone cells can be seen towards the top of the image matching the $^{31}P^{16}O^-$ image in distribution. This co-localisation is more evident in the top right of the $^{56}Fe^{16}O^-$ image where individual phytate granules can almost be resolved. The second and most obvious region of localisation is the hotspots of $^{56}Fe^{16}O^-$. These are distributed across both the aleurone and sub-aleurone and have high signal intensity

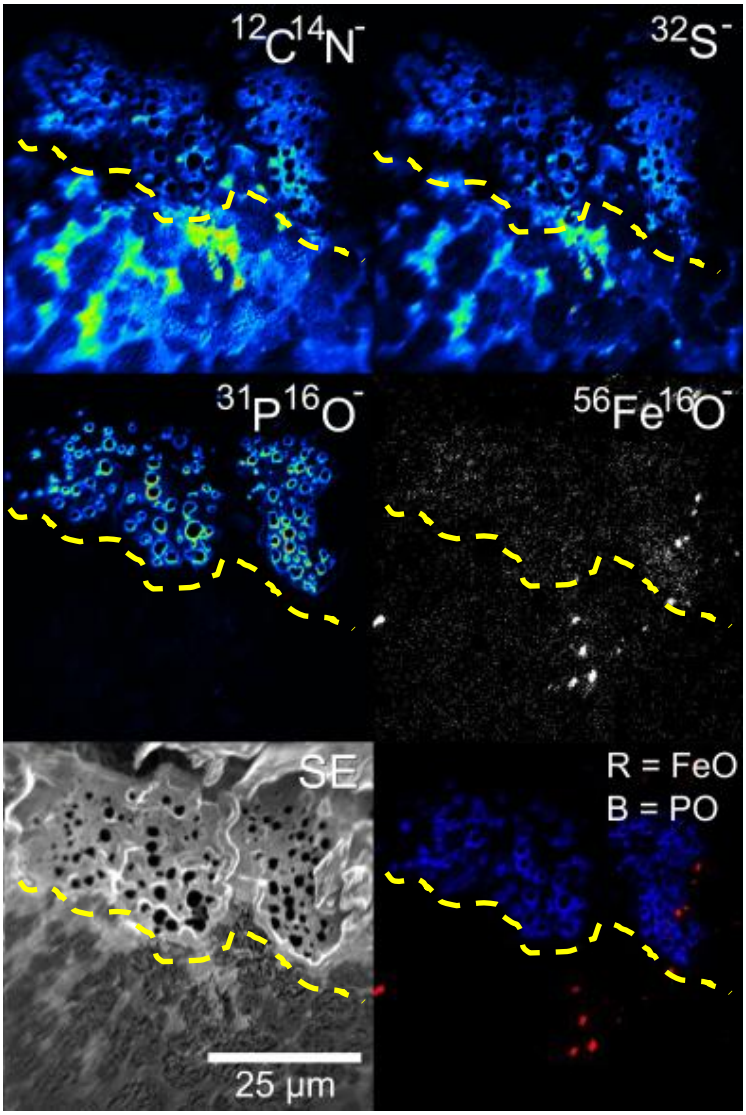

Figure 3: NanoSIMS imaging of grain

NanoSIMS images showing the aleurone (above yellow dashed line) and sub-aleurone regions (directly below yellow dashed line) of a wild-type rice grain. The distributions of $^{12}C^{14}N^-$, $^{32}S^-$, $^{31}P^{16}O^-$ and the SE image are from a single image. The $^{56}Fe^{16}O^-$ image has been summed together from 13 separate images to improve the counts. The colour merge shows the relative locations of the $^{56}Fe^{16}O^-$ (red) and $^{31}P^{16}O^-$ (blue) signals from summed images.

3.3.5 Synchrotron radiation XRF with transgenic material

Work presented in Chapter Two of this thesis shows a considerable increase in grain Fe when rice over expresses *OsNAS2* in root cortex specific cell types. This line (RC *OsNAS2*) produced grain with 66 μg g^{-1} and 13 μg g^{-1} Fe in brown and polished grain respectively. The use of colourimetric stains such as PPB, to visualise the distribution of Fe within the endosperm was unsuccessful and instead synchrotron radiation analysis was pursued to investigate the distribution of Fe within the transgenic grain.

As discussed in Chapter Two, PPB staining was not entirely suitable for Fe distribution analysis as more detailed analyses was required. Consequently, SXRF was used to yield quantifiable element-specific colour distribution images. Images A-E of Figure 4 show SXRF maps of the same 60 um thick section of a brown grain from a transgenic RC *OsNAS2* line and 4F-J show a 60um thick section of a wildtype brown rice grain. For the two single lines, the ICP-OES data showed the concentrations of Fe, Mn, Zn and P to be 16, 11, 24, and 3800 μg $g^{-1,}$ respectively, in wild-type brown grains; and 66, 14, 83 and 5600 μg g^{-1}, respectively, in the transgenic brown grains (see Chapter Two for details).

The maps generated for the transgenic line as depicted in Figure 4 and show an obvious increase in colour depth for Fe (B), Mn (C) and Zn (D), with Zn being the most notable increase compared with wildtype. Distribution of Fe in both transgenic and wildtype grains appears localised to the aleurone and periphery of the embryo. The deposition of Fe in the scutellum is more obvious in the wildtype grain than the transgenic and this may be due to the slicing of the grain with the vibratome,

shearing off a section of tissue during the process. Interestingly, there appears to be no Fe counts within the endosperm for either the wildtype or the transgenic line. The ICP-OES analysis of polished transgenic grain would suggest otherwise, with 13 μg g^{-1} Fe present in the sample. This is almost as much Fe present in the wildtype brown grain.

Distribution of Mn according to the maps in Figure 4C and 4H of the transgenic and wildtype grains respectively appears slightly enhanced in the plumule of the embryo in the transgenic grain compared to the wildtype. However Mn accumulation appears to remain the same for both lines, limited to the outer edge of the aleurone and embryo periphery. The difference in Mn concentrations between the two samples is only small and this is noted in the images with little colour intensity difference noted between the two maps.

The distribution of Zn appears no different between the transgenic and the wildtype grains with accumulation of the element being the only difference, as expected with the Zn concentration increasing almost 3.5-fold in the transgenic grain compared to the wildtype (83 μg g^{-1} versus 24 μg g^{-1}, respectively). Again the distribution pattern of Zn in the transgenic does not differ from the wild type, with loading being dominated by the endosperm and deposition accounted for in the aleurone and embryo, including what appears to be the plumule.

Particularly interesting information from this analysis is the composite colour images (4E and 4J) where Fe, Mn and Zn energy counts are overlayed with each other to obtain a more detailed distribution map. Here it can be seen in 4E, the intensities of each element in the transgenic (4E) greater than that of the wildtype sample (4J). It

becomes clear that Mn is deposited on the outer most edge of the aleurone and embryo (red) and Zn is almost evenly distributed across the whole grain surface. The plumule tissue and the tip of the embryo is the only area where all three elements are co-deposited. Interestingly, the pattern of Fe and Mn appear identical in 4B and 4C. However, in the composite image, it is quite clear the Mn does not penetrate the grain to as greater extent as Fe, with a wide green band lying further into the grain, within the sub-aleurone or exterior of the endosperm.

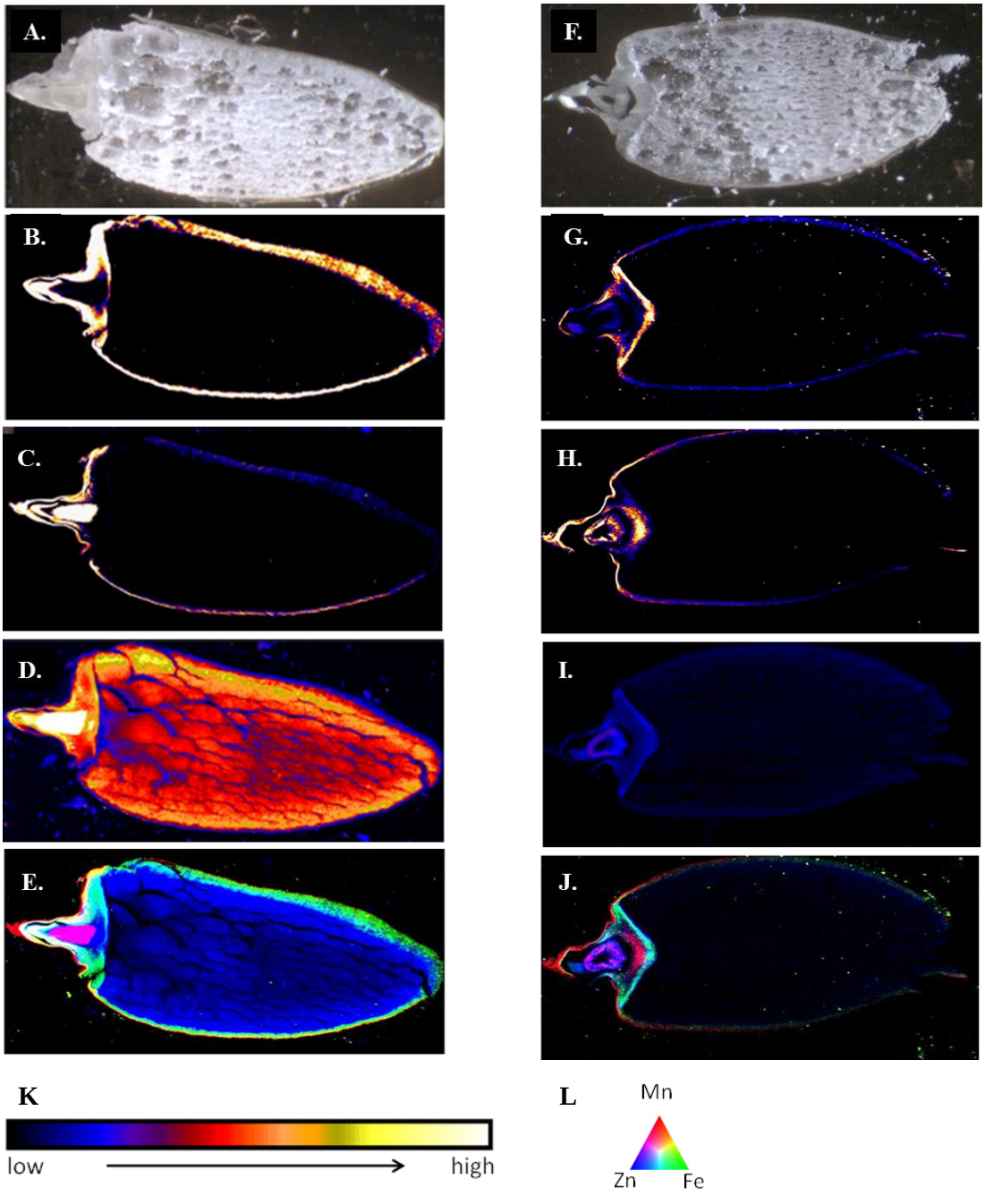
A.
F.
B.
G.
C.
H.
D.
I.
E.
J.
K
low
high
L
Mn
Zn
Fe

Figure 4: Synchrotron Radiation X- Ray Fluoroscence microscopy images illustrate the distribution of Fe, Mn and Zn in transgenic (left) and wildtype (right) rice grains.

Light microscope image of 60 μm thick section of transgenic brown rice grain and wildtype respectively (A, F), SXRF image of Fe distribution (B, G), Mn distribution (C, H), Zn distribution (D, I) and SXRF composite image (E, J) (red Mn, blue Zn, green Fe). Images generated using GeoPIXE software. Elemental values based on WT%. Values for different elements are not scaled equally. The whole-seeds maps refer to areas of approximately 5.5 x 2.2 mm and where mapped at 1.25 μm resolution. Sections of brown rice grain (60 μm thick) were prepared using Leica 1200 Vibratome. Sections were mounted on Kapton tape. The spectrum gradient (K) shown applies to all images, except for (E) and (J), where colours represent metal count intensity (L).

Synchrotron XRF line scans of 100 μm into the interior of the grain from the aleurone edge were obtained for the transgenic grain that show the distribution of Fe and P. Three dimensional maps generated from the recorded counts can be seen in Figure 5. Quite clearly it can be seen that the distribution of Fe extends further into the grain interior than does P. This is an important finding considering Fe is predominantly co-localised to P atoms in rice aleurone as this comprises the Fe-phytate anti-nutrient complex and is in agreement with findings from wildtype rice (Figure 1). To be able to show that Fe is not limited to the aleurone, and is not solely deposited in the same location as P atoms suggests the transgenic grain may have enriched Fe in a more bioavailable form. This work compliments findings in Chapter two where Caco-2 studies identified an increase in ferritin production in transgenic rice grains, therefore strongly suggesting increased bioavailable Fe is present in these rice grains.

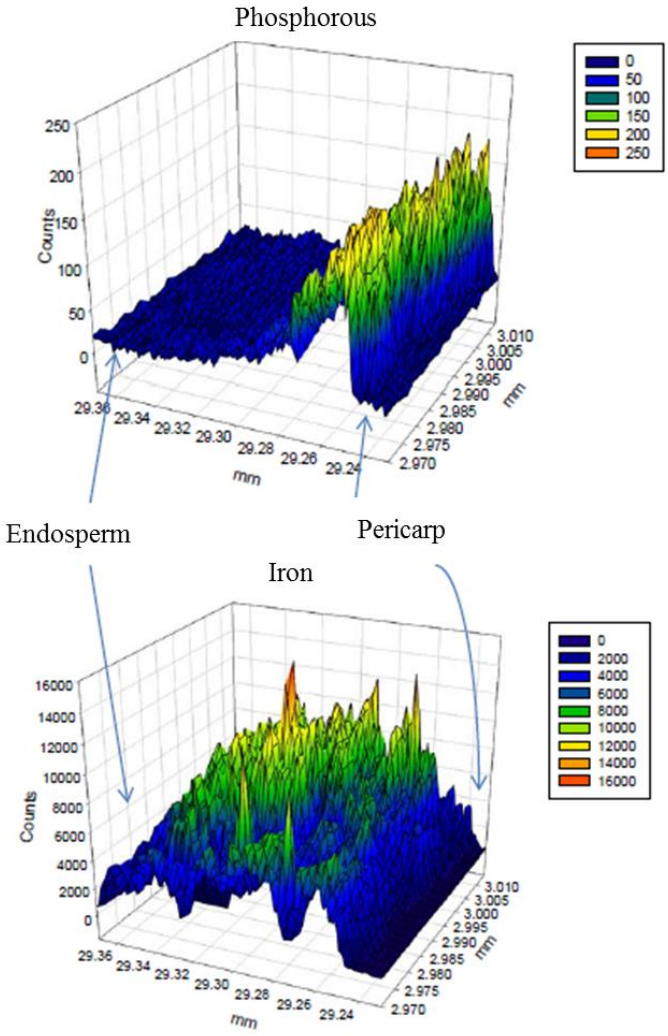

Figure 5: SXRF line SXANES of transgenic brown rice grains show Fe extends further into the grain than P.

3.4 Discussion

3.4.1 High resolution maps of Fe distribution *in situ*

Current knowledge of Fe distribution in rice grains is limited to elemental analysis (i.e. by ICP-OES and AAS) from brown and polished grains which indicates that 80% of Fe is in the aleurone, which in itself only comprises 20% of the grain. Images from SEM or PIXE have been utilised to image the localisation of Fe in rice grains (Bechtel and Juliano, 1980, Bechtel and Pomeranz, 1977) but this work was reported over 30 years ago and there remains a great lack in defined spatial resolution of Fe in rice grains. Whilst efforts have been made to image the Fe distribution in rice, imaging techniques have improved but the images generated to date have not (Lombi et al., 2009). The highly specific and detailed images in this project uncover greater information about Fe distribution.

The high definition images obtained in Figure 1 show highly distinct Mn, Zn and Fe accumulation across the grain surface. Accumulation of Mn was used as an indicator of the aleurone cells because it is enriched specifically in the aleurone (Tanaka et al., 1973) thereby acting as a 'marker' for the tissue. Whilst it is known that the majority of Fe lies within aleurone and embryonic tissue, this is the first time that images have provided a clear map supporting and extending this information. Interestingly, it was noted in Table 5A/B of Chapter Two that both P and Fe concentrations decreased approximately 70-80% post-milling. This suggests a commonly known relationship between phytate (potentially represented by P) and Fe, and thus all losses were due to strong bonds between the two in the aleurone. However from the SXRF imaging in Figure 1, it is evident that Fe extends well into the endosperm of the grain whereas P

concentration decreases significantly beyond the first 40 µm from the grain edge (aleurone). Additionally the Fe distribution extends well beyond that of Mn, supporting the hypothesis that Fe also lies in the sub-aleurone and outermost edge of the rice grain. The SXRF images also support ICP data where it is clear that there is Fe accumulation in the endosperm, as seen in endosperm, (Table 5B, Chapter Two). Both Mn and Fe (Figure 1B and 1D, respectively) comprise embryonic tissue, namely the primordial leaf tissue, scutellum, with a greater concentration of Mn in the outer most region of the aleurone than Fe, as expected (Wada and Lott, 1997).

These findings are extremely important with respect to Fe concentrations in polished grain. It is well known that Fe does exist, albeit at low concentrations, within the endosperm of rice and this was supported by ICP data in Table 5A/B of Chapter Two. The distribution of Fe in aleurone is also supported by whole grain maps and line scans by SXRF in Figure 1. Fe distribution in the endosperm was clearly defined in the fine detailed maps of the rice grain as being limited to the outer edge of the grain. Unlike Zn, which is uniformly distributed across the grain surface (Figure 1E and F), Fe accumulation is greatest within the aleurone and sub-aleurone. This finding is imperative when considering how important milling conditions are for polished grain preparation.

3.4.2 Ferric ion speciation in bran and flour

Within the plant, Fe is known to be bound to chelators such as NA, citrate, and storage proteins such as ferritin, but little research has demonstrated conclusive evidence for the species of Fe, Fe chelators and potential bioavailablility of Fe within the grain. Sperotto et al. (2010) suggest that Fe^{3+} is most prevalent with the rice grain

and go on to hypothesise that the ions may be phytate bound. Research conducted by demonstrated a strong affinity of NA for Fe^{2+} in phloem, however this work was not extended to the grain. To expand and compliment SXRF maps in this study, SXANES spectra were obtained for bran and flour samples. Bulk SXANES was used to determine the Fe speciation in each sample, and to identify chelating molecules. The bulk SXANES spectra generated for photon energies detected for rice bran and flour in this project are the first of its kind in regards to Fe speciation and chelation in rice. The photon energy absorption spectra represented in Figure 2A clearly suggest a strong trend in phytate:Fe^{3+} in bran. Furthermore, the bulk SXANES data in Figure 2B clearly shows NA:Fe^{3+} was strongly detected in flour more so than the NA:Fe^{2+} complex. This is in agreement with research showing the strong relationship between phytate and Fe (Inoue et al., 2003) and NA:Fe^{3+} (von Wiren et al., 1999). Whilst our results do not suggest exclusivity to NA:Fe^{3+} chelation, the difference between the two species and chelation of Fe specifically in the endosperm is a novel finding as a result of this work. As previously mentioned, true and precise molecular standards are difficult to source, thus, future work is required to fully identify this chelate body.

3.4.3 Iron is not bound to phytate in endosperm

The data and images presented in this project support and expand the existing knowledge regarding Fe localization and speciation within rice grain. The fine resolution maps of rice endosperm tissue generated using NanoSIMS technology contradicts some of the data from XANES, in particular, Fe bound to phytate in flour. In Figure 3, there is a clear distinction between the aleurone and the endosperm, with $^{56}Fe^{16}O^-$ (red) visible in the endosperm without $^{31}P^{16}O^-$ present

(phytate is depicted as blue rings). In fact all phytate appears limited to the aleurone. This is interesting as SXANES suggests the presence of phytate:Fe^{2+} in flour (Figure 2A). Synchrotron XANES were performed on bulk bran and flour fractions. Clearly it appears that some bran could have been retained on the endosperm therefore contaminating the sample. Images from NanoSIMS clearly indicate phytate molecules are not co-located with Fe atoms in the sub-aleurone and this supports the hypothesis of this project which states multi-spectroscopic analysis will provide more accurate elemental distribution and speciation data than single tooled approaches.

NanoSIMS also demonstrated that Fe is present in the sub-aleurone and co-located with proteinaceous molecules. The probability of a protein rich sub-aleurone is in agreement with Bechtel and Juliano (1980), who stated that the sub-aleurone layer consists of a protein and lipid rich bilayer. Moreover, the presence of Fe in the sub-aleurone as detected by NanoSIMS supports the SXRF maps of Figures 1, 4 and 5 where there is a distinct deposition of Fe in the sub-aleurone.

The analysis in this project clearly suggests that a range of spectroscopic tools should be used to confirm findings with regards to Fe distribution in rice. It is believed that multi-spectroscopic analysis must be employed to identify 'false positive' information and to provide concise elemental analysis. A combination of multi-spectroscopic techniques can accurately define the distribution, speciation and chelation of Fe and Zn in rice grains; allowing for improved targeted research into cereal biofortification.

3.4.4 Increased iron in transgenic rice clearly visualised by synchrotron spectra

The high resolution images of Fe distribution in SXRF maps demonstrate strong deposition in the sub-aleurone (outer edge of endosperm), interior to Mn (Figure 4) and P (Figure 5). It was expected that a greater accumulation of Fe would be detected further into the centre of the endosperm due to ICP analysis showing relatively high Fe concentrations in polished rice (Table 5B, Chapter Two), however these images are in agreement with spectra in Figure 1.

The images generated from SXRF scans of the transverse section of transgenic grain show dramatically higher elemental counts for Fe, Zn and Mn compared to similar images taken with wildtype grain. As expected, Zn localisation is not particularly limited to any specific tissue on the grain with uniform distribution across the whole surface and slightly increased accumulation in embryonic tissue, both in wildtype and transgenic grain (Figure 4E and 4J respectively). Manganese is limited to outer edge of grain, most likely the aleurone (Tanaka et al., 1973) again as shown in both wildtype and transgenic grain images of Figure 4D and 4I, respectively. Iron lies predominately in embryo, scutellum and primordial tissue, as expected, but there exists extensive deposition in the grain's outer edge. Whilst it is expected that Fe would be limited to aleurone due to binding of phytate, further analysis shows the Fe lies interior to Mn and also as per Figure 5 it can be seen that the Fe extends further into the endosperm, beyond the limits of the P deposition (indicative of phytate globoids). This information may not have been recognised due to minimal detection in endosperm but SXRF line scans (Figure 5) and ICP-OES (Table 5B of Chapter

Two) of polished grain does indeed demonstrate the presence of Fe in the endosperm, at levels higher than that of wildtype. It is therefore clear that multi-spectroscopic analysis is required to further investigate Fe distribution and speciation which may further elucidate the complex potential of Fe in the transgenic rice lines.

Chapter Four: The effects of soil applied cadmium on iron uptake in transgenic rice overexpressing *OsNAS*

4.1 Introduction

In plants, cadmium (Cd) reduces photosynthesis, water and nutrient uptake (Sanita di Toppi and Gabbrielli, 1999), inhibits enzyme activities and disrupts cellular transport (Clemens, 2001). In humans, Cd accumulates mostly in kidneys (Kawada and Suzuki, 1998), resulting in severe renal dysfuntion (Yamaguchi et al., 2012). Disruptions to bone structure and the development of osteomalacia, or Itai Itai disease, failure of reproductive systems and elevated risk of cancers has also been reported as a result of chronic Cd accumulation in the body (Chen et al., 2008, Fechner et al., 2011). Like all metals, plants are unable to produce Cd, but instead take up this element from the soil into the plant; as such elevated levels of Cd in the soil can result in increased Cd levels in the edible rice grain. Up to 50% of dietary Cd intake is attributed to contaminated white rice consumption in Japan (Yamaguchi et al., 2012).

A major focus of this thesis has been the development of transgenic rice with Fe enriched endosperm, as a proof of concept to ultimately combat human micronutrient deficiencies. As described in Chapter Two (Cell Type Specific Over-Expression of *OsNAS1, 2, 3*), these results indicate that increasing nicotianamine (NA) results in an increase in Fe uptake from the soil and increases Fe accumulation in the grain. Nicotianamine is ubiquitous in the plant kingdom and is known to bind several micronutrients including: Fe, Zn, Cu, Mn (Anderegg and Ripperger, 1989, Husted et al., 2011, Pich et al., 1994, von Wiren et al., 1999) and the heavy metal Ni (Douchkov et al., 2005). Douchkov et al. (2005) showed the potential for NA to

chelate Ni in *Arabidopsis*, however tests did not confer any suggestion that NAS over-expression in *Arabidopsis* had any effect on Cd uptake. Nevertheless, it is important to show whether increased *NAS* (and hence PS) in the transgenic *OsNAS* rice lines are capable of increasing Cd accumulation.

Whilst little has been shown to implicate NAS in any way to Cd, there is considerable data suggesting Cd may compete for Fe or Zn uptake due to analogous or isomorphous identities of the ions (Stillman et al., 1987). Cadmium transport into cells via the Fe and Zn transporter, IRT1 has been proposed (Clemens, 2001, Korshunova et al., 1999) with Fox and Guerinot (1998) suggesting inhibition of Fe uptake due to Cd completion at the transporter site. Several transporters specific to cations like Fe, Zn and Mn have been implicated in Cd transport (Dufner-Beattie et al., 2007). Homologous to rice genes, human Zn and Fe transporters ZIP4 and ZIP8 have also demonstrated Cd transport in mice *in vivo* studies (Himeno et al., 2009, Leung et al., 2012). A relationship has been also drawn between the upregulation of *AtNAS* and *AtZIP* genes and their response to Zn deficiency (Assuncao et al., 2013). This supports the potential for the involvement of NAS, be it directly or indirectly, in Cd uptake or transport in rice.

The development of *OsNAS* overexpressing rice in this study has led to the generation of several lines that are capable of accumulating up to three times more Fe in the endosperm than non-transgenic rice. It has been suggested that the increase in Fe demonstrated within these lines is directly due to the cell type specific expression of the *OsNAS* genes. The focus of this chapter is to investigate the effect of this *OsNAS* transformation when plants are grown in soils with elevated Cd levels. It is hypothesised that the resulting increase in NA will result in increased Cd uptake

(as Cd has similar properties to Fe) and possibly result in increased Cd accumulation in the grain. This difference between what is expected in rice and what is known in dicots stems from what has already been described in Chapter Two. In brief, it is known that NA behaves differently in monocots and dicots. Strong elemental chelation between several divalent cations has been widely published and it is therefore suggested that Cd may indeed bind to NA in monocots. Conversely a contrary hypothesis has been proposed stating that these transgenic lines may have the potential to preferentially transport Fe over Cd, creating a target for enhanced grain Fe without increasing toxic heavy metals such as Cd, which could have exciting benefits for growing this plant in Cd contaminated soils without resulting in potentially toxic Cd levels in the edible grain.

4.2 Materials and methods

4.2.1 Development of transgenic plant material

Generation of transgenic rice (*Oryza sativa* s*sp. Japonica cv.* Nipponbare) is described in section 2.2 of this thesis. Several combinations of T1 and T2 generations of the cell type specific *OsNAS* expression lines were used independently in this current study and are described in the results section. Generation T2 grains used in this study were genotyped for the presence of the NPTII selection marker in the second transformation event (as detailed in section 2.2). Transformed T1 generation rice shown not to express constitutive *OsNAS2* (35S:*OsNAS2*) called null transformant and thus act as controls (Johnson et al., 2011).

4.2.2 Cadmium uptake

Plants were grown in UC Davis soil (prepared according to methods published by Hoagland and Arnon (1950) which was contaminated with $CdCl_2$ to reach 3μg g^{-1} Cd in the soil, and mixed thoroughly. Soil was placed in 1 L pots and onto large trays to contain water. T1 seeds were germinated as per 4.2.3. UC Davis soil was used as a non-contaminated soil. Note, Cd contaminated soils are called CdCS and non-contaminated soils are called NCdS.

4.2.3 Growth conditions

Cell type specific Root Cortex (RC) *OsNAS2* and Developing Flower: Lodicule (DF:L *OsNAS3*) rice (*Oryza sativa ssp. Japonica cv.* Nipponbare) seeds were soaked in 70% ethanol for 5 minutes, washed with 30% bleach (v/v) and 1% Tween 20 (v/v)

and agitated for 30 minutes at 25°C. Seeds were washed with reverse osmosis (RO) water 3 times, with 10 minutes between washes. Seeds were then placed on Petri dishes lined with Whatman filter paper Number 1 and 5 ml RO water. Plates were sealed with parafilm and incubated at 28°C with 24 hours light for one week. Seedlings were planted in CdCS or NCdS. Pots were placed on large trays of water and partially submerged.

Plants were cultivated in glasshouse conditions or controlled environment growth rooms (CER) (12 day light hours, 28/24 ºC day/night temperature, 70% humidity). Plants were grown in winter months, and those grown in glasshouse conditions had semi-controlled temperatures, within 10 ºC of the outside environment. Additional supplementary 1000W lighting was also required for glasshouse grown plants. Plants were watered until physiological maturity (five months post germination) and watering ceased until plants were dry. Grain was harvested and dried in a 37 ºC oven for 3 days.

4.2.4 Cadmium concentration analysis

After four weeks of seedling growth, the youngest emerged leaf blades (YEB) were collected from each plant and dried at 30°C for three days. Grains were harvested once the plants reached full maturity (post grain filling) and dried at 30°C for 24 hours to ensure all tissue was void of moisture.

Grains were threshed and either analysed directly (as brown grains) or milled using a modified commercial bench-top miller (Kett Electrical Laboratory, Tokyo, Japan).

Note that the mill had previously been modified to prevent metal contamination of the grain (as discussed in Chapter Two) (Stangoulis, 2010).

Elemental concentrations were investigated in dried, youngest emerged blade (YEB), leaf tissue, and 25 brown and 50 polished grains, via ICP-OES (Wheal et al., 2011). Cd concentrations in soil for both CdCS and NCdS were determined by AAS according to methods published by McLaughlin et al. (1995).

4.3 Results

4.3.1 T1 grains grown in modified and unmodified soils present stressed phenotypes

Transgenic rice lines over-expressing *OsNAS* genes under cell-type specific promoters were grown in 3 μg g^{-1} CdCS. This was to establish whether plants with increased NA also had increased Cd accumulation in the endosperm. Note that in this and subsequent experiments in this chapter the term 'control' refers to both wildtype and null 35S *OsNAS2* transgenics, not soil contamination status.

Due to the nature of PS secretion from roots in rice plants, it was proposed that the over expression of *OsNAS* could potentially result in increased PS that are capable of binding Fe in the rhizosphere of neighbouring, non-transgenic / non-overexpressing plants. Thus, *OsNAS* over-expressing plants were grown in separate water trays to null transformants and wildtype controls.

There was a considerable difference in shoot growth between plants in the two Cd treatments, as illustrated in Figure 1A (CdCS in pink pots, NCdS in black pots). Here plants were four months post germination and control plants appeared fuller, with

more foliage and deeper green leaf. However, both plants in NCdS and CdCS presented features of stressed phenotypes, including few and weak and thin tillers (Figure 1C) and chlorosis (Figure 1D). The controlled temperature of the glasshouse in which these plants were grown was within 10ºC of outside temperatures. As plants were grown during winter with average temperatures of 15°C (Climate Data Online, 2013), it is possible that there were low temperatures within the glasshouse. This may have stressed the plants, explaining poor vegetative growth.

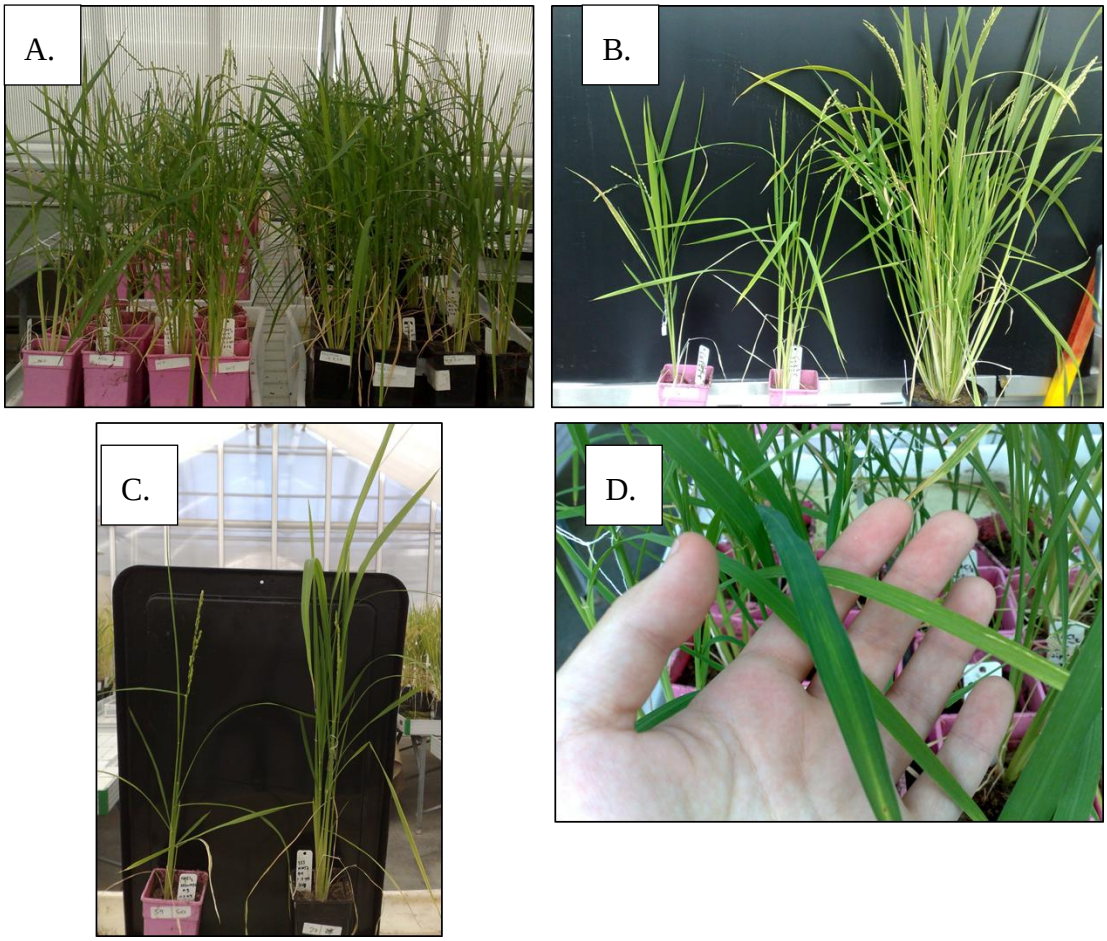

Figure 1: Cadmium contaminated rice and non contamined rice both look weak during growth.

A: Transgenic and wildtype rice plants in pink containers (left) growing in CdCS looking markedly weaker with less leaf tissue than the control soil plants (transgenic and wildtype rice plants in black containers (right) growing in NCdS). B: 35S *OsNAS2* (left) and wildtype (centre) grown in CdCS compared to a *OsNAS2* transgenic plant (right) grown in same glasshouse conditions at same time as Cd experiment plants (*OsNAS2* not part of this project, and thus grown in NCdS.) C: Same 35S *OsNAS2* plant in CdCS shown in B, photo taken one week later, (left) shown next to NCdS 35S *OsNAS2* (right). D: chlorosis shown in leaves of one randomly selected plant from the contaminated range.

Figure 1B illustrates the null 35S *OsNAS2* plant compared to a wildtype plant grown in the same CdCS, which is further compared to a rice plant grown simultaneously in unmodified UC Davis soil in the same greenhouse. The comparative 35S *OsNAS2* plant shown on the far right of Figure 1B was planted in the same week as the plants grown in NCdS and CdCS of this study, in the same glasshouse. This shows that the reduced growth in the NCdS and CdCS grown plants is indeed significant and unlikely to be a result of glasshouse conditions. Figure 1C shows a transgenic 35S *OsNAS2* null from both the CdCS and NCdS (left and right respectively) where it can be seen that the CdCS plant has fewer tillers and less vegetative tissue than its corresponding control on the right. However, both plants are unexpectedly small, indicating less growth in either Cd treatments. Figure 1D shows the chlorosis in the leaf tissue, noted in majority of both CdCS and NCdS grown plants. At this point, youngest emerged leaf blades (YEBs) were harvested from several plants showing particularly concerning levels of chlorosis. These YEBs were analysed for elemental composition via ICP-OES.

4.3.2 Cadmium in leaf tissue

The addition of Cd to the soil resulted in a noticeable increase in Cd in the leaves (Figure 2). When grown in 3 μg g^{-1} Cd, leaf Cd concentrations were increased by up to a six-fold (up to a maximum of approximately 18 μg g^{-1} Cd) compared to plants grown in NCdS. Samples of soil were analysed for Cd content to ensure there were indeed Cd present in the soils. The AAS analysis of soils shows that approximately 2.5 μg g^{-1} Cd was present in the soils. This is slightly less than the expected concentration but not in excess, therefore unlikely to contribute to the toxicity of

plants. There is no indication that the concentration of B, Fe, Mn or Zn are of concern, however boron (B) does vary from 8.92 μg g^{-1} in NCdS to almost double at 16.4 μg g^{-1} in CdCS. From this information, little can be extrapolated to define why the plants did not grow well in this particular experiment, while it is clear that toxic levels of Cd are not present in the prepared soils.

Generally, plants maintain Fe Fe concentrations of approximately 100 μg g^{-1} in leaf tissues under Fe adequate conditions (Taiz and Zeiger, 2002). In Figure 2, it can be seen that the level of Fe is at a normal range for both NCdS and CdCS plants (ranging from 94 - 178 μg g^{-1} and 89-107 μg g^{-1} in NCdS and CdCS, respectively). There is a 5% decrease in leaf Fe concentrations of wildtype plants when grown in CdCS, 15% decrease in the RC *OsNAS2* lines (NCdS vs CdCS) and a 40% decrease in the 35S *OsNAS3* plants (NCdS vs CdCS). However, with the ranges of Fe being within the normal range expected in leaf tissues, it could not be said that the presence of Cd in the soil was high enough to restrict Fe from entering the plant, nor could it be suggested that the Cd was competing for Fe transport.

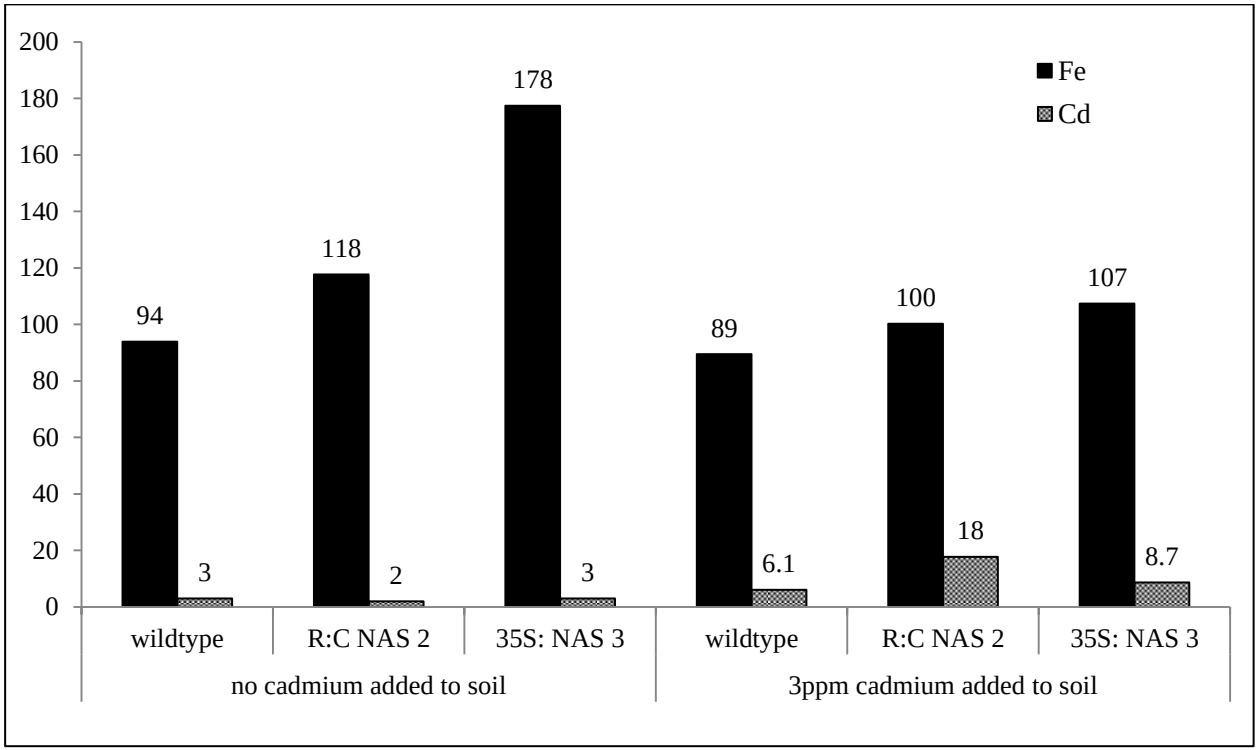

Figure 2: Cd concentration in leaves of stressed plants as determined by ICP-OES.

Concentrations of Fe and Cd in the leaf tissue do not appear to be of any concern, with Fe levels relatively stable and not of level that could induce severe Fe deficiency. The same can be said about the Cd concentrations, where it can be seen that the concentrations of the heavy metal increase in the three lines when introduced to CdCS. Values represent $\mu g\ g^{-1}$.

Table 1: Elemental concentration in leaf tissue of CdCS and NCdS plants

ICP-OES analysis shows the elemental composition (μg g^{-1}) of the YEB's harvested from plants presenting stressed phenotypes.

		Cd	Fe	Mn	Zn	P	B	Cu	Ca	Mg	Na	K	S
NCdS	wildtype	< 3	178	460	34	10700	103	35	4500	4100	181	27000	5800
	RC NAS 2	< 2	118	410	27	5200	150	15	5300	3300	115	28000	4800
	35S: NAS 3	< 3	94	290	24	3500	111	14	5000	3000	193	25000	3800
3 μg g^{-1} CdCS	wildtype	6	89	185	33	6300	69	16	3000	2700	186	27000	5400
	RC NAS 2	18	100	290	34	6100	120	14	7500	3200	220	25000	5700
	35S: NAS 3	9	107	144	29	5200	79	13	3900	2500	196	27000	4800

Table 2: Concentration of CdCS is under 3 μg g^{-1} but not at a level would attribute to decreased plant health.

AAS was performed on the soils used in this experiment to determine whether the Cd concentration used to contaminate the soils was incorrect. A 3 μg g^{-1} Cd concentration was desired for CdCS however it is apparent that approximately 2.5 μg g^{-1} Cd has been reached. Samples were taken from bulk soils from which no plants had been grown.

	Cd	B	Fe	Mn	Zn
NCdS	0.003	8.92	2752	9.8	5.08
	0.002	14.72	2424	8.88	5.2
	0.272	11.6	3056	11.8	4.92
3 μg g^{-1} CdCS	2.56	14.84	2528	8.96	3.56
	2.46	11.28	2332	8.44	4.16
	2.36	16.4	2348	8.24	4.56

The data obtained for Zn, Ca, Mg, Na, K, S in CdCS (Table 1) illustrate no significant change between genotypes and soil conditions, with values still within an acceptable range (Taiz and Zeiger, 2002). Mn concentrations (Table 1) appeared stable in the three NCdS but much higher than the expected value of 50 μg g^{-1} (Taiz and Zeiger, 2002). However, these concentrations decreased for all three tissues harvested from plants grown in CdCS. Concentrations for B were also much higher than the expected 40 μg g^{-1} (Nable et al., 1997), ranging from 103-150 μg g^{-1} in NCdS and 69-120 μg g^{-1}, enough to be considered toxic specifically in rice (Cayton, 1985). This could explain the symptoms of poor growth in all plants. This high concentration of B could be contributed by the water supply, which can vary in B and in this case, water coming into the growth facility was excessive in B. This was also confirmed by the large differences in B concentration found in soils extracted from plants showing weakened phenotypes (Table 1) (Palmer, 2013 personal communication). The same could be proposed of the P concentrations in leaves, however, the values for the wildtype leaves grown in NCdS were not considered to be of concern.

4.3.3 Cadmium in the T1 grain

Plants did not show any significant improvement in their overall growth or yield, and of the 95 plants grown from T1 seed, only 12 plants produced enough seed for ICP-OES analysis (as shown in Figure 3). Brown grains were not analysed by ICP-OES due to constraints with the mass of seeds, and also because the primary aim of this experiment is to determine if Cd has competed with Fe and accumulating in the endosperm.

The analysis of transgenic white grains harvested from plants grown in CdCS both showed a considerable level of Cd accumulation in the endosperm. As expected, in all plants grown in NCdS, the level of Cd in the grain is below the 0.4 μg g^{-1} limit (Commission and Commission, 2011) as depicted in Figure 3. The Fe concentration in wildtype grain of plants grown in CdCS or NCdS is 75% less than previously seen in ICP-OES data of white grain (Chapter Two, Table 6). In this study, Fe concentrations were around 1 μg g^{-1} in CdCS as opposed to the expected 4 μg g^{-1}. Concentrations were also lower than expected for RC *OsNAS2* grains and DF:L *OsNAS3* with levels previously reported at 13 and 8 μg g^{-1} respectively in white grains. In this study 50% less Fe was detected in the white grains at 6.3 and 4.6 μg g^{-1}, respectively.

Referring to Figure 3, trends in the data for Fe accumulation in individual wildtype plants for both soil treatments show little change, however there is an increase in Cd accumulation in the endosperm with a change from 0.1 μg g^{-1} in NCdS to 0.98 and 1.4 μg g^{-1} in CdCS. In CdCS, the RC *OsNAS2* plants yielded grains with reduced Fe compared to NCdS plants, ranging from 1.9 - 2.4 μg g^{-1}, a significant decrease from 6.3 μg g^{-1} in NCdS ($P < 0.05$). DF:L *OsNAS3* also contains significantly less Fe decreasing from 4.6 to between 1.4 and 2 μg g^{-1} ($P< 0.002$). Cd accumulation increased in both RC *OsNAS2* and DF:L *OsNAS3* contaminated plants. Concentrations ranged from 0.3 and 0.2 μg g^{-1} in NCdS, up to 3 μg g^{-1} and 3.6 μg g^{-1} in CdCS (RC *OsNAS2* and DF:L *OsNAS3*, respectively). This is well above the 0.4 μg g^{-1} Cd limit allowed for human consumption (Commission and Commission, 2011).

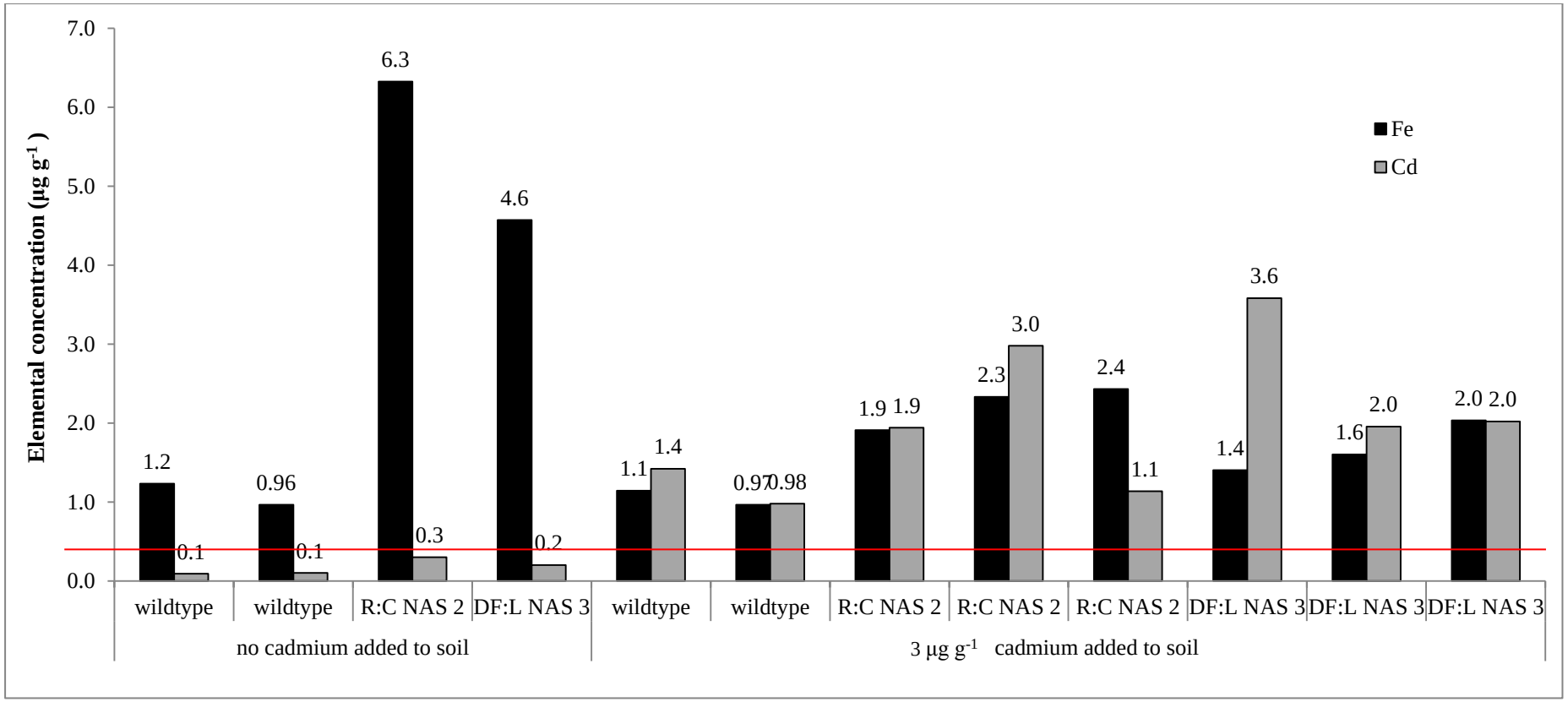

Figure 3: Cadmium concentrations in grain of white grains as determined via ICP-OES.

Cadmium concentrations for the lines grown in NCdS were detected as less than the values shown in this figure (< 0.1, < 0.3, < 0.2). The red line denotes the 0.4 µg g^{-1} contamination limit for rice. Data represents individual plants therefore error bars are not present.

4.3.4 Zinc and Cadmium correlations

The decrease in Fe concentrations between NCdS and CdCS was also noted in Zn concentrations. Figure 4 shows the negative correlation (R^2 value of 0.187) between increasing Cd and decreasing Zn levels in white grains. This data is representative of all samples grown in NCdS and CdCS. As leaf tissue ICP-OES data suggests in Table 1, Zn concentrations were not unstable and appeared to be within homeostatic levels. It is therefore believed that the apparent competition between Cd and Zn in the rice plants has occurred within the plant during grain loading and not during uptake from soil and transport in vegetative tissue. The data obtained from this experiment warrants further investigation.

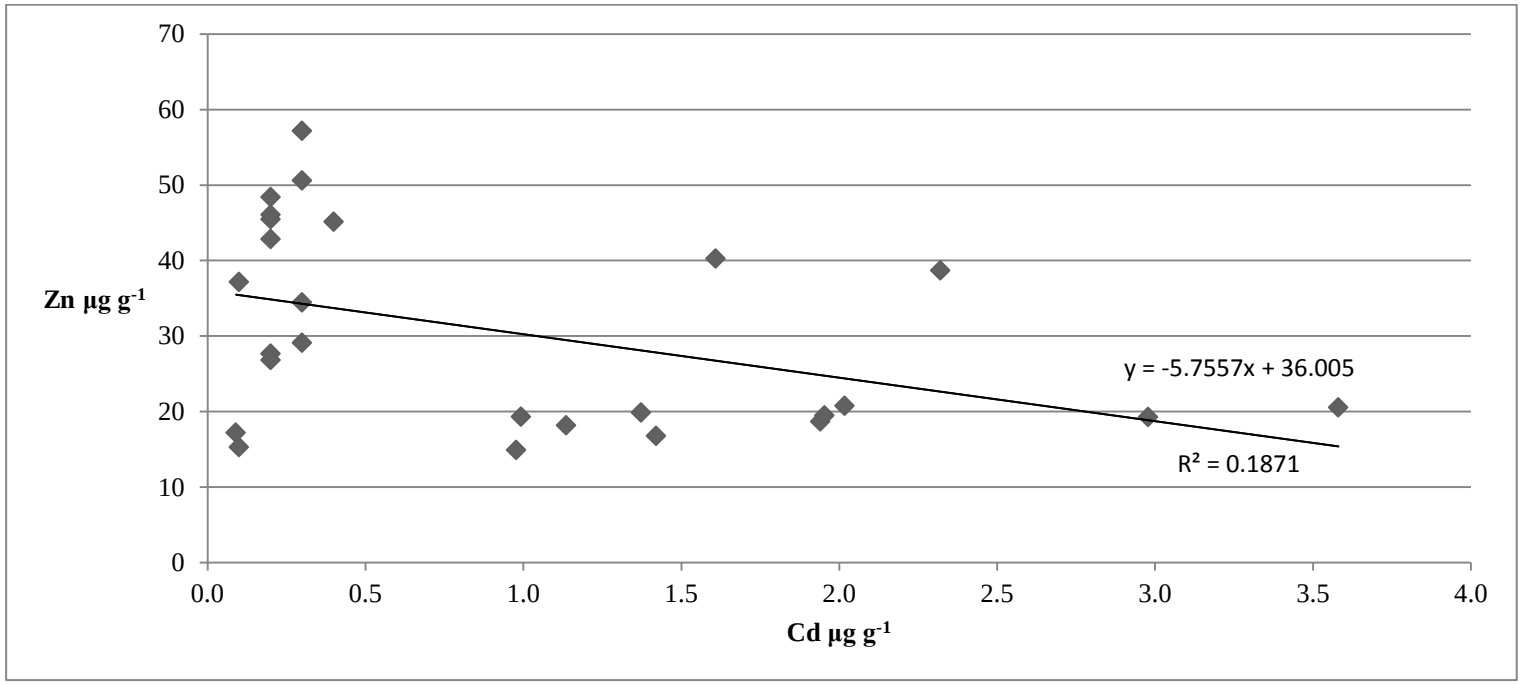

Figure 4: Increasing [Cd] in white grains produces a decrease in [Zn] as determined via ICP-OES.

The relationship between Cd and Zn in the data obtained for white grains grown NCdS and CdCS shows a clear decrease in Zn as Cd increases.

4.3.5 Cadmium trial repeated with transgenic T2 cell type specific *OsNAS* grain

T2 grain harvested from plants infected with *Sarocladium oryzae* (see section 2.3.7 Expanding progeny to T2 and T3 seed) were grown in a control environment growth room in soils contaminated with 3 μg g^{-1} Cd (from $CdCl_2$) to replicate and expand the previous Cd uptake experiment. Upon germination of T2 grain, only 20% of grain successfully germinated. This was at first an unexpected result, however, investigations into the pathology of *Saracladium oryzae* revealed the pathogen imbeds grains of infected plants with high levels of helvonic acid and subsequently reducing germination rates by 80% and producing plants with weakened growth (Ayyadurai et al., 2005, Gopalakrishnan et al., 2010).

Soil pH was investigated to establish whether poor plant health was specific to the growing conditions or related to the pathogen infection. Using a Soil pH Test Kit (Manutech), soils of both treatments appeared to be within an approximate range of pH 5-5.5 which is slightly acidic but not detrimental for rice growth according to the advice given with the product (preferred range of 5-6.5 pH). As this pH is ideal for Fe, Zn, Mn and B ions it could not be said that there was a heightened release of ions causing a concern of toxic levels in leaves and therefore weakening plants. It was therefore determined that weak plant growth was attributed to the pathogen.

The Fe concentration in T2 grain was not found to be as high as the T1 parent lines, as shown in Table 3. All plants were weaker and low grain quantities yielded. As a result of continuous pathogen infections in glasshouses, the Cd experiment was finally aborted as all rice related experiments were placed on an embargo until

further notice, which in effect lasted nearly one year. Further investigations could not be made during the timeline of this project.

Table 3: Fe concentrations of T1 and T2 rice grains grown in glasshouse conditions, showing decrease in [Fe] between generations. Values represent μg g^{-1}

Plant Genotype		T1		T2	
control		21	n/a	21[a] ± 2.5[b]	(18-24)[c]
root: stele	*OsNAS3*	40	n/a	35 ± 9	(24-46)
developing flower: lodicule	*OsNAS2*	46 ± 1.4	(45-47)	30 ± 10.8	(21-41)
	OsNAS3	47± 2.9	(45-50)	39 ± 12.8	(18-47)
root: cortex	*OsNAS1*	41 ± 3.5	(38-45)	29 ± 6.4	(22-36)
	OsNAS2	50 ± 14.2	(41-66)	32 ± 8.2	(23-47)
	OsNAS3	43 ± 2.1	(42-46)	32 ± 6.5	(21-40)

a = mean, b = standard deviation, c = range of data

4.4 Discussion

4.4.1 Over-expression of *OsNAS2* and *OsNAS 3* under cell type specific promoters leads to increases in cadmium loading in rice endosperm

It is common knowledge that a great proportion of ingested Cd is derived from foods such as white rice. In Japan alone, white rice has been shown to attribute to 50% of ingested Cd (Leung et al., 2012). With these statistics in mind it was pertinent that Cd uptake was investigated to determine if the result of cell-type specific over-expression of the *OsNAS* genes affected grain Cd levels. It was hypothesised that as there is a difference in Fe accumulation in the grain as a result of the three genotypes, there could also be a preferential uptake of Fe and Zn compared to Cd in the endosperm.

The CdCS used in this experiment was prepared to have a concentration of 3 μg g^{-1} Cd, the minimum level of Cd considered to be 'contaminated and potentially harmful' (ANZECC/NHMRC, 1992). Less than 0.4 μg g^{-1} Cd in white grain is permissible for human consumption (Arao and Ishikawa, 2006, Commission and Commission, 2011). From the small range of samples available to analyse, it is clear that Cd accumulation increased for both wildtype and transgenic white grains when grown in CdCS when compared to NCdS where grain Cd levels were almost undetectable. When grown in CdCS it was determined that the Cd level in wildtype grains increased to a level up to three times above the acceptable level of Cd in white, ranging from 0.9 - 1.4 μg g^{-1}. A more dramatic increase in Cd is noted in the transgenics where levels range from 1.1 - 3 μg g^{-1} in the RC *OsNAS2* grains and 2 - 3.6 μg g^{-1} in the DF:L *OsNAS3* grains. Most concerning is the decrease in both Fe

and Zn which was observed only in the transgenic grains; a decreases of up to 70% and 50% Fe and Zn, respectively, was noted for several samples of transgenic lines. Our initial data attributed the poor plant growth in the glasshouse to the decrease in Fe and Zn uptake and high levels of Cd (as observed in leaf tissue). However, it is known that Cd levels that are known to be toxic to humans and animals are not necessarily toxic to plants, as they can tolerate much higher levels of the heavy metal (Satarug and Moore, 2004), and these levels were not even exceeded in these plants. So the possibility that the reduced plant growth occurred as a result of Cd toxicity can be ruled out. Additionally, no decrease in Fe and Zn was observed in the wildtype grains grown in contaminated soils indicating that there was no competition with Cd during transport to grains at least.

The decrease in Zn and increase in Cd is consistent with evidence that Cd is chemically isomorphic to and can 'mimic' Zn and compete for binding affinity with several chelating molecules (Palmgren et al., 2008). Nicotianamine is known to bind other divalent ions such as Zn^{2+}, Fe^{2+}, Mn^{2+} and Ni^{2+}. Whilst NA has been reported not to chelate Cd (Kato et al., 2010), DMA, a product of NA catabolism does in fact bind Cd (Meda et al., 2007, Schaaf et al., 2005). However the data in this project contradicts the work by Kato et al. (2010). Considering Fe and Zn did not decrease in wildtype grains harvested from CdCS, it is possible that the over-expression of *OsNAS* could be responsible for the increased Cd loading. It is proposed that this was due to an abundance of NA molecules capable of binding Cd^{2+} ions and due to the 'mimic' nature of Cd to Zn ions. It is also possible that Cd transport has occurred via Zn or Fe -specific transporters. This hypothesis has previously been supported in several studies providing strong evidence that the Fe transporters *OsIRT1* and

OsIRT2 are partly responsible for Cd^{2+} influx into root cells (Eide et al., 1996, Vert et al., 2002). Nakanishi et al. (2006) also suggested the involvement of other transporters such as *OsZIP1* as possible Cd^{2+} transporters. This was further confirmed by Lee and An (2009) who reported that *OsIRT1* can transport Cd^{2+} as well as Fe^{2+} and Zn^{2+} in *OsITR1*-overexpressed rice plants. To truly explore this hypothesis, large scale trials, with an expansion of cell-type specific controlled over-expression of all three *OsNAS* genes, preferably in existing CdCS would be required in any future work.

There is a trend in decreasing Fe concentration in T2 seed when compared to that of T1 (Table 3). This was originally attributed to the pathogen infection, which is known to affect the subsequent generation. However, as controls do not seem affected this was not the likely cause. Sterility and poor germination rates (decrease of 80% compared to non-infected plants) could be due to the deposition of helvonic acid produced by the pathogen (Bridge et al., 1989, Rahman et al., 2007).

4.4.2 Closing remarks

It is tempting to suggest that the increased NA in transgenic *OsNAS* lines has resulted in increased Cd accumulation compared to WT plants. However, this experiment was compromised by considerable factors. An original objective of this project was to perform destructive elemental analysis on plants at varying growth periods to ascertain the impact of Cd uptake in the plant. This may shed light on the Cd uptake mechanism and its relationship to Fe uptake and NA transport and should not be omitted in future analysis.

Subsequent research must investigate the true chelation potential of Cd within the plant. This can be performed using qPCR analysis to understand the up-regulation of other transporters and expression of proteins that may be implicated in the Cd uptake and transport due to the over-expression of *OsNAS* in the plant. This might provide clues as to how Cd is complexed within the cell.

The potential for *OsNAS* over-expression plants to be used in phytoremediation of Cd contaminated soils could also be an important investigation in future work, taking a new direction and moving away from human health. This has been reported as a positive method to remove Cd from rice fields with a reduction in both soil and grain Cd content as a result of growing high Cd accumulating rice crops on contaminated land (Ibaraki et al., 2009, Murakami et al., 2009).

Chapter Five: Endosperm specific over-expression of *OsVIT1*

5.1 Introduction

5.1.1 Iron deficiency- the human epidemic

Iron deficiency affects over a third of the world's population, with the same proportion of people living in extreme poverty. The epidemic of extreme poverty, poor human health and food security has been of great concern over the past six decades. As a means to target the impending food security crisis during the 1960's, the Green Revolution sought to increase production of cheap cereals like rice and wheat, in turn, reducing production of relatively expensive livestock. Arguably, this may have had a negative implication on the moderation of diets (Graham et al., 2012). As millions suffer extreme poverty around the world, more rely on inexpensive foods like rice while nutrient rich vegetables or animal products are often neglected, thus resulting in a nutrient deplete diet. This has now led to a new movement - combating human micronutrient deficiencies with biofortified cereal crops.

The enormity of such a challenge is exacerbated by the lack of understanding regarding micronutrient storage in plants. Mechanisms implicated in Fe distribution, loading and storage within the grain are of particular importance. Recent characterisation of the vacuolar iron transporter (VIT) in *Arabidopsis* and its two homologs in rice (*OsVIT1* and *OsVIT2*) has revealed the vacuole as a key target to investigate new sink-source relationships in plants, as a means to further enhance Fe levels in the grain.

5.1.2 Vacuolar protein storage in plants

Iron storage proteins such as ferritin, are limited to chloroplasts in plants (Li et al., 2001), however, the vacuole is also a vital Fe storage unit. Vacuole development during parenchyma differentiation plays an important role in osmotic turgor and cytoplasmic homeostasis (Johnson et al., 1990). The vacuole is also important in protein and enzymatic storage. Protein storage vacuoles (PSV) develop during seed development (Hohl et al., 1996) and lytic vacuoles (LV) are abundant in vegetative tissue. The PSV is a tripartite organelle comprised of matrix, crystalloid and globoid regions (Lott and Spitzer, 1980, Weber and Neumann, 1980). Investigations of the rice grain PSV have shown matrix and crystalloid regions that specifically house storage proteins (Jiang et al., 2001) such as prolamin and glutamin (Takahashi et al., 2005). The globoid inclusion of the PSV stores the cation deposit phytin, contributing 90% of the grains total P (Otegui et al., 2002).

5.1.3 Vacuolar iron storage gene families

The first described vacuolar Fe storage transport protein was the cation Ca^{2+}-sensitive cross-complementer in yeast (*ScCCC1*) (Li et al., 2001). It was shown that the yeast can survive without exogenous Fe and was concluded that the yeast internalise the ions for latent distribution. However, *CCC1*-knockout yeast mutants (*ccc1*) accumulated less Fe in vacuoles, and showed reduced Fe toxicity tolerance. Complementation of *ScCCC1* in *ccc1* mutants resulted in an increase vacuolar Fe and Mn.

An increase in vacuolar Fe and Mn was also observed when the *Arabidopsis* ortholog (*AtVIT1*) was over-expressed in the *Δccc1* mutant yeast (Kim et al., 2006). In this study three dimensional synchrotron tomography images have captured the localisation of *AtVIT1* to provascular strands of the *Arabidopsis* seed, with significant increases in gene expression identified during embryogenesis. This would be in agreement with reports showing expression of the tonoplast intrinsic protein (αTIP) is elevated during late seed maturation, for the distribution of essential nutrients to the developing grain (Herman and Larkins, 1999). There exist two orthologs to the *ScCCC1* gene in the plant kingdom in rice, *OsVIT1* and *OsVIT2*. (Zheng et al., 2009) has shown *OsVIT1* to be important in the regulation of intracellular transport and storage of Fe, with expression down-regulated during Fe deficiency. This is in contrast to *AtVIT1* which is not Fe homeostatically-dependent (Kim et al., 2006). (Zhang et al., 2012) published interesting data implicating the role of *OsVIT1* and *OsVIT2* as Fe and Zn localisation regulators in flag leaves, with regulation in vacuoles important during potential sink-source mode of nutrient transport. This is similar to findings in *Arabidopsis* where localisation of Fe was controlled by *AtVIT1* in the seed (Kim et al., 2006, Roschzttardtz et al., 2010).

5.1.4 Nicotianamine - a means to increase grain iron

Unlike the Fe storage properties within the *VIT* family, *OsNAS1*, *OsNAS2* and *OsNAS3* are known to be directly involved in Fe uptake from soil, long distance transport and grain loading. Nicotianamine synthase (NAS) is important in the production of NA, a known metal chelator. Nicotianamine binds Fe (and other cations such as Zn) and transports the metals from roots, to shoots and grain. In rice,

NA is metabolised to produce PS that are released from the roots and bind rhizospheric ferric ions (Fe^{3+}). This complex re-enters the plant, allowing NA to bind the newly acquired Fe and transport it through the plant. In this thesis, *OsNAS2* has proven to be a promising candidate for Fe enrichment in transgenic rice grains (see Chapter Two for more details). Furthermore, similar findings have been published for rice and wheat (Johnson et al., 2011).

Whilst there have been increases in Fe levels in the *OsNAS2* transgenic grain, and ICP evidence to suggest Fe is enriched in the endosperm (compared to non-transformed grain), it has been noted that this elevation in endosperm Fe is limited to the outer edge of the grain, both in the aleurone and sub-aleurone (see Chapter Three of this thesis). Figure 1 below schematically represents the distribution of Fe in typical, non-transformed rice grains. This pattern is similar for the *OsNAS2* transgenic lines, but with the spread of Fe deposition extending further into the grain, as shown. More detail on Fe deposition can be seen in the synchrotron XRF images available in Chapter Three of this thesis. The Fe distribution in both non-transformed and transgenic rice grains impacts rice preparation in commercial practises, for example milling conditions for commercial use can result in reduced retention of enriched Fe. It is therefore important to focus on increasing Fe further into the endosperm. Over-expression of *OsVIT1* has been chosen as a candidate to achieve this.

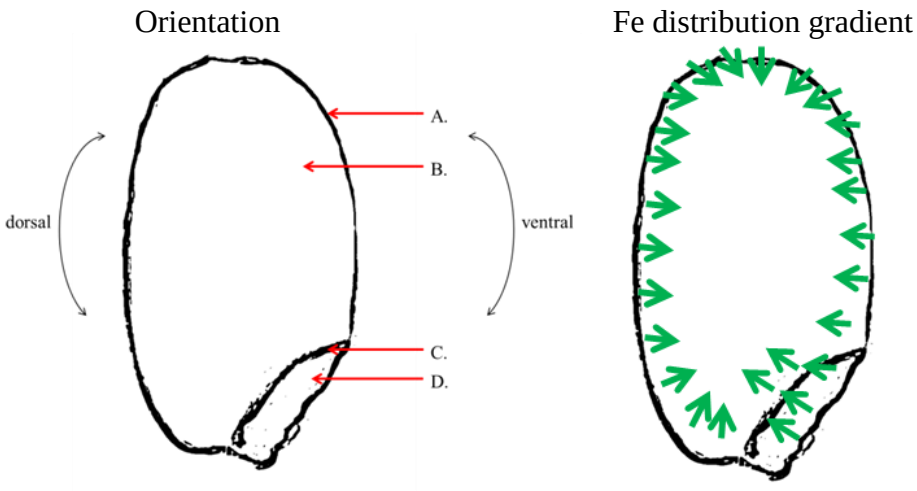

Figure 1: Schematic representation of Fe distribution across the whole rice grain

5.1.5 Aims of current study

It is believed that *OsVIT1* over-expression, controlled by the endosperm specific promoter *TdPR60* will result in Fe deposition centralised in the endosperm and not limited to the outer edge of the grain. More specifically, it is hypothesised that this will result in elevated Fe accumulation in vacuoles in the endosperm.

Furthermore, in the background of an *OsNAS2* over-expression line, it is expected that the over-expression of *OsVIT1*, again controlled by *TdPR60*, will result in enhanced Fe accumulation in the grain, with an increased source/sink relationship (source/sink referring to a concentration gradient dynamic occurring at the site of interest, in this case the endosperm). By increasing the trafficking of Fe into the endosperm via *OsNAS2*, more Fe could be made available in the cytoplasm for *OsVIT1* to deposit Fe into the vacuole of endospermic cells. It is expected that the distribution of Fe in the grain will be both centralised in the endosperm and externalised to the endosperm, giving greater uniformity to Fe deposition.

5.1.6 Endosperm-specific control of *OsVIT1*

To achieve endosperm specific expression of *OsVIT1* in this study, a wheat-derived promoter, *TdPR60*, was used. It has been shown that expression of *TdPR60* is endosperm specific in wheat grains. This work by (Kovalchuk et al., 2009), identified the control of *TdPR60* by β-glucuronidase (GUS) expression resulted in expression localised to endosperm transfer cells surrounding the nucellar projection of the grain. Interestingly when expressed in rice, *TdPR60* was localised centrally within the starchy endosperm.

5.2 Materials and methods

5.2.1 Plasmid vector construction (*TdPR60:OsVIT1*)

The sequence for *OsVIT1* was compared to the *AtVIT1* gene sequence and was found to share 64% homology according to the Rice Genome Annotation Project (2013). The locus for this gene is Os04g0463400 (Accession number NM_001059545.1). The cDNA fragment for *OsVIT1*, of 759 bp (see Appendix Three) was synthesised by DNA2.0 (Menlo Park, California, USA) which was inserted into an Invitrogen Gateway pDONR221 donor vector as per DNA2.0 procedures.

5.2.2 Agarose gel electrophoresis

DNA products from PCR or restriction enzyme digests were analysed via agarose gel electrophoresis using a 1% agarose (w/v) and 1x TAE buffer (0.04 M Tris acetate and 0.001 M EDTA) solution. Syber Safe DNA Gel Stain (Invitrogen) added as per manufacturer's instruction prior to solidifying allowing the DNA products/ fragments to be imaged under UV light. Samples were combined 1:1 with 0.15% Orange G loading buffer (Sigma-Aldrich), loaded into gel and run at 130V for approximately 1 hour. Images viewed under GelDoc imaging system (BioRad).

5.2.3 Generation of *Td:PR60::OsVIT1* vectors

Sequence verified endosperm specific promoter (*TdPR60*), in a destination vector (pMDC32), was made available by Sergiy Lopato at the Australian Centre for Plant Functional Genomics. A Gateway® ligation was performed according to protocols established by Invitrogen to place the *TdPR60* construct upstream of the *OsVIT1*

construct. Prior to ligation, a restriction enzyme digest using *EcoR*V was used to linearise DNA of the *OsVIT1* pDONR221 vector (see details below regarding restriction enzyme digests).

5.2.4 Bacterial transformations

For later infection of *Agrobacterium tumerfaciens* cells, *E.coli* cells were transformed with the ligated *TdPR60:OsVIT1* vector. The TOPO Cloning reaction with OneShot® chemically competent *E.coli* cells was used and protocols were followed according to Invitrogen standard instructions. *E.coli* colonies were grown overnight at 37°C on Luria Broth (LB) plates with 50 $\mu l.ml^{-1}$ Kanamycin- resistance selection (Kan50). Single isolated white opaque colonies were selected and grown in 5 ml LB/Kan50 cultures overnight and shaken at 37°C. To prepare plasmid DNA from bacterial transformations prior to transfection of *Agrobacterium turmerfaciens*, QIAprep Spin Miniprep kits (Qiagen®) were used according to manufacturer's instructions.

5.2.5 Preparing competent *Agrobacterium* cells

Competent *Agrobacterium tumefaciens* cells, strain AGL1, encoding resistance to rifampicin were prepared in autoclaved 10 ml cultures with 50 $\mu l.ml^{-1}$ rifampicin selection (TYNG/Rif50). TYNG media comprised of 10 g/L bacto-tryptone, 5 $g.L^{-1}$ yeast extract, 5 $g.L^{-1}$ NaCl, 0.2 $g.L^{-1}$ $MgSO_4.7H_2O$ prepared in RO water, pH adjusted to 7.5. After 24 hours, 1 ml of the culture was added to 30 ml TYNG/Rif50 cultures. Cultures were oscillated for 5 hours at 28°C until opacity was visible and cultures were placed on ice for a further 10 minutes. Samples were centrifuged at

4500 rpm, 4°C for 10 minutes and supernatant discarded. Pellets were resuspended in 500 µl of 20 mM $CaCl_2$ which had been stored on ice. AGL1 cells were transformed with linearised *TdPR60:OsVIT1* plasmid using the freeze-thaw method.

5.2.6 Freeze-thaw transformations of *Agrobacterium*

For the freeze-thaw procedure, 1 µg of plasmid DNA was extracted from *E.coli* cells (1 µl of minipreped plasmid DNA was used). Plasmid DNA was added to 100 µl of competent AGL1 cells and gently mixed and frozen in liquid nitrogen (N_2) for 1 minute. Cells were immediately thawed for 5 minutes in a 37°C water bath before adding 500 µl TYNG media. Solutions were cultured on a shaking incubator at 28°C for 2 hours. Cells were spread plated on LB/Rif50/Kan50 plates and incubated at room temperature for two days.

5.2.7 Restriction enzyme digests

Restriction digests were used to confirm DNA fragment insertions during vector ligations or to linearise the *OsVIT1* vector prior to Gateway® recombination reactions. Enzymes were provided by New England biolabs (NEB) and digests performed according to Table 1.

Table 1: Restriction Digest conditions

Additive	Volume for single reaction (µl)
DNA	2
Buffer	2
Bovine serum albumin (BSA) solution	2
H20	13.7
Restriction Enzyme	0.3
total volume	**20**
Incubated at 37°C for 90 minutes	

*EcoR*V was used to lineasise *OsVIT1* pDONR221 vector prior to Gateway® recombination reactions. Double restriction digests of *TdPR60:OsVIT1* ligated plasmid DNA from *E.coli* were used to confirm vector insertions post QIAprep Spin miniprep procedure, using both *Sac*I and *Hind*III enzymes. Appropriate buffers pertaining to each enzyme were used according to the manufacturer's instructions. Digests were confirmed on a 1% agarose gel.

5.2.8 Generating transgenic plant material

The rice transgenesis protocols were modified from those established by Sallaud et al. (2003). Briefly, embryogenic nodular units arising from scutellum-derived callus were generated using transgenic constitutive *OsNAS2* over-expression rice grains (Johnson et al., 2011). Calli were then co-incubated with AGL1 cells containing the *TdPR60:OsVIT1* construct and grown on LB and geneticin plates for two weeks. Geneticin-resistant shoots were regenerated after nine weeks, after which vigorous shoot and root development on calli was noticed. Rooted T0 calli were prepared, placed in growth media tubes and grown in growth chambers for four weeks (110-

130 mM/mPAR, cycle of 12 hours light/dark, 28°C). Specific materials and methods, including media preparation are available in Appendix Six a. and Six b. of this thesis.

Rooted regenerated plantlets were transferred to the growth room in Jiffy peat pots, acclimatised to glasshouse conditions under mini-greenhouse units and moved to soil after 15 days. Soil used was a modified version of soils published by Hoagland and Arnon (1950) which was comprised of sterilised sand, peatmoss and hydrated agricultural lime at a pH of 6.5 (UC Davis mix). Plants were cultivated in a greenhouse (12 day light hours, 28ºC / 24ºC day/ night temperature, 70% humidity). Plants were destroyed post seed-filling due to Australian Quarantine Inspection Services (AQIS) regulations implemented during an infestation of *Saracladium oryza* in the greenhouse.

This process was repeated using non transformed (wildtype) *Orzya sativa ssp. Japonica cv.* Nipponbare grains to create endosperm specific *OsVIT1* transgenic lines (without the background of 35S:*OsNAS2* over-expression).

T1 grain was sterilised in 70% ethanol for 5 minutes 30% bleach (v/v) and 1% Tween 20 (v/v) and agitated for 30 minutes in reverse osmosis (RO) water for 10 minutes. Seeds were placed on Petri dishes lined with Whatman filter paper Number 1 containing 5 ml RO water, and incubated at 28°C with 24 hours light for one week. Seedlings were grown in similar soil and greenhouse conditions as stated for T0 plants. After 1 month plants were destroyed due to AQIS instruction, no seed was collected.

5.2.9 Iron concentrations of grain

Iron concentrations were determined for T1 grain only. Grains were manually threshed, and 25 brown grains were randomly selected for analysis. Inductively coupled plasma optical emission spectroscopy (ICP-OES) was used to determine elemental concentrations in brown grains, using methods described by (Wheal et al., 2011).

5.3 Results

5.3.1 Growth of transgenic plant material

Transgenic T1 rice grains constitutively over-expressing *OsNAS2* were used to generate 'twice transformed' plants. Calli generated from once-transformed *35S:OsNAS2* were transformed a second time, to over express *TdPR60:OsVIT1*.

We successfully developed 18 *35S:OsNAS2: TdPR60:OsVIT1* rice plant events using stable *Agrobacterium* transformation methods (see Figure 2). Interestingly, calli generated from wildtype rice grains and transfected with AGL1 cells containing *TdPR60: OsVIT1* vectors did not progress beyond the stage of producing geneticin-resistant shoots as depicted in Figure 2B. Calli became dry and unsuitable for shoot proliferation, unlike the well-developed calli in Figure 2D below. Therefore, no plants were generated with endosperm specific over-expression of *OsVIT1* in a non-transformed background line.

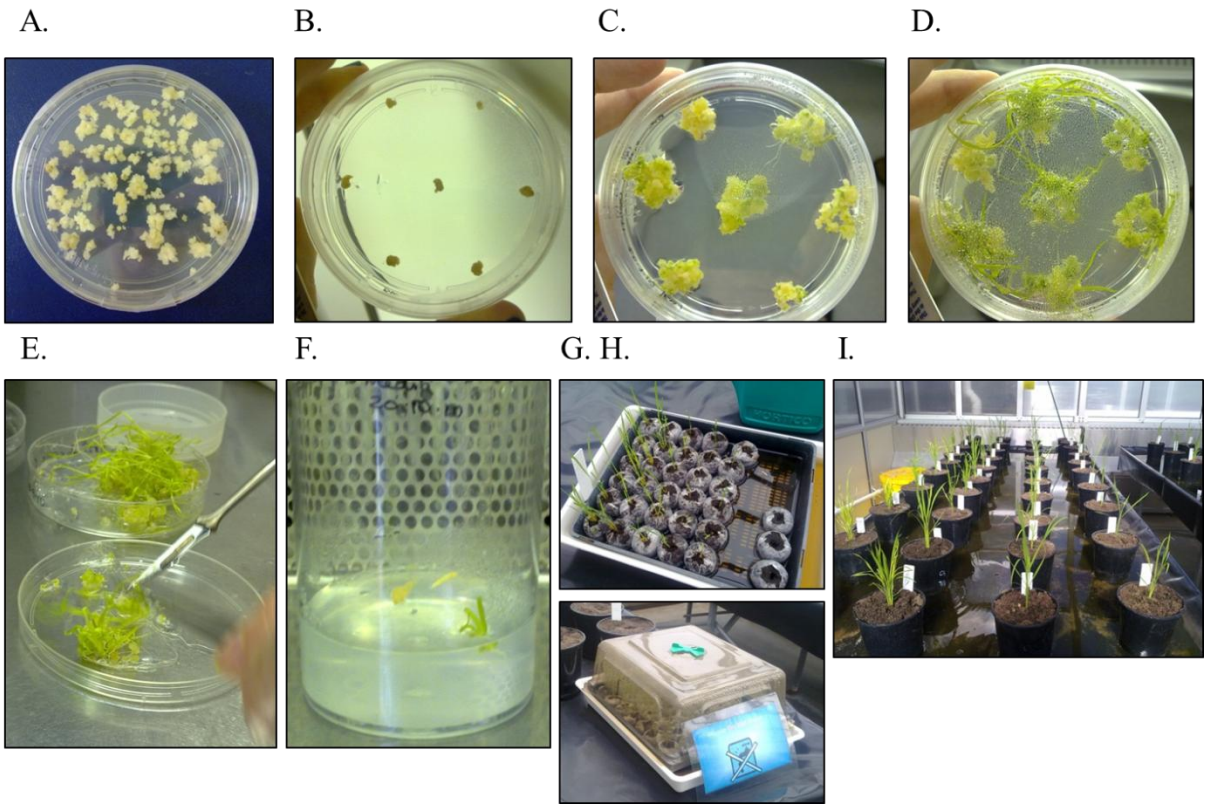

Figure 2: *Agrobacterium* mediated transformations of rice (previously transformed to constitutively over-express *OsNAS2*) with the endosperm specific over-expression of *OsVIT1*.

Calli developed from 35S:OsNAS2 rice grains (A) were inoculated with *Agrobacterium* carrying *TdPR60:OsVIT1* constructs (B). Two week old geneticin resistant calli (C) were allowed to generate shoots for nine weeks (D), after which time, strong plantlets were isolated (E) and grown on rooting media (F) for four weeks. Plantlets were then moved to jiffy pots (G) in miniature greenhouses (H) to acclimatise for over two weeks. Plants were then transferred to 1L UC Davis soil and cultivated in greenhouse conditions (12 day light hours, 28 ºC/ 24 ºC day/ night temperature, 70% humidity for three months. At this point, plants with mature seed were destroyed due to pathogen infection. T1 seed was collected.

5.3.2 Destruction of T0 and T1 plants due to pathogen infections

As it has been mentioned previously in this thesis, several outbreaks of *Sarocladium oryzae*, or sheath rot, occurred in the glasshouse containing plants belonging to this project and those of other students (see Chapter Two section 2.3.7 Expanding progeny to T2 and T3 seed). In this particular instance, the T0 plants were involved in the second outbreak of the pathogen (in reference to Chapter Two circumstances pertaining to the first outbreak). According to Australian Quarantine Inspection Services (AQIS) all plants grown in implicated glasshouses were ordered to be destroyed by autoclave treatment, regardless of pathogen infection. Any T1 grain collected was harvested and ICP analysis was performed on this grain. Samples of T1 grains were also planted to generate T1 plants (and thus T2 grain), once the glasshouse reached acceptable improvements outlined by AQIS. However, a third outbreak of the pathogen occurred, and T1 plants were destroyed prior to the reproductive stage, no material was analysed for genetic or phenotypic identification.

5.3.3 Phenotypic analysis of T1 grain

There is great potential for Fe enhancement within several *35S:OsNAS2: TdPR60:OsVIT1* lines. Lines 7 and 18 have over 35 μg g^{-1} Fe in the brown grain (Table 2), over 40% more than the majority of the lines generated. The most interesting line is Line 12 with 57 μg g^{-1} Fe in the whole grain. More importantly, when compared to wildtype grain used in Chapter Two of this thesis (grown independently of these lines but in similar conditions), it is clear lines 7, 12 and 18 exceed the Fe loading of wildtype grain. Strong increases in Zn are also noted in this line, with findings consistent with those in brown and white transgenic cell type

specific *OsNAS* grains presented in Chapter Two of this thesis and those published by Johnson et al. (2011). Of note is the minimal increase in P in all lines which may suggest little change to phytate concentrations in the grain, further implying less potential anti-nutrient activity and increased Fe bioavailability. Interestingly, Line 4 shows limited Fe increase, enhanced Zn concentration (41 μg g^{-1} compared to the mean 35 μg g^{-1}) and higher P than most lines (4400 μg g^{-1} compared to a mean of 3600 μg g^{-1}). Future genotypic analysis on this line would provide important information regarding this difference in elemental concentrations in this line and its relationship with *OsVIT1*.

Without true controls it is impossible to assign any significance to these findings. Trends in the data can however be compared to non transformed rice grown and presented in Chapter Two of this thesis (see Section 2.3.3). Average element concentrations for wildtype plants are shown in Table 2 below. It is clear that the four lines (4, 7, 12 and 18) do present themselves as interesting lines compared to wildtype rice as they are well within two standard deviations of the Fe concentration amongst all the lines (Figure 3) with Line 12 well exceeding the range found in wildtype grain.

Table 2: Elemental concentrations in T1 transgenic *OsNAS2:TdPR60:OsVIT1* brown grain

Values for wildtype grain samples are averages of values used in Chapter Two of this thesis (see Section 2.3.3 and Appendix One) and serve as a comparison tool only. These plants were not grown simultaneously to those used in this chapter. Lines 1-18 represent individual plants and single sample analysis.

	element concentration µg g^{-1}		
	Fe	**Zn**	**P**
wildtype*	**19**	**29**	**4317**
Line 1	25	31	3300
Line 2	20	28	3300
Line 3	21	26	3400
Line 4	26	41	4400
Line 5	22	30	3800
Line 6	19	26	3000
Line 7	36	44	3400
Line 8	21	33	3700
Line 9	21	29	3600
Line 10	21	32	3300
Line 11	20	29	3600
Line 12	57	69	4800
Line 13	24	37	3900
Line 14	18	30	3500
Line 15	19	33	3800
Line 16	23	38	3700
Line 17	18	29	3700
Line 18	37	46	3900

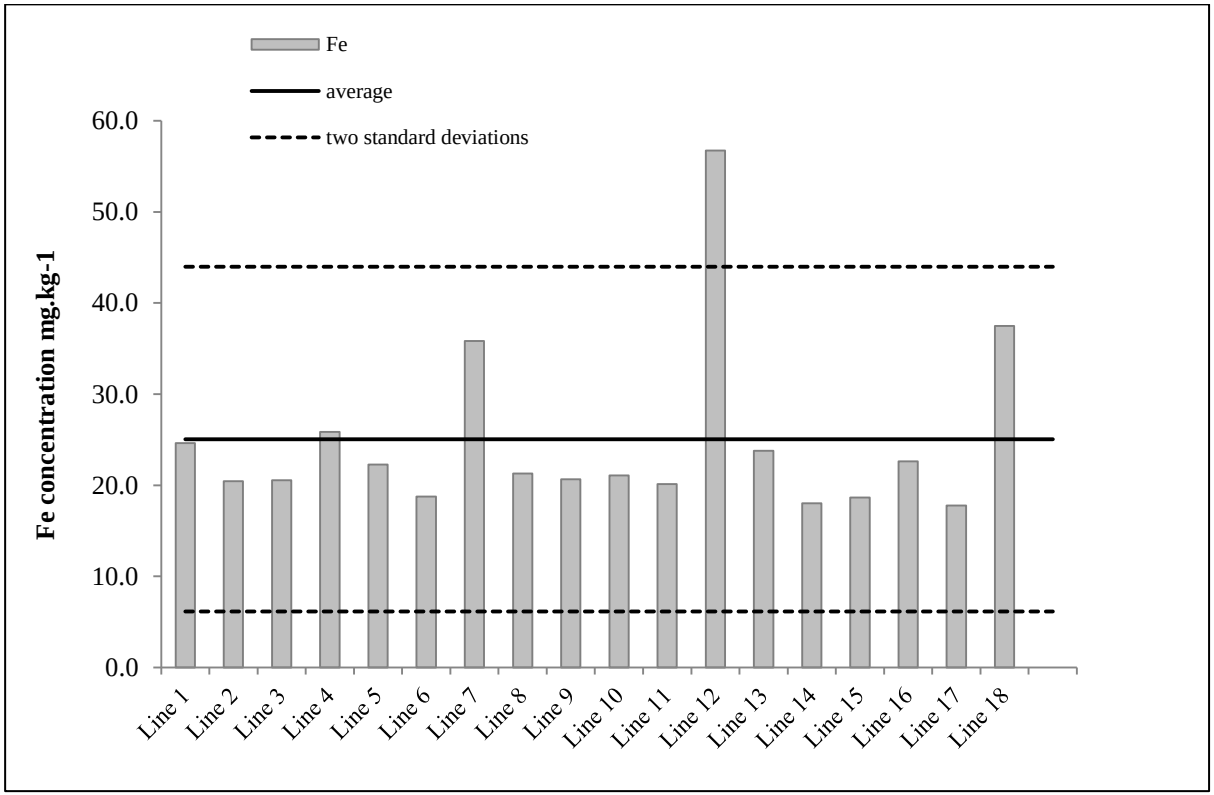

Figure 3 : Fe concentrations are within two standard deviations of the mean for all transgenic lines. Brown grain (n=25) were analysed via ICP-OES to obtain concentrations available in Table 2.

5.4 Discussion

5.4.1 Project development

It is important to note that at the time of project development for this current study little research on *OsVIT1* was published, with the Rice Genome Annotation Project being the only source of expression data available (Rice Genome Annotation Project, 2013). From here it was understood that *OsVIT1* was expressed in leaf tissue, with little or negligible expression observed in the endosperm. This current project was designed as a proof-of-concept study with the aim of using *OsVIT1* to enhance Fe loading into rice grains, therefore, it was important to establish whether *OsVIT1* was expressed in grain at all or if the negligible expression data was indicative of little or low vacuolar development in endosperm. Several attempts to synthesise cDNA from grain RNA were unsuccessful (data not shown) however the presence of vacuoles in rice endosperm is well reported (Bechtel and Juliano, 1980, Bechtel and Pomeranz, 1977). As a result commercially synthesised *OsVIT1* cDNA was obtained for this study.

5.4.2 Lacking controls

Due to previous issues with the destruction of crops due to fungal pathogen (see Chapter Two), it was decided that the generation of these transgenic plants would be a preliminary test for the transformation process. If strong plants developed, subsequent genotypic and phenotypic analysis would have been performed on progeny and not on T0 lines. It is for this reason that no wildtype, non-transformed or null segregant controls are present in the elemental analysis of T1 grain (Table 2 and

Figure 2). Attempts were made to generate *TdPR60:OsVIT1* transgenics using only wildtype grains (no transgenic over-expression of *OsNAS2*), therefore acting as the single transformation event; however these lines did not develop beyond callus stage. Such controls were intended to be used once it was certain that no pathogen existed in the glasshouses where the transgenic rice plants were grown. As mentioned above, a new pathogen infection did result in the destruction of this crop, and embargos imparted by AQIS prevented the growth of any further progeny. The preliminary analysis of T1 grain is merely a hopeful insight into the potential for future work. Interestingly we see in Figure 2 that all lines produced grain with Fe concentrations within two standard deviations of the mean, and that three of these lines have over 35 μg g^{-1} Fe in the brown grain. With up 56 μg g^{-1} Fe in the *OsNAS2::TdPR60::OsVIT1* line 12, it is clear that there is a great deal of potential for future work with this project. Clearly presence of the transgenes needs to be confirmed, and it is recommended that both Southern Analysis and qPCR be performed on future progeny, to compare transcript levels within the lines. Also it is necessary to perform ICP-OES on milled grain to determine the Fe content within the endosperm. Synchrotron radiation of endosperm would also contribute greatly to the need to understand whether this multiple transformant has in fact encouraged more Fe loading into the endosperm compared to single transformants and wildtype grain.

5.4.3 Future projections still stand

It is hypothesised that Fe concentrations of twice-transformed rice will be greater than that of wildtype rice as a result of the increased source/sink (*OsNAS2 / OsVIT1*) relationship. It is uncertain as to whether the Fe concentration of *OsVIT1* grain will

vary significantly compared to wildtype grain however it is expected that more Fe will be stored in the vacuoles of the endosperm, resulting in higher concentrations of Fe in milled grain compared to wildtype grain. As depicted in Figure 4, we propose that the distribution of Fe in the new transgenic rice grains will differ to patterns normally seen in wildtype rice (Figure 4B) where Fe distribution dominates embryo, scutellum and aleurone. As shown in Chapter Three and confirmed by Johnson et al. (2011), this distribution extends further into the grain towards the endosperm in transgenic *OsNAS2* over-expression lines, in higher concentrations than wildtype. This is formulated in Table 3. It is expected that the distribution of Fe in rice grain over expressing *OsVIT1* under the control of the endosperm specific promoter *TdPR60* will be centralised in the endosperm, extending out toward the edge of the grain (Figure 4C). Therefore it was hypothesised for this project that the combination of endosperm specific *OsVIT1* in *OsNAS2* over-expression lines will result in grain with increased Fe, localised to the centre of the endosperm (compared to non-transformed wildtype rice) (Figure 4D). A hypothesised projection of Fe concentration in transgenic grain is also presented in Table 3, with the expected trends in concentrations increasing in transgenics compared to non-transformed rice. As it is already known that the T1 *OsNAS2* lines have positive increases in Fe concentrations compared to wildtype, it is suggested that this trend will continue in twice-transformed *OsVIT1* lines, resulting in Fe enhanced rice endosperm. It is not possible to assume *OsVIT1* over-expression will result in significant increases in Fe, however, it is possible to suggest that the promotion of *OsVIT1* expression by *TdP60* will result in higher accumulation of Fe in vacuoles within the starchy endosperm.

Therefore, this may increase the level of Fe retained in milled grain post-milling, resulting in greater bioavailability.

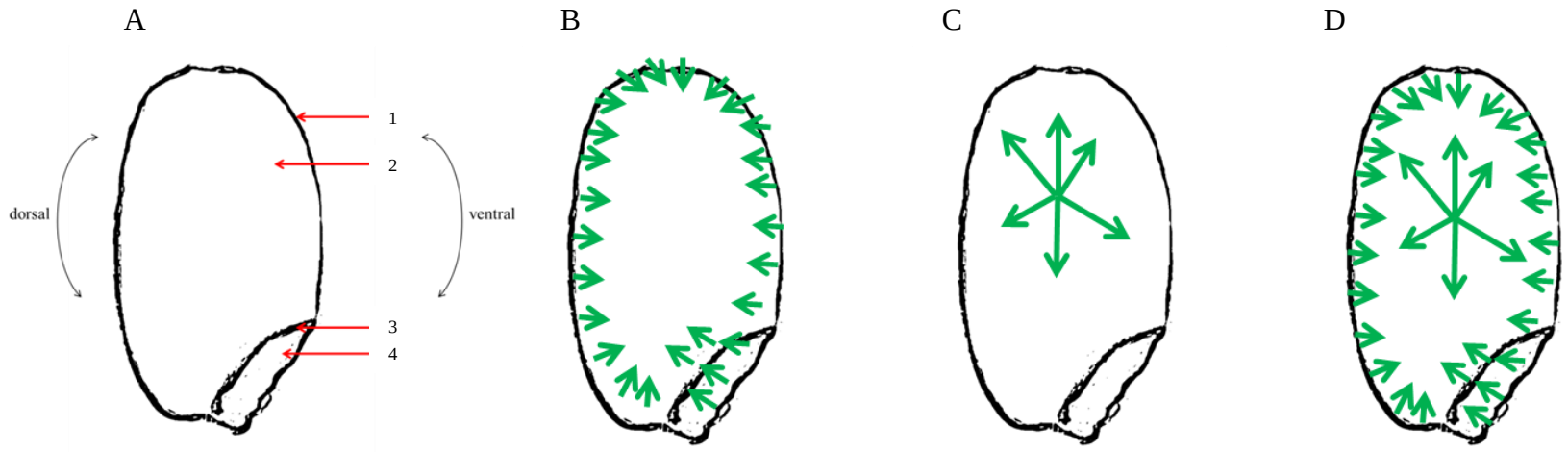

Figure 4: A simplified schematic of hypothesised trends in rice endosperm concentrations and distributions for new transgenics

(A.) The entire grain is enclosed by pericarp tissue and a single cell layer of aleurone tissue (1); directly interior to the aleurone lies the starch filled parenchyma of the endosperm (2); on the ventral side of the grain sits the scutellum (3); and the embryo (4).
(B.) Fe distribution in wildtype, non-transformed rice entering the endosperm via aleurone, pericarp, embryo and scutellum.
(C.) Hypothesised Fe distribution in endosperm specifically controlled *OsVIT1* over-expression lines showing more centralised loading of Fe into endosperm than wildtype
(D.) projected schematic of Fe distribution in *OsNAS2::TdPR60::OsVIT1* grains with additionally enhanced Fe loading in the grain with heightened Fe deposition in the centre of the endosperm.

Table 3: Iron concentration trend projection for transgenic varieties.

Transformation event	genotype	Fe concentration trends
nil	wildtype	x
single	*35S::OsNAS2*	x + y
single	*TdPR60::OsVIT1*	x + z
double	*35S::OsNAS2* + *TdPR60::OsVIT1*	x + y + z

The insight into increased sink/source relationships with *OsNAS2* and *OsVIT1* and the impact on Fe enrichment in the endosperm has not conclusively been investigated within this chapter. The development of these lines and the preliminary Fe concentrations within the transgenic plants does warrant further investigation and the potential for a plethora of informative and interesting data is certain to develop with future analysis within this project.

Chapter Six: Final Discussion

The incidence of human micronutrient malnutrition reportedly affects over 30% of the world's population (Graham et al., 2012). This value hasn't changed in over 20 years of scientific publications. In this time, the global population has grown 40%, from 5 billion to 7 billion people, demonstrating that this apparent, stagnant epidemic has in fact been spreading as fast as the population has increased. The need for biofortified food products to act as a vehicle to combat this problem has triggered a plethora of recently conducted research in this field.

This project was designed to enter this field with a sole purpose of generating Fe-rich, Fe-bioavailable rice that could provide a model for improving the Fe nutrition of the staple food crop, rice. To explore this, there were four major objectives. Firstly, the potential for cell type specific over-expression of *OsNAS* genes to explicitly and efficiently enhance Fe in the endosperm of the rice grain was investigated in Chapter Two. Synchrotron technologies were used to elucidate the distribution of the enhanced level of Fe, to establish how Fe was deposited in the grain (Chapter Three). An enhanced uptake of Cd was a concern as nicotianamine is able to bind with this toxic metal, and Chapter Four strongly suggests that NA may be directly involved in the uptake and loading of Cd in the rice grain. Finally, double transformants were developed (Chapter Five) to explore the potential of *OsNAS2* and *OsVIT1* to further enhance Fe loading into the rice endosperm.

The most interesting conclusion from this entire project is that *OsNAS2* over-expression in root cortical cells provides the greatest Fe loading into the grain, which is highly bioavailable and can be seen by synchrotron radiation imaging. The work with Cd and Os*VIT1* represent preliminary studies and while further research must be

conducted to validate results obtained in this thesis, there is a clear need for caution in over-expression of Os*NAS* genes as this has the potential to lead to enhanced Cd uptake on soils with a higher level of available Cd.

This entire body of work has yielded several highly relevant results in the biofortification research area, that enable one to design a network of projects that would further develop the biofortification strategy into the future. It cannot be ignored that many obstacles stood in the path of success. The profound loss of data and material due to the pathogen infections resulted in compromised data, loss of controls and lack of yields. Embargo requirements placed by quarantine regulations meant grain could not be milled for analysis and time inhibitions prevented further data collection. Southern blots, genotyping and strong controls were to be included in subsequent progeny and must not be ignored in future work. The negative impact left on this work is not to the detriment of its potential success, and future publications will certainly arise if the grain can be grown in approved quarantine conditions.

The finding that *OsNAS2* over-expression yields the greatest Fe accumulation in the endosperm is the most important finding of this thesis. Constitutive over-expression was further investigated by (Johnson et al., 2011) and as this work contributes greatly to this thesis, it has been included as Appendix One. A suggestion was made in this thesis that cell-type specific over-expression of *OsNAS2* may up-regulate endogenous *OsNAS* genes, therefore producing more NA and Fe uptake. To fully attribute the increases in Fe seen in Chapter Two to the root cortex specific genotype, expression of all the *OsNAS* genes should be investigated. It would also be interesting to overexpress RC *OsNAS2* in the background of an RNAi line to suppress endogenous gene expression. The complexity of a twice- transformed plant

may be an issue, considering we don't fully understand the genetic disruptions occurring in our transformants. However, a single transformation event with a two-gene cassette producing concomitant expression could alleviate this problem. This was successful for (Masuda et al., 2013) where soybean ferritin and barley promoter genes were expressed in rice to produce Fe biofortified grain. Interestingly, rice genes were not used to produce these biofortification lines and less than 6 μg g^{-1} Fe was found in the endosperm. Whilst this was a positive increase in Fe concentrations, we clearly see that over-expression of rice *OsNAS* genes far exceeds the Fe accumulation in grain published, demonstrating the importance of pursuing further research in the *OsNAS* genotype. Southern Blots and qPCR are vital for future analysis to confirm single gene copy and expression levels of our genotypes however we strongly believe these lines will still prove to be efficient Fe accumulators in subsequent progeny. Similar work has yet to be published with many reports focussing solely on a single *OsNAS* orthologue (Lee et al., 2012).

In Chapter Two we saw a strong increase in ferritin production from transgenic lines, and Chapter Three showed no phytate granules in the sub-aleurone; according to nano-SIMS analysis. Phytate analysis of the grains via HPLC methods is also vital to fully appreciate the bioavailable state of the acquired Fe in the endosperm. Also, investigations into DMA chelation of Fe in the endosperm could help explain whether we are indeed seeing Fe bind to NA or DMA in non-proteinogenic complexes noted in nano-SIMS. It would be interesting to gain a better understanding of the PS, DMA influx and efflux transporters like *OsYSL16* (Kakei et al., 2012), *OsYSL18* (Aoyama et al., 2009) and *OsTOM1* (Nozoye et al., 2011) respectively, in our *OsNAS* over-expression lines. As we suggest RC *OsNAS2* may

trigger a false state of Fe deficiency in the plant and therefore up-regulate endogenous *OsNAS*. It is without doubt that several related transporters may also receive similar signals. It would be interesting to see if this gene signalling extends beyond the *OsNAS* family so transciptomic profiling might be of use to achieve this. Also, if deficiency is triggered within the plants, this is a cause for some concern and will need further evaluation; ideally in a field setting. Outside of a field screening of the transgenic and wild-type genotypes, one could look at running critical deficiency studies in greenhouses which will give you information on external and internal nutrient requirements that will elucidate whether the transgenic plants are more sensitive to Fe (or another element) deficiency.

It then follows that several of these potential gene up-regulations may involve those implicated in Cd uptake, such as *OsIRT1* (Vert et al., 2002). Ogawa et al. (2009) demonstrated that *OsIRT1* expression indeed increased more than two fold when plants were exposed to Cd stress, by the use of rice microarray data. Whether this has occurred in our transgenics, thus enhancing the potential for Cd accumulation is yet to be explored. Again, it is important that a more global genetic analysis be performed in the cell type specific *OsNAS* lines to fully garner an appreciation for the genetic network that is developing upon the stimulus of excess NA and Fe in the plant. This has secondary implications on a subcellular level within the grain. It is known that *OsNRAMP1* (Takahashi et al., 2011) and *OsNRAMP5* (Ishimaru et al., 2012) are implicated in both Fe and Cd efflux from the cell into the cytosol. More interestingly, *OsNRAMP5* expression has been detected on the root cortex, localised to the plasma membrane (Ishimaru et al., 2012). It is possible that we have induced

Cd uptake via increased *OsIRT1* if one considers the potential that we have falsely triggered a state of Fe deficiency in the RC *OsNAS2* lines.

Interestingly this implicates the *OsNAS2::OsVIT1* lines too, as it is known that the antiporter to the *OsVIT1* is the *OsNRAMP* gene family. The efflux capacity of *OsNRAMP* is not limited to Fe. Therefore, *OsVIT1*, or an unknown transporter, could export Cd from the cytosol into the vacuolar space. Of course the *OsVIT1* lines documented in this thesis are in their infancy and remain in a preliminary state of investigation. Due to *OsVIT1* repression during Fe deficiency (Zheng et al., 2009) it is important to ascertain whether the over-expression of *OsNAS* is indeed signalling a false state of Fe deficiency in the plant as speculated in this thesis. If so, it is imperative that qPCR analysis of the *OsVIT1* transgene be obtained from subsequent plants to establish the true function of both the transgenic and endogenous genes to determine whether the transgenic plant will override the innate repression of *OsVIT1*. Analysis of the endosperm specific *TdPR60* promoter should also be investigated.

In fact due to the nature of the state of this body of work, a great deal of speculation can be extrapolated from the results. A schematic of results and projections below summarises many of these ideas. It is expected that future plans depend on the growth of cell-type specific *OsNAS* and *OsNAS2::OsVIT1* progeny to then identify single copy, genetically stable lines, and continued Fe biofortification, with no sign of pathogen induced stress. Once this is achieved, it is recommended that destructive plant analysis for phytate, NA, DMA and Fe concentrations be performed on young seedlings at critical developmental stages of growth. An example of such analysis is one that was originally designed for this thesis based on work by (Hoshikawa, 1989). Harvests of seedlings at second leaf emergence would identify significant elemental

homeostasis conditions during the development of first crown roots from the coleoptile node. A second harvest between the 10^{th} and 14^{th} leaf stage may inform us about elemental transport during the development of the flowering grain. Once the flag leaf has emerged, the plant is commencing its maturation phase and both the panicle and pollen develop. Analysis at this stage would contribute greatly to the understanding of nutrient requirement and ligand trafficking. This phenotypic and biochemical work would complement microarray technology and qPCR quantification techniques that would explore a global genetic expression map of the plants.

The successes and potential future research that have arisen from this work has far surpassed the hurdles encountered. Without doubt, the ultimate aim is to support the development of Fe-biofortified rice crops with the great and ultimate goal of combatting human nutrition. We can see from this work that the information gleaned from this thesis can lead to further, high quality research.

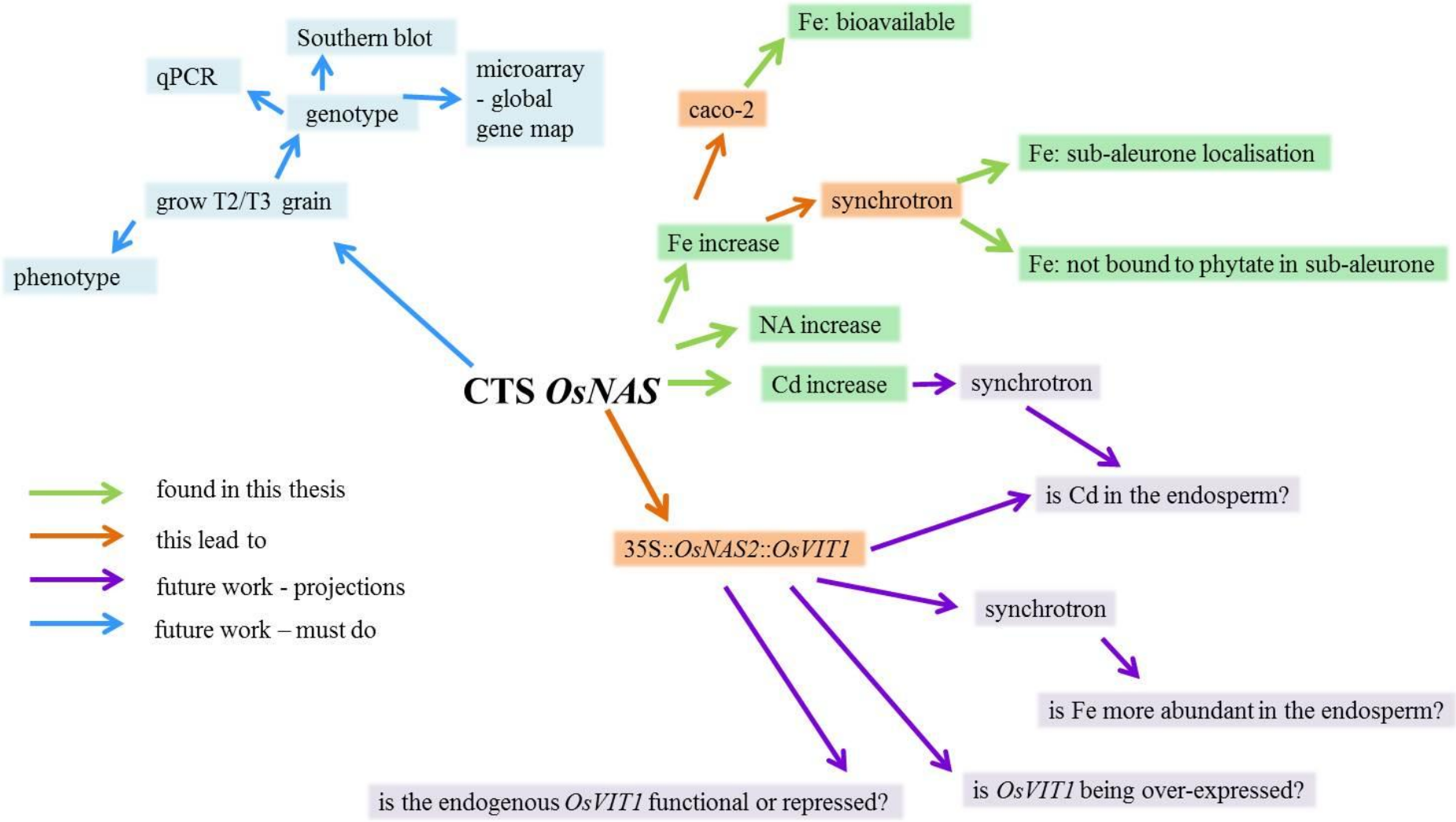
Southern blot
qPCR
genotype
microarray
- global
gene map
grow T2/T3 grain
phenotype
Fe: bioavailable
caco-2
Fe: sub-aleurone localisation
synchrotron
Fe increase
Fe: not bound to phytate in sub-aleurone
NA increase
CTS OsNAS
Cd increase
synchrotron
found in this thesis
this lead to
future work - projections
future work – must do
is Cd in the endosperm?
35S::OsNAS2::OsVIT1
synchrotron
is Fe more abundant in the endosperm?
is the endogenous OsVIT1 functional or repressed?
is OsVIT1 being over-expressed?

Appendix One- Constitutive Over-expression of the *OsNAS* Gene Family Reveals Single-Gene Strategies for Effective Iron- and Zinc-Biofortification of Rice Endosperm

Alexander A. T. Johnson[1, 2 *], Bianca Kyriacou[2, 3], Damien Callahan[1], Lorraine Carruthers[2], James Stangoulis[3], Enzo Lombi[4] and Mark Tester[2]

1 School of Botany, The University of Melbourne, Victoria 3010, Australia

2 Australian Centre for Plant Functional Genomics, University of Adelaide, PMB1, Glen Osmond, South Australia 5064, Australia

3 School of Biological Sciences, Flinders University of South Australia, GPO Box 2100, South Australia 5001, Australia

4 Centre for Environmental Risk Assessment and Remediation, University of South Australia, Building X, Mawson Lakes Campus, Mawson Lakes, South Australia 5095, Australia

*Email: johnsa@unimelb.edu.au

Abstract

Background: Rice is the primary source of food for billions of people in developing countries, yet the commonly consumed polished grain contains insufficient levels of the key micronutrients iron (Fe), zinc (Zn) and Vitamin A to meet daily dietary requirements. Experts estimate that a rice-based diet should contain 14.5 μg g^{-1} Fe in endosperm, the main constituent of polished grain, but breeding programs have failed to achieve even half of that value. Transgenic efforts to increase Fe content of rice endosperm include expression of ferritin genes, nicotianamine synthase genes (NAS) or ferritin in conjunction with NAS genes, with results ranging from two-fold increases via single-gene approaches to six-fold increases via multi-gene approaches, yet no approach has reported 14.5 μg g^{-1} Fe in endosperm.

Methodology/Principal Findings: Three populations of rice were generated to overexpress *OsNAS1, OsNAS2* or *OsNAS3*, respectively. Nicotianamine, Fe and Zn concentrations were significantly increased in unpolished grain of all three of the over-expression populations, relative to controls, and highest in the *OsNAS2* and *OsNAS3* over-expression populations. Selected lines from each population had at least 10 μg g^{-1} Fe in polished grain and two *OsNAS2* over-expression line had 14 and 19 μg g^{-1} Fe in polished grain, representing a four-fold increase in Fe content. Two-fold increases of Zn content were also observed in the *OsNAS2* population. Synchrotron X-ray fluorescence spectroscopy demonstrated that *OsNAS2* ovexpression leads to significant enrichment of Fe and Zn in P-free regions of rice endosperm.

Conclusions: We have found that the *OsNAS* genes, particularly *OsNAS2*, show enormous potential for Fe and Zn biofortification of rice endosperm. The results demonstrate that rice cultivars overexpressing single rice *OsNAS* genes could provide a sustainable and genetically simple solution to Fe and Zn deficiency disorders affecting billions of people throughout the world.

Introduction

Rice is the primary source of food for roughly half of the world's population yet the polished grain, also known as white rice, contains nutritionally insufficient concentrations of iron (Fe), zinc (Zn) and pro-vitamin A to meet daily requirements in diets based on this staple (Kush 2005; Mayer et al. 2008). Other widely consumed cereals, such as wheat and maize, are also poor sources of several key micronutrients. As a result, micronutrient deficiencies afflict billions of people throughout that world and are particularly prevalent in developing countries where cereals are widely consumed. Fe deficiency affects more than two billion people worldwide, with symptoms ranging from poor mental development, depressed immune function to anaemia, and is the most widespread nutritional deficiency in the world (Ramakrishnan 2002). The development of new cereal varieties containing increased concentrations of Fe and other essential micronutrients, an approach known as biofortification, offers an inexpensive and sustainable solution to the chronic micronutrient malnutrition problems that currently plaque people in developing countries.

Rice has the lowest Fe content of the cultivated cereal crops and a striking lack of genetic variation for this trait has hindered conventional breeding efforts from increasing its Fe content beyond 6 $\mu g\ g^{-1}$ in polished grain (Pfeiffer and McClafferty 2008, Kennedy and Burlingame 2003). To produce polished grain with 14.5 $\mu g\ g^{-1}$ Fe, the target concentration that nutritionists have recommended to meet Fe requirements in a rice-based diet, novel sources of genetic diversity for grain Fe concentration are required (Lucca et al. 2002, Hotz and McClafferty 2007). Numerous biotechnological strategies have been employed to produce rice with increased concentrations of Fe in endosperm tissues, the principle constituent of polished grain. Grain-specific over-expression of genes encoding ferritin, a Fe storage protein found in plants, animals and bacteria, has been utilized to increase the "sink" for Fe in endosperm. While this approach has resulted in 2-fold increases in endosperm Fe content (Goto et al. 1999), the relatively modest increases in Fe

content do not match the 13-fold increases in endosperm ferritin protein levels that often occur via this strategy (Qu et al. 2005), suggesting that transport of Fe to the endosperm sink is also limiting.

Nicotianamine (NA) is a chelator of transition metals that plays important roles in long- and short-distance transport of metal cations, including Fe^{2+} and Fe^{3+}, in higher plants (von Wiren et al. 1999, Takahashi 2003). NA is biosynthesized by trimerization of S-adenosylmethionine, a reaction catalyzed by the NA synthase (NAS) enzymes. Genes encoding NAS are known to be differentially regulated by iron status in a variety of plant species including maize, *Arabidopsis*, barley and rice (Mizuno et al. 2003, Klatte et al. 2009, Higuchi et al. 1999, Inoue et al. 2003), and show strong induction by Fe deficiency. Aside from its role in metal transport in plants, NA is an antihypertensive substance in humans and rice lines with enhanced NA content have been developed as potential candidates for the functional food industry (Usuda et al. 2009).

Transgenic approaches to increase NA content have often focused on over-expression of exogenous *NAS* genes in plants. Constitutive over-expression of a barley NAS gene, *HvNAS1*, in *Arabidopsis* and tobacco led to several-fold increases in seed Fe, Zn and Cu concentration of both species (Kim et al. 2005). Similar over-expression of *HvNAS1* in rice led to greatly enhanced NA concentration (15-fold increase over wild type) and 2.3- and 1.5-fold increases in Fe and Zn concentrations of polished grain, respectively (Masuda et al. 2009). Constitutive expression of an *Arabidopsis NAS* gene, *AtNAS1*, in conjunction with seed-specific expression of ferritin and phytase, led to a 6.3-fold increase in Fe concentration of rice endosperm (Wirth et al. 2009).

Relatively few studies have been done to overexpress the endogenous rice *NAS* genes (*OsNAS*) in rice. Endosperm-specific over-expression of *OsNAS1* resulted in polished grain with significantly increased concentrations of NA and Zn. While Fe

concentration was not increased by this strategy, the bioavailability of Fe was double that of controls as measured by ferritin synthesis in Caco-2 cells (Zheng et al. 2010). Recently, two activation tagged lines of rice with increased expression of *OsNAS2* and *OsNAS3*, respectively, were identified and characterized (Lee et al. 2011, Lee et al. 2009). The *OsNAS2* activation tagged line had 20-fold more NA and significantly increased Zn content in polished grain, while the *OsNAS3* activation tagged line had 9-fold more NA, 2.6 fold more Fe and 2.2 fold more Zn in polished grain. Most significantly, polished grain from the *OsNAS3* activation tagged line reversed signs of Fe-deficiency when fed to anemic mice (Lee et al. 2009).

The overall aim of this study was to constitutively overexpress all three members of the *OsNAS* gene family, individually, to assess their utility for Fe biofortification of polished rice grain via a single-transgene approach. Characterization of more than 90 independent transgenic lines overexpressing these genes revealed that all three *OsNAS* genes increase not only Fe, but also Zn, concentrations in unpolished and polished grain when expressed constitutively and those increases are positively correlated with NA concentration. One member of the *OsNAS* gene family, *OsNAS2*, was particularly effective at increasing Fe and Zn concentrations in rice endosperm and this increase was mapped in unprecedented detail using synchrotron X-ray fluorescence spectroscopy (μ-XRF).

Results

Construction of three rice populations overexpressing OsNAS1, OsNAS2 and OsNAS3

The 0.7 kb dual CaMV 35S promoter contained in the pMDC vector system (Curtis and Grossniklaus 2003) was used to drive constitutive expression of the *OsNAS1* (LOC_Os03g19427), *OsNAS2* (LOC_Os03g19420) and *OsNAS3* (LOC_Os07g48980) coding sequences in rice. The T-DNA region of the binary vectors used for transformations also contained the selectable marker gene *neomycin phosphotransferase II* that detoxifies aminoglycoside antibiotics such as geneticin (G418) and kanamycin (Figure 1). Embryogenic callus of japonica rice cultivar Nipponbare was used for *Agrobacterium*-mediated transformation of the binary vectors containing the three different *OsNAS* coding sequences. The production of 30 independent transgenic lines carrying the *OsNAS1* over-expression vector, designated the OE-*OsNAS1* population, 39 independent transgenic lines carrying the *OsNAS2* over-expression vector, designated the OE-*OsNAS2* population, and 24 independent transgenic lines carrying the *OsNAS3* over-expression vector, designated the OE-*OsNAS3* population, was confirmed by resistance to geneticin in T_0 and T_1 plants, PCR and Southern blot analysis (data not shown).

Constitutive over-expression of the OsNAS genes leads to increased Fe and Zn concentrations in unpolished and polished grain

Because nicotianamine is known to chelate and mobilize a variety of metal cations including Fe, Zn, Mn, Cu and Ni in plants (Beneš et al. 1983, von Wiren et al. 1999) we employed inductively coupled plasma atomic emission spectroscopy (ICP-AES) to characterize the elemental composition of unpolished T_1 grain harvested from the three transgenic rice populations. Two metals in particular, Fe and Zn, were several-fold higher in unpolished grain of the OE-*OsNAS* population, relative to WT grain (Figure 2), while Mn, Cu and Ni did not show significant differences from WT grain (Supplementary Table 1).

Unpolished grain Fe concentrations ranged from 25 to 56 $\mu g\ g^{-1}$ dry weight (DW) in the OE-*OsNAS1* population, 19 to 81 $\mu g\ g^{-1}$ DW in the OE-*OsNAS2* population and

21 to 63 μg g^{-1} DW in the OE-*OsNAS3* population, representing up to 2.4-fold, 3.5-fold and 2.7-fold increases, respectively, over wild type (WT) in each population (Figure 2A). Unpolished grain Zn concentrations ranged from 40 to 59 μg g^{-1} dry weight (DW) in the OE-*OsNAS1* population, 30 to 95 μg g^{-1} DW in the OE-*OsNAS2* population and 30 to 79 μg g^{-1} DW in the OE-*OsNAS3* population, representing up to 1.6-fold, 2.5-fold and 2.1-fold increases, respectively, over wild type (WT) in each population (Figure 2B). Furthermore, Fe and Zn concentrations of unpolished grain were highly correlated in transgenic lines (r = 0.83, 0.94 and 0.97 for the OE-*OsNAS1*, OE-*OsNAS2* and OE-*OsNAS3* populations, respectively) which accounts for the similar Fe and Zn profiles in Figure 2A and 2B (genotype order is the same in both panels).

Polished grain was produced from selected transgenic lines using a Kett Mill. One transgenic line overexpressing *OsNAS1* (OE-*OsNAS1S*), two independent transgenic lines overexpressing *OsNAS2* (OE-*OsNAS2B* and OE-*OsNAS2J*) and one transgenic line overexpressing *OsNAS3* (OE-*OsNAS3B*) were selected for this analysis based on large numbers of available grain to mill and Fe concentrations that fell within the upper 20% of each over-expression population. WT lines retained approximately 20% of Fe through milling, resulting in a concentration of 4.5 μg g^{-1} DW Fe in the polished grain (Table 1). The OE-*OsNAS1S* and OE-*OsNAS3B* lines retained similar amounts of Fe through milling, resulting in unpolished grain with approximately 10 μg g^{-1} DW Fe, representing a 2-fold increase over WT. The two *OsNAS2* over-expression lines (OE-*OsNAS2B* and OE-*OsNAS2J*) retained more Fe through milling (26-30%), and had up to 19 μg g^{-1} DW Fe in polished grain, representing a 4.2-fold increase in Fe content over WT. Zinc concentrations were also increased in polished grain of the transgenic lines. The OE-*OsNAS1S* and OE-*OsNAS3B* lines had approximately 49 μg g^{-1} DW Zn in polished grain, representing a 1.4-fold increase over WT. The OE-*OsNAS2B* and OE-*OsNAS2J* lines had up to 76 μg g^{-1} DW Zn in polished grain, representing a 2.2-fold increase in Zn content over WT. As with unpolished grain, the Fe and Zn concentrations in polished grain were highly correlated (r = 0.94).

Constitutive over-expression of the OsNAS genes leads to increased NA concentrations in unpolished grain that are positively correlated with Fe and Zn content

Liquid chromatography-mass spectrometry (LC-MS) was employed to determine if *OsNAS* over-expression leads to significantly increased NA concentration of the grain. Single-insert transgenic lines were selected for nicotianamine quantification experiments to ensure that null segregant lines (lines that have the lost the over-expression vector due to meiotic segregation) were produced as additional controls to WT. Three sibling T_1 lines, comprising two transgenic lines and one null segregant line, were derived from a single T_0 parental line within each of the three OE-*OsNAS* populations and grown to maturity in the glasshouse to yield T_2 grain. In addition to nicotianamine quantification by LC-MS, the Fe and Zn concentrations of T_2 grain were determined by ICP-AES.

The unpolished grain NA concentration was 18 μg g^{-1} DW for WT and did not differ significantly from unpolished grain NA concentrations of null segregant (NS) lines (Figure 3A). By contrast, unpolished grain NA concentrations ranged from 96 to 115 μg g^{-1} DW in the OE-*OsNAS1* sibling lines, 152 to 168 μg g^{-1} DW in the OE-*OsNAS2* sibling lines and 174 to 210 μg g^{-1} DW in the OE-*OsNAS3* sibling lines, representing up to 6.4-fold, 9.3-fold and 11.7-fold increases, respectively, over wild type (WT) concentrations of NA. Figure 3B demonstrates the statistically significant, positive correlation that was found between unpolished grain NA concentration and Fe and Zn content for the ten genotypes utilized in this experiment.

XRF elemental maps reveal significant increases in Fe and Zn accumulation in specific tissues of OE-OsNAS2 grain

Synchrotron X-ray fluorescence spectroscopy (μ-XRF) was used to generate colour distribution maps of several NA-related cations (Fe, Zn, Mn and Cu) in two longitudinal sections each of WT and OE-*OsNAS2A* grain. Elemental distribution in the two longitudinal sections of each grain type was very similar and therefore only one set of images is presented in Figure 4.

The maps of Fe distribution in WT and OE-*OsNAS2A* grain (Figures 4B and C, respectively) show a striking lack of this element in large portions of the endosperm. In WT grain, the highest signal occurs in scutellum and outer regions of the embryo while a very low Fe signal is detected in the outermost layers of the endosperm and the single-layered aleurone that surrounds the endosperm. No signal is detected from the inner layers of the endosperm. The OE-*OsNAS2A* grain, by contrast, has a high Fe signal in the outer endosperm and aleurone layers in addition to high aleurone and embryo signals. The inner layers of endosperm, as with WT grain, have no signal.

The maps of Zn distribution in WT and OE-*OsNAS2A* grain (Figures 4D and E, respectively) depict a radically different distribution of this element compared to Fe. In WT grain, the highest signal is observed inside the embryo (likely corresponding to the plumule) while the scutellum and outer embryo has intermediate signals A low signal is detected in a thick band comprising many outer layers of endosperm and the single-layered aleurone that surrounds the endosperm. Unlike Fe, the Zn signal extends (albeit at very low levels) throughout the endosperm of WT grain. In OE-*OsNAS2A* grain a similar pattern of Zn distribution is observed, however, the signal in the embryo and throughout endosperm tissues is considerably higher. In the outermost layers of the endosperm and the single-layered aleurone, the signal borders on intermediate signal intensity.

The maps of Mn and Cu in WT and OE-*OsNAS2A* grain (Figures 4F and G, 4H and I, respectively) show that these metals, like Fe, have no signal in much of the endosperm. The Mn signal is higher in the outermost layers of the endosperm and the single-layered aleurone of OE-*OsNAS2A* compared to WT, and this may be explained by the slightly higher Mn concentration detected by ICP-AES for the OE-*OsNAS2A* grain relative to WT (14 vs. 11 $\mu g\ g^{-1}$ DW Mn, respectively). The Cu signal is higher in the embryo of OE-*OsNAS2A* compared to WT, and this may be explained by the slightly higher Cu concentration detected by ICP-AES for the OE-*OsNAS2A* grain relative to WT (9 vs. 7 $\mu g\ g^{-1}$ DW Cu, respectively).

XRF line scans reveal significantly more Fe and Zn, and larger Fe:Zn ratios, in aleurone, sub-aleurone and endosperm tissues of OE-OsNAS2 grain

Two 135 μm line scans across the ventral portion of grain, away from the embryo region, are reported for WT and OE-*OsNAS2A* in Figure 5 (line scan region is indicated by the green box in Figure 4A). The dorsal side of rice grain contains a single aleurone layer that is rich in phosphorus (P, primarily in the form of phytic acid) while starchy endosperm tissues contain only trace P (Ogawa et al. 1979, Liu et al. 2004). The P distribution, which had highly similar counts and profile in both WT and OE-*OsNAS2A* grain, was thereby used to assign regions of the line scan to aleurone, sub-aleurone and endosperm layers of grain. As the rectangular-shaped aleurone cells of rice endosperm are approximately 25-30 μm in length (Luh 1991), we conservatively assigned the first 50 μm of the line scan to the aleurone layer (the additional 20 μm accounting for the pericarp, seed coat and nucellus that preceed the aleurone layer). Consistent with the phytic acid-enriched aleurone layer, the average P counts for both WT and OE-*OsNAS2A* grain were by far the highest in this 50 μm section (70 and 81 counts, respectively). P counts began to rapidly drop off after 50 μm and we assigned 51-90 μm to the sub-aleurone layer and 91-135 μm to the endosperm (assuming average cell lengths of 40 μm in these two layers). Average P counts for WT and OE-*OsNAS2A* grain were roughly halved in the sub-aleurone layer (44 and 30 counts, respectively) and nearly background levels in the endosperm layer (20 and 18 counts, respectively).

The line scan of WT grain (Figure 5A) shows that Fe and Zn counts increase rapidly through the aleurone layer and are nearly equal towards the start of the sub-aleurone layer (~1550 counts for both Fe and Zn at 50 μM). The Fe count begins to drop off beyond this point while Zn continues to climb for most of the sub-aleurone and endosperm layers before leveling off in the last 10 μm of the scan. The results demonstrate that while the aleurone layer has significant amounts of Fe and Zn, the sub-aleurone layer and endosperm layers, combined, have higher amounts of both of these metals. The results also show that there is more Zn relative to Fe for nearly all of the scanned region, leading to Fe:Zn ratios of <1 for the aleurone, sub-aleurone and endosperm layers (Table 2).

The line scan of OE-*OsNAS2A* grain (Figure 5B) shows that Fe and Zn counts increase rapidly through the aleurone layer but at a much steeper slope for Fe, so that

Fe counts surpass Zn counts early in the aleurone layer. The Fe count shows a first peak in the aleurone layer (5482 counts at 41 μm), similar to WT. Unlike the WT grain, however, the OE-*OsNAS2A* grain has two, successively higher, Fe peak regions in the sub-aleurone (6498 counts at 81 μm) and endosperm (6958 counts at 101 μm) layers. The Fe count begins to drop off beyond this point, most rapidly in the final 20 μm of the scan. The Fe counts in WT and OE-*OsNAS2A* grain are plotted on linear scale in Figure 6 to clearly visualize the differences in Fe quantity and distribution between the two genotypes.

The Fe count is approximately 4.4 fold higher in the aleurone, sub-aleurone and endosperm layers of OE-*OsNAS2A* grain relative to WT (Table 2). The Zn count in OE-*OsNAS2A* grain rises progressively through the scan, but does not surpass the Fe count until the final 20 μm of the scan. The Zn count is 1.4 fold higher in the aleurone layer and 2-fold higher in the sub-aleurone and endosperm layers of OE-*OsNAS2A* grain relative to WT. These fold increases for Fe and Zn count are remarkably consistent with the 4.2-fold and 2.2-fold increases of Fe and Zn concentration, respectively, that were reported for polished OE-*OsNAS2B* grain, relative to WT, as determined by ICP-AES (Table 1). Because Fe counts are higher than Zn counts for most of the line scan, Fe:Zn ratios are much larger for OE-*OsNAS2A* and >1 for both the aleurone and sub-aleurone layers (Table 2).

Discussion

The results of this study demonstrate significantly increased Fe and Zn concentrations in rice grain as a result of constitutive over-expression of single *OsNAS* genes. Within each of the three transgenic rice populations – OE-*OsNAS1*, OE-*OsNAS2* and OE-*OsNAS3* –lines were identified with at least 2- and 1.5-fold increases in Fe and Zn concentrations, respectively, of unpolished grain. Large differences, however, were observed regarding the upper limits of Fe and Zn enrichment that were found in each population (Figure 1). The OE-*OsNAS1* and OE-*OsNAS2* populations differed most significantly from each other, with the highest Fe-containing OE-*OsNAS1* line (56 μg g^{-1} DW) representing only 70% of the unpolished grain Fe concentration of the highest OE-*OsNAS2* line (81 μg g^{-1} DW). In fact, the five highest Fe-containing OE-*OsNAS2* lines had more than 60 μg g^{-1} DW Fe in unpolished grain. The observed differences between the OE-*OsNAS1* and OE-*OsNAS2* populations are surprising considering that the coding sequences of *OsNAS1* and *OsNAS2* share 87% identity and the first 233 amino acids of the two, roughly 330 aa long enzymes, are identical. The *OsNAS*1 and *OsNAS*2 enzymes may show differential activity in the synthesis of NA, or over-expression of the *OsNAS1* and *OsNAS2* coding sequences may cause significant, as yet unknown, pleiotropic effects on nutrient transport processes in rice. Studies regarding both of these possibilities are now underway.

While only a subset of lines were milled to produce polished grain, results obtained with the two OE-*OsNAS2* lines revealed some of the highest Fe concentrations that have been reported for rice endosperm. OE-*OsNAS2B* and OE-*OsNAS2J* had Fe concentrations of 19 and 14 μg g^{-1} DW, respectively, in rice endosperm (Table 1). These concentrations are 4.2- and 3-fold higher, respectively, than the Fe concentration observed for WT polished grain (4.5 μg g^{-1} DW) and represent the first time that rice lines have been reported with Fe concentrations at or above the 14.5 μg g^{-1} DW threshold recommended for an Fe-biofortified rice diet (Hotz and McClafferty 2007). Zn concentrations of the two OE-*OsNAS2* lines were also 1.5- to 2.2-fold higher than WT polished grain. The increased Fe contents of polished OE-

OsNAS2 grain appear due to not only higher metal content in unpolished grain, but also reduced losses of Fe during milling of the grain. While WT, OE-*OsNAS*1 and OE-*OsNAS3* grains consistently retained 20% of Fe concentration after milling, the two OE-*OsNAS2* lines retained 26-30% of Fe after milling. These results suggest that Fe penetrates further into rice endosperm tissues relative to WT grain, however, more over-expression lines within each of the three populations require similar characterization to determine whether this trait is specific to only the OE-*OsNAS2* population. The OE-*OsNAS2* over-expression lines should also be evaluated under field conditions to determine the stability of the high-Fe trait under different environments where Fe may be more limiting. Field trials will also enable agronomic performance of the lines to be accurately assessed.

The positive correlations between Fe and Zn concentrations in both unpolished and polished grain of the three OE-*OsNAS* populations provided strong evidence that a common mechanism – most likely NA – was responsible for transporting these micronutrient metals into the grain. The LC-MS experiments with segregating T_1 lines confirmed this hypothesis and showed that NA concentrations in unpolished grain were 6.4- to 11.7-fold higher in the *OsNAS* over-expression progeny relative to WT and null segregant lines. The NA concentration that we calculated for WT unpolished grain using the LC-MS method – 18 $\mu g\ g^{-1}$ DW – is very close to published values of 21.2 $\mu g\ g^{-1}$ DW for unpolished rice grain (Wada et al. 2007) and gave us confidence that our analytical technique was accurate and representative of actual NA concentrations. The fact that null segregant lines did not differ significantly from WT with respect to unpolished grain NA concentration, while all of the transgenic progeny had significantly higher concentrations, provided conclusive evidence that the OE-*OsNAS* constructs were responsible for the increases in NA concentration (Figure 3A). Additionally, these experiments demonstrated that the OE-*OsNAS* constructs of single-insert lines were transmitted to progeny lines in typical Mendelian fashion and stably expressed in progeny. The statistically significant, positive correlations between NA concentration and Fe and Zn concentrations ($r = 0.9769$ and 0.9288, respectively) demonstrated that increased NA concentrations of unpolished seed were not only higher in the *OsNAS* transgenic

progeny, but also indicative of Fe and Zn concentration (Figure 3B). NA concentration can therefore be considered a major regulator of Fe and Zn concentrations in rice grain, and NA may very well be a limiting factor in the accumulation of Fe and Zn in WT rice grain.

To further explore the distributions of Fe, Zn and other metal cations (that are known to chelate with NA) in rice grain, we employed synchrotron X-ray fluorescence spectroscopy (μ-XRF) to generate detailed elemental maps of WT and OE-*OsNAS2* longitudinal grain sections. A single-insert transgenic line from the OE-*OsNAS2* population, OE-*OsNAS2A*, with high levels of Fe and Zn (64 and 80 μg g^{-1} DW, respectively) was selected as a comparison to WT grain. The elemental maps of Fe and Zn in WT grain (Figure 4B and D) are in agreement with what we know about the distribution of these two metals in cereal grain – namely that Zn has a higher concentration and more broad distribution profile in the grain compared to Fe and, away from the embryo region, is not limited to outer layers of endosperm and the aleurone. The abundance of Zn in the central portion of the embryo, most likely in the plumule, has been observed in similar μ-XRF studies of barley grain (Lombi et al. 2009). The complete absence of Fe signal from much of the endosperm, as opposed to Zn which extends (faintly) throughout the endosperm, demonstrates why polishing of rice grain causes much greater losses of Fe compared to Zn. When maps of WT grain were compared to those of OE-*OsNAS2A* grain, one of the most striking differences concerned Fe distribution (Figure 4B and C). Whereas WT had very low signals of Fe in the outer endosperm and aleurone layer of the seed, OE-*OsNAS2A* grain had intermediate to high signals in the same position. Another major difference between WT and OE-*OsNAS2A* grain concerned the overall higher signals for Zn throughout the transgenic grain. Although the Zn distribution pattern did not appear altered in OE-*OsNAS2A* grain, the signal intensity was considerably higher. The small differences observed in Mn and Cu intensity between the two grain types were likely due to small (2-3 μg g^{-1} DW) increases of those elements in the embryo and/or aleurone layer of OE-*OsNAS2A* grain.

Line scans allowed us to focus in on the ventral portion of the grain, away from the embryo region (the area highlighted in green in Figure 4A), where the large

differences for Fe signal intensity had been observed between WT and OE-*OsNAS2A* grain. Of crucial importance to this experiment was the ability to detect phosphorus (P) as a direct indicator of the aleurone layer. The aleurone cells of cereals accumulate high levels of phosphorus-containing phytic acid (PA), which normally occurs as a mixed salt of potassium (K), magnesium (Mg), calcium (Ca), Fe and Zn in the cells (Liang et al. 2008). The primary function of PA is to provide storage of phosphorus and minerals for germinating seeds. The consequences of PA binding to minerals and micronutrients such as Fe and Zn, however, are undesirable from a nutritional point of view. PA is a strong inhibitor of mineral and micronutrient absorption and is reported to inhibit Fe, Zn, Ca and Mn absorption in humans (Hurrell 2003). It is thought that mineral binding to PA forms an insoluble complex that precipitates, thereby rendering the mineral unavailable to human intestinal absorption. By detecting P in our line scans, we were able to not only distinguish aleurone cells from starchy endosperm (which has only trace levels of P), but also accurately determine if Fe and Zn were localized to a region where they were likely to be bound by PA (and therefore unlikely to be bioavailable).

The line scans of WT grain showed the highest counts of Fe towards the aleurone/sub-aleurone junction, after which Fe counts began to slowly decline through the sub-aleurone and endosperm layers (Figure 5A). Zn counts, on the other hand, steadily increased through the aleurone, sub-aleurone and endosperm layers, so that the highest Zn counts were detected in the endosperm. Because Zn count was higher than Fe for most of the scan, the Fe:Zn ratio in all three layers was < 1 (Table 2). The line scan of WT grain provides novel insights into the distribution of Fe in the outer layers of rice grain. While significant quantities of Fe and Zn are localized in the aleurone cells, and therefore likely bound to PA, the sub-aleurone and endosperm contain substantial quantities of Fe and Zn that are likely to be bioavailable; particularly in the endosperm region where only trace P was detected. What molecule(s) the micronutrient metals are chelated to in this region remains unknown.

The line scans of OE-*OsNAS2A* grain revealed a radically different distribution and quantity of Fe and Zn in all three layers (Figure 5B). A major difference was

apparent in the relative amounts of Fe and Zn, with more Fe than Zn counts detected in most of the scanned region. This is essentially the reverse of what was seen in WT grain, and is reflected in Fe:Zn ratios of > 1 for aleurone and sub-aleurone cells, and close to 1 in the endosperm, for OE-*OsNAS2A* grain (Table 2). Furthermore, the Fe count did not trail off after a peak in the sub-aleurone layer, rather, it continued to peak at progressively higher levels in the sub-aleurone and endosperm layers. In fact, the highest count of Fe in OE-*OsNAS2A* grain (6958 at 101 μm) occurred in a region of endosperm where only trace counts of P (21) were detected, thereby indicating that most of the Fe could not be complexed with PA and may be readily bioavailable. To better visualize the distribution of Fe in OE-*OsNAS2A* grain, and how it differs from that of WT, the Fe counts for both grain types were plotted on linear scale in Figure 6. Increased Fe concentrations in the aleurone, sub-aleurone and endosperm layers of OE-*OsNAS2A* grain, relative to WT, are readily apparent in this chart and, furthermore, the enrichment of Fe in the endosperm layer of transgenic grain is clear. The Zn counts in OE-*OsNAS2A* grain were also significantly higher than those of WT grain, but followed a similar trend to that of WT by gradually increasing towards the endosperm.

It is tempting to speculate that the increased concentrations of Fe and Zn in aleurone, sub-aleurone and endosperm layers of OE-*OsNAS2A* grain are present as complexes with NA. NA is known to have high binding affinities for Fe and Zn at alkaline pH, while the Fe^{2+}NA complex in particular demonstrates unusually high kinetic stability that does not show autoxidation at physiological pH ranges (von Wiren et al. 1999). Preferential binding of NA to Fe^{2+} as it is transported to the seed through phloem tissues, and high stability of the Fe^{2+}NA complex within the grain, could explain why the trend of Zn > Fe counts in WT grain is reversed in OE-*OsNAS2A* grain. The hypothesis that Fe and Zn are bound to NA is bolstered by recent analyses of grain from the *OsNAS3* activation tagged line of rice discussed earlier (Lee et al. 2009) which contains 9-fold more NA in the grain. Whereas WT and the *OsNAS3* activation tagged grain did not differ with regards to the amount of PA-bound Fe, the *OsNAS3* activation tagged grain had 7-fold more Fe bound to a low molecular weight mass compound that is likely to be NA. A similar result was found in grain of the

OsNAS2 activation tagged line with regards to Zn (Lee et al. 2011). We are currently using X-ray Absorption Near Edge Structure (XANES) to identify compounds that bind to Fe and Zn in the endosperm of WT and OE-*OsNAS2A* grain. XANES should also yield speciation information for Fe (Fe^{2+} vs. Fe^{3+}), and we expect the OE-*OsNAS2A* grain to have more Fe^{2+} relative to Fe^{3+} due to preferential chelation of Fe^{2+} by NA under aerobic conditions (von Wiren et al. 1999).

More than 2 billion people are currently afflicted by iron deficiency, a serious nutritional problem that has been exacerbated by high dependences on nutrient poor cereal crops in many developing countries of the world. Billions also suffer from equally devastating micronutrient disorders such as Zn and Vitamin A deficiency. Worryingly, micronutrient malnutrition problems may become even more prevalent as the Earth's atmospheric concentration of carbon dioxide (CO_2) continues to rise. Many studies have shown that carbon enrichment, while increasing productivity of many crops, also causes significant decreases in the concentration of key micronutrients such as Fe and Zn (Loladze 2002). In light of these results it is imperative that conventional breeding and biotechnology are exploited to the fullest extent to increase nutritional composition of the world's major food staples. Using constitutive over-expression of single members of the *OsNAS* gene family, we have produced biofortified rice lines that contain significantly enhanced Fe and Zn concentrations in polished grain. The use of rice genes to increase the micronutrient content of rice shows that cisgenic plants could be developed using similar technology (Schouten et al. 2006). Most importantly, the Fe concentrations detected in particular *OsNAS2* overexpressing lines meet or surpass the target concentration for Fe biofortification of rice endosperm. The enhanced Fe concentrations are preferentially located in areas of the rice grain where they are likely to be unbound by phytic acid and therefore likely to be bioavailable in human diets.

Materials and methods

Plant growth conditions

Oryza sativa ssp. *japonica* cv. Nipponbare was used for all experiments. Seeds were germinated on filter paper in RO water for one week before transfer to pots in UC Davis soil mix in a growth room maintained at 28°C day, 24°C night, 12 h light/dark. Transgenic plantlets were grown under the same conditions. Grain harvested from plants was dried for 3 d at 37°C and then used for elemental, NA and μ-XRF studies.

Vector construction and rice transformation

RNA was extracted from 2-week old seedlings of japonica rice cultivar Nipponbare and used for cDNA synthesis. The *OsNAS1* coding sequence was PCR amplified from cDNA with forward primer 5' – ATGGAGGCTCAGAACCAAGAGGTCG – 3'and reverse primer 5' – GTTAGACGGACAGCTCCTTGTTGGC – 3' to yield a 1000 bp fragment containing the *OsNAS1* cDNA; the *OsNAS2* coding sequence was PCR amplified with forward primer 5'-ATGGAGGCTCAGAACCAAGAGGTCG – 3' and reverse primer 5' – ATGCACGCACTCAGACGGATAGCCT – 3'to yield a 991 bp fragment containing the *OsNAS2* cDNA; and the *OsNAS3* coding sequence was PCR amplified with forward primer 5' – ATGACGGTGGAAGTGGAGGCGGTGA – 3' and reverse primer 5' – GGTGAGGTAGCAAGCGATGGAAGCA – , 3' to yield a 1072 bp fragment containing the *OsNAS3* cDNA. The three PCR fragments were cloned, separately, into the Invitrogen entry vector pCR8. Error free sequences were then recombined into a modified pMDC100 vector that placed the *OsNAS* coding sequences under the control of dual CaMV 35S promoter (Figure 1). Embryogenic nodular units arising from scutellum-derived callus were inoculated with supervirulent *Agrobacterium tumefaciens* strain AGL1 (carrying the *OsNAS* over-expression vectors) and 200 mg l^{-1} geneticin-resistant shoots were regenerated after nine weeks using established protocols (Sallaud et al. 2003). Rooted T_0 plantlets were transferred to the growthroom in Jiffy peat pots, and moved to soil after 15 days.

Elemental analyses of rice grain

An average of 25 brown grains and 34 milled grains per line were analyzed by ICP-AES to determine metal concentrations. Milling was carried out using a Kett Mill for 150 seconds, as preliminary studies with KOH staining had shown this time period to be sufficient for removal of the bran layer.

Liquid chromatography-mass spectrometry (LC-MS)

The LC-MS method is based on published methods (Callahan et al. 2007). Four individual rice grains were extracted from each line. 20 mg of ground rice was weighed into an Eppendorf tube then 200 µL of an EDTA solution (5 mM) was added. The EDTA was used to release any metal complexed with NA. The derivatization of nicotianamine involved mixing of 10 µL supernatant with 70 µL borate buffer (0.2 M; pH 8.8), followed by the addition of 10 µL of AQC solution (10 mM) in dry acetonitrile. The reaction mixture was then heated at 55°C for 10 minutesand analyzed by LC-MS. Chromatograms and mass spectra were evaluated using the MassHunter Quantitative analysis program (Agilent). Quantification was based on the external calibration curve method. A 1 mg/mL stock nicotianamine standard was prepared and subsequently diluted with the EDTA solution (5 mM) to prepare calibration standards in the concentration range between 2.75 - 100 pmol/µL.

Synchrotoron X-ray fluorescence spectroscopy (µ-XRF)

Thin longitudinal sections of rice grain were obtained using published methods (Lombi et al. 2009). Briefly, grains were glued to a plastic support and then sliced using a vibrating blade microtome in order to obtain a flat surface (Leica VT1000 S). A piece of Kapton polyimide film was then pressed on the surface of the sample with the blade of the microtome cutting underneath. In this way, longitudinal sections were directly placed on Kapton tape without the need for embedding. Two longitudinal sections each of WT and OE-*OsNAS2A* grain were analyzed. µ-XRF elemental maps were collected at the X-ray Fluorescence Microscopy (XFM) beamline at the Australian Synchrotron. Elemental maps were collected at 7.5 keV using a 96-element prototype Maia detector. The detector was placed perpendicular to the beam path at a distance of 20 mm and was used to collect the full spectra fluorescence signal from the sample. The samples were analysed continuously in the

horizontal direction with steps of 1.25 μm in the vertical direction. The sample stage was set to a speed of 2 mm s^{-1}, resulting in a pixel transit time of roughly 0.6 ms. The full XRF spectra were analysed using GeoPIXE. The line scans were obtained by laterally averaging a box (depicted in green in Figure 4A) with a width of 40 μm (84 pixels) and a length of 135 μm.

Acknowledgments

The synchrotron X-ray fluorescence microscopy work was undertaken on the X-ray fluorescence microscopy beamline at the Australian Synchroton, Victoria, Australia. Financial support was provided by the Australian Research Council (LP0883746) and the HarvestPlus Challenge Program.

References

Beneš I, Schreiber K, Ripperger H, Kircheiss A (1983) Metal complex formation by nicotianamine, a possible phytosiderophore. Experientia 39: 261-262.

Callahan DL, Kolev SD, O'Hair RAJ, Salt DE, Baker AJM (2007) Relationships of nicotianamine and other amino acids with nickel, zinc and iron in Thlaspi hyperaccumulators. New Phytol 176: 836-848.

Curtis MD, Grossniklaus U (2003) A gateway cloning vector set for high-throughput functional analysis of genes in planta. Plant Physiol 133: 462-469.

Goto F, Yoshihara T, Shigemoto N, Toki S, Takaiwa F (1999) Iron fortification of rice seed by the soybean ferritin gene. Nat Biotech 17: 282-296.

Higuchi K, Suzuki K, Nakanishi H, Yamaguchi H, Nishizawa N-K, et al. (1999) Cloning of nicotianamine synthase genes, novel genes involved in the biosynthesis of phytosiderophores. Plant Physiol 119: 471-480.

Hotz C, McClafferty B (2007) From harvest to health: challenges for developing biofortified staple foods and determining their impact on micronutrient status. Food Nutr Bull 28: S271-279.

Hurrell RF (2003) Influence of vegetable protein sources on trace element and mineral bioavailability. J Nutr 133: 2973S-2977S.

Inoue H, Higuchi K, Takahashi M, Nakanishi H, Mori S, et al. (2003) Three rice nicotianamine synthase genes, *OsNAS*1, *OsNAS*2, and *OsNAS*3 are expressed in cells involved in long-distance transport of iron and differentially regulated by iron. Plant J 36: 366-381.

Kennedy G, Burlingame B (2003) Analysis of food composition data on rice from a plant genetic resources perspective. Food Chemistry 80: 589-596.

Klatte M, Schuler M, Wirtz M, Fink-Straube C, Hell R, et al. (2009) The analysis of *Arabidopsis* nicotianamine synthase mutants reveals functions for nicotianamine in seed iron loading and iron deficiency responses. Plant Physiol 150: 257-271.

Khush G (2005) What it will take to feed 5.0 billion rice consumers in 2030. Plant Mol Biol 59: 1-6.

Kim S, Takahashi M, Higuchi K, Tsunoda K, Nakanishi H, et al. (2005) Increased nicotianamine biosynthesis confers enhanced tolerance of high levels of metals, in particular nickel, to plants. Plant Cell Physiol 46: 1809-1818.

Lee S, Jeon US, Lee SJ, Kim Y-K, Persson DP, et al. (2009) Iron fortification of rice seeds through activation of the nicotianamine synthase gene. P Natl Acad Sci USA 106: 22014-22019.

Lee S, Persson DP, Hansen TH, Husted S, Schjoerring JK, et al. (2011) Bio-available zinc in rice seeds is increased by activation tagging of nicotianamine synthase. Plant Biotechol J 9: 1-9.

Liang J, Li Z, Tsuji K, Nakano K, Nout MJR, et al. (2008) Milling characteristics and distribution of phytic acid and zinc in long-, medium- and short-grain rice. J Cereal Sci 48: 83-91.

Liu JC, Ockenden I, Truax M, Lott JNA (2004) Phytic acid-phosphorus and other nutritionally important mineral nutrient elements in grains of wild-type and low phytic acid (lpa1-1) rice. Seed Sci Res 14: 109-116

Loladze I (2002) Rising atmospheric CO2 and human nutrition: toward globally imbalanced plant stoichiometry Trends Ecol Evol 17: 457-461.

Lombi E, Scheckel KG, Pallon J, Carey AM, Zhu YG, et al. (2009) Speciation and distribution of arsenic and localization of nutrients in rice grains. New Phytologist 184: 193-201.

Lombi E, Smith E, Hansen TH, Paterson D, de Jonge MD, et al. (2010) Megapixel imaging of (micro)nutrients in mature barley grains. Journal of Exp Bot 62: 273-282.

Lucca P, Hurrell R, Potrykus I (2002) Fighting iron deficiency anemia with iron-rich rice. J Am Coll Nutr 21: 184S-190.

Luh BS (1991) Rice volume II: production and utilization, 2nd edition. New York, New York: Van Nostrand Reinhold. 413 p.

Masuda H, Usuda K, Kobayashi T, Ishimaru Y, Kakei Y, et al. (2009) Over-expression of the barley nicotianamine synthase gene HvNAS1 increases iron and zinc concentrations in rice grains Rice 2: 155-166.

Mayer JE, Pfeiffer WH, Beyer P (2008) Biofortified crops to alleviate micronutrient malnutrition. Curr Opin Plant Biol 11: 166-170.

Mizuno D, Higuchi K, Sakamoto T, Nakanishi H, Mori S, et al. (2003) Three nicotianamine synthase genes isolated from maize are differentially regulated by iron nutritional status. Plant Physiol 132: 1989-1997.

Ogawa M, Tanaka K, Kasai Z (1979) Accumulation of phosphorus, magnesium and potassium in developing rice grains: followed by electron microprobe X-ray analysis focusing on the aleurone layer. Plant Cell Physiol 20: 19-27.

Pfeiffer WH, McClafferty B (2008) Biofortification: breeding micronutrient-dense crops. Breeding Major Food Staples: Blackwell Publishing Ltd. pp. 61-91.

Qu LQ, Yoshihara T, Ooyama A, Goto F, Takaiwa F (2005) Iron accumulation does not parallel the high expression level of ferritin in transgenic rice seeds. Planta 222: 225-233.

Ramakrishnan U (2002) Prevalence of micronutrient malnutrition worldwide. Nutrition Rev 60: S46-S52.

Sallaud C, Meynard D, van Boxtel J, Gay C, Bès M, et al. (2003) Highly efficient production and characterization of T-DNA plants for rice (Oryza sativa L.) functional genomics. Theor Appl Genet 106: 1396-1408.

Schouten HJ, Krens FA, Jacobsen E (2006) Cisgenic plants are similar to traditionally bred plants. EMBO Rep 7: 750-753.

Takahashi M, Terada Y, Nakai I, Nakanishi H, Yoshimura E, et al. (2003) Role of nicotianamine in the intracellular delivery of metals and plant reproductive development. Plant Cell 15: 1263-1280.

Usuda K, Wada Y, Ishimaru Y, Kobayashi T, Takahashi M, et al. (2008) Genetically engineered rice containing larger amounts of nicotianamine to enhance the antihypertensive effect. Plant Biotechnol J 7: 87-95.

von Wiren N, Klair S, Bansal S, Briat J-F, Khodr H, et al. (1999) Nicotianamine chelates both FeIII and FeII. Implications for metal transport in plants. Plant Physiol 119: 1107-1114.

Wada Y, Yamaguchi I, Takahashi M, Nakanishi H, Mori S, et al. (2007) Highly sensitive quantitative analysis of nicotianamine using LC/ESI-TOF-MS with an internal standard. Biosci Biotechnol Biochem 71: 435-441.

Wirth J, Poletti S, Aeschlimann B, Yakandawala N, Drosse B, et al. (2009) Rice endosperm iron biofortification by targeted and synergistic action of nicotianamine synthase and ferritin. Plant Biotechnol J 7: 631-644.

Zheng L, Cheng Z, Ai C, Jiang X, Bei X, et al. (2010) Nicotianamine, a novel enhancer of rice iron bioavailability to humans. PLoS ONE 5: e10190.

Figure Legends

Figure 1. Schematic representation of the T-DNAs used for constitutive over-expression of the three *OsNAS* genes. RB, right border; 2 × 35S, dual CaMV 35S promoter; *OsNAS*, coding sequence of *OsNAS1* (999 bp), *OsNAS2* (981 bp) or *OsNAS3* (1032 bp); nos T, nopaline synthase terminator; 35S, CaMV 35S promoter; nptII, *neomycin phosphotransferase II*; LB, left border.

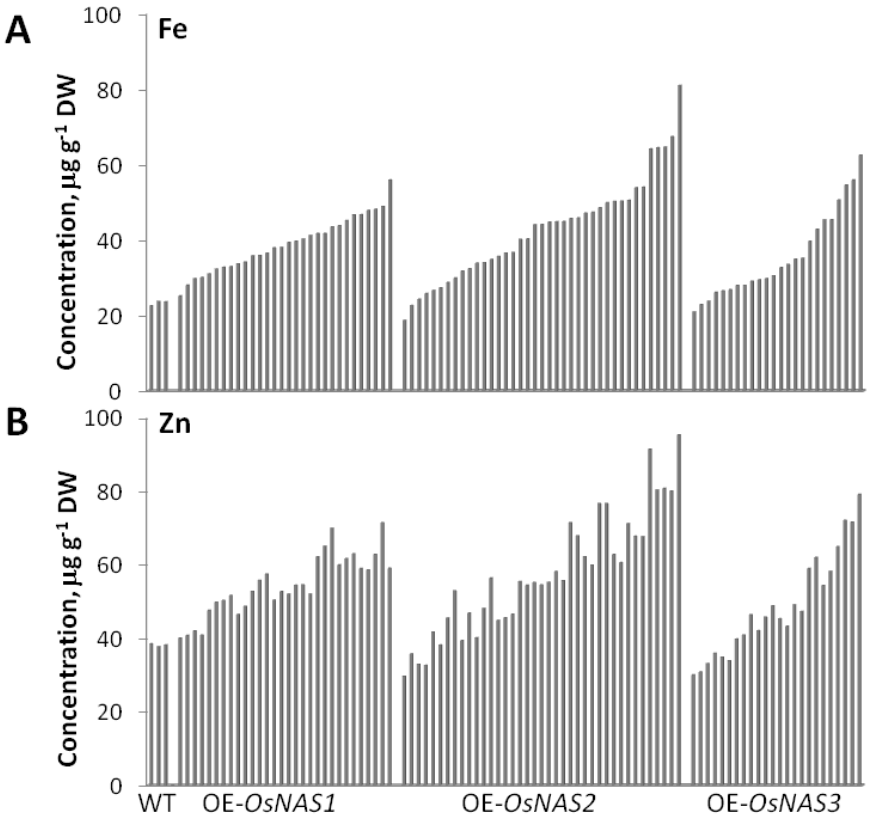

Figure 2. Fe (A) and Zn (B) concentrations in unpolished grain of wild type and transgenic rice. WT, three wild type lines of rice; OE-*OsNAS1*, 30 independent transgenic lines overexpressing *OsNAS1*; OE-*OsNAS2*, 39 independent transgenic lines overexpressing *OsNAS2*; OE-*OsNAS3*, 24 independent transgenic lines overexpressing *OsNAS3*. Unpolished grain was analyzed by inductively coupled plasma atomic emission spectroscopy to determine Fe and Zn concentrations. The three populations of over-expression lines are sorted in order from lowest to highest Fe content in panels A and B.

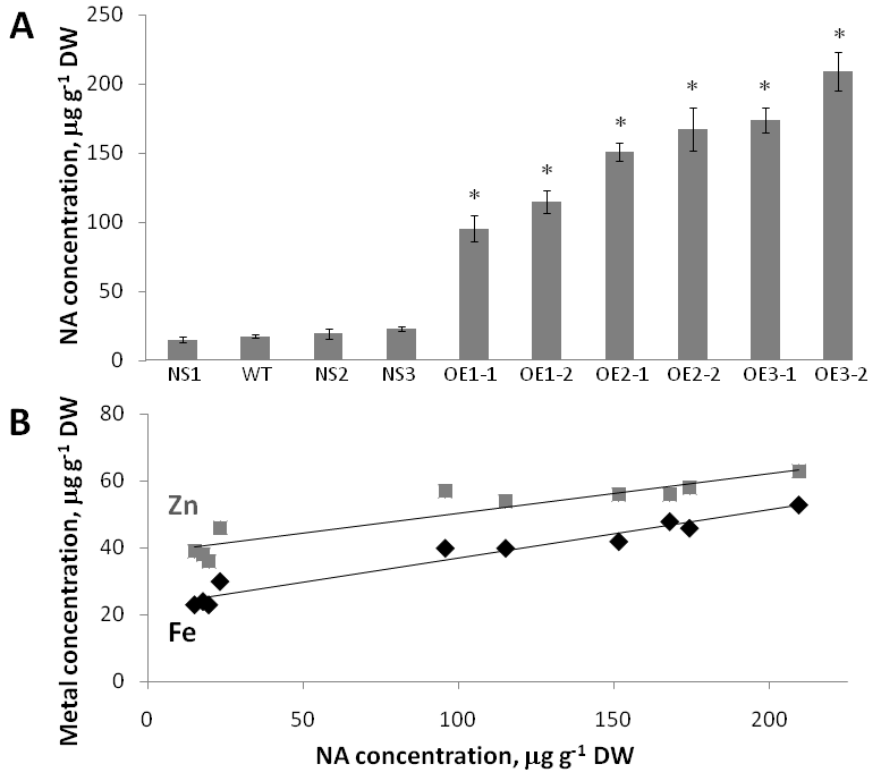

Figure 3. Nicotianamine (NA) concentrations in unpolished grain and positive correlation with Fe and Zn content. (A) NS, null segregant lines of rice; WT, wild type line of rice; OE, over-expression lines of rice. Three sibling T_1 lines, consisting of two OE lines and one NS line, were obtained from a single-insert T_0 mother line in each of the three *OsNAS* over-expression populations. The three *OsNAS1* sibling lines are labeled OE1-1, OE1-2 and NS1; the three *OsNAS2* sibling lines are labeled OE2-1, OE2-2 and NS2; the three *OsNAS3* sibling lines are labeled OE3-1, OE3-2 and NS3. Unpolished grain was analyzed by LC-MS to determine nicotianamine content (mean ± SE, n =4). Significant differences from WT are indicated by asterisks ($P < 0.05$). (B) Statistically significant positive correlations were found between unpolished grain NA concentration and Fe (black diamonds; $r = 0.9769$ and $p < 0.01$) and Zn (gray squares; $r = 0.9288$ and $P < 0.01$) concentrations for the ten genotypes described in panel A.

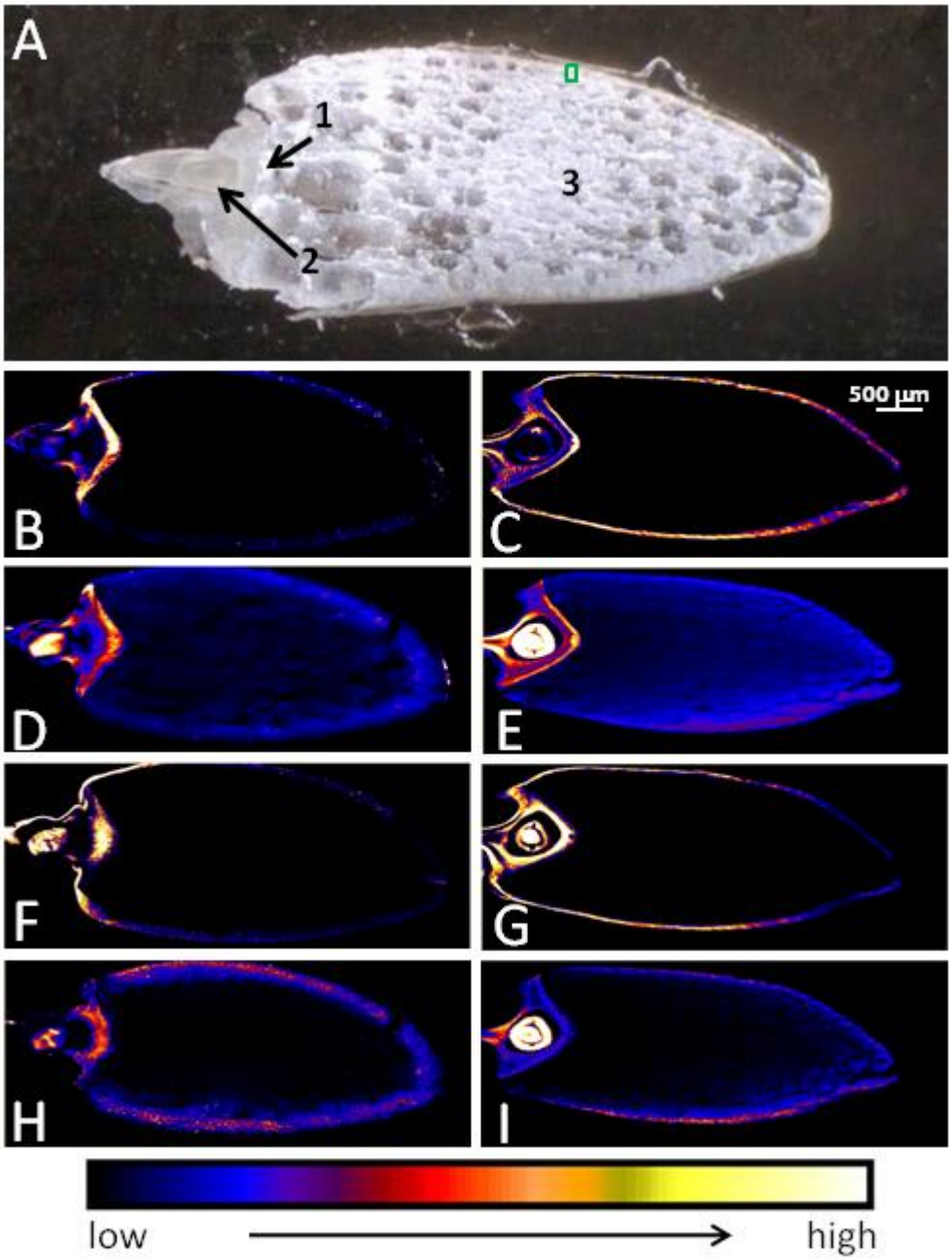

Figure 4. XRF elemental maps of WT and OE-*OsNAS2A* longitudinal grain sections (ventral side on top). WT grain had 23 µg g^{-1} DW Fe and 38 µg g^{-1} DW Zn while OE-*OsNAS2A* grain had 64 µg g^{-1} DW Fe and 80 µg g^{-1} DW Zn, as determined by ICP-AES. (A) Light microscopy photo of a representative grain section with numbers indicating the location of scutellum (1), embryo (2) and endosperm (3); the

green box on ventral side corresponds to the area used to obtain the line scans in Figures 5-6. (1), embryo (2) and endosperm (3). (B-I) Elemental maps of Fe distribution in WT (B) and OE-*OsNAS2A* (C) grain; Zn distribution in WT (D) and OE-*OsNAS2A* (E) grain; Mn distribution in WT (F) and OE-*OsNAS2A* (G) grain; Cu distribution in WT (H) and OE-*OsNAS2A* (I) grain. The colour scale represents different elemental concentrations, with black and white corresponding to the lowest and highest concentration, respectively.

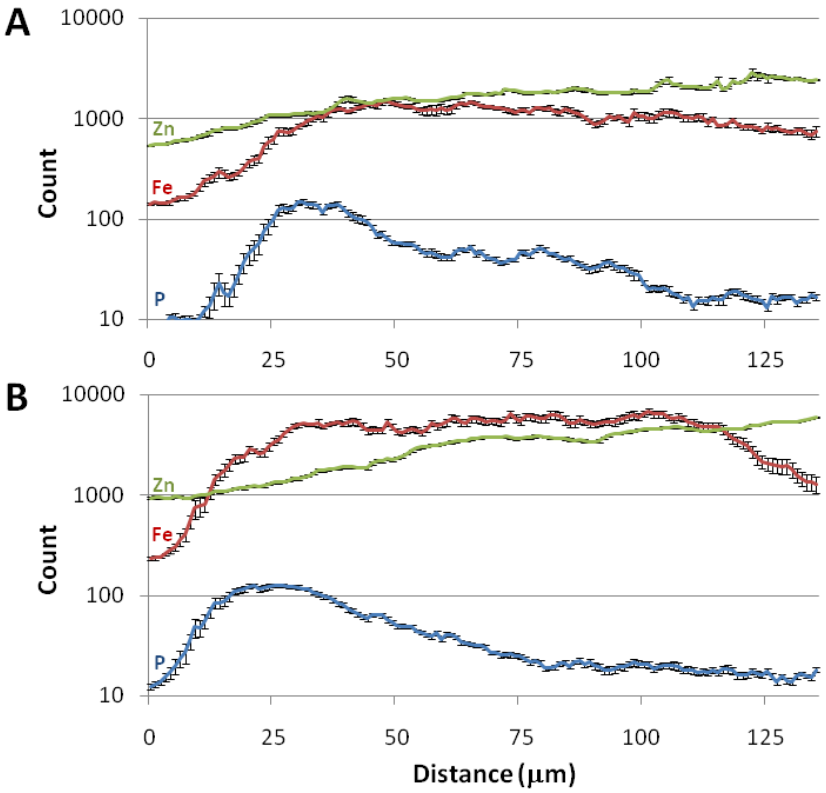

Figure 5. Line scans for P, Fe and Zn in WT (A) and OE-*OsNAS2A* (B) grain. Line scans begin on the ventral side of grain and continue 135 μm towards the endosperm; data is displayed as average count (mean ± SE, n = 23). Counts are plotted on logarithmic scale in the y-axis to account for the low P counts (blue) relative to Fe (red) and Zn (green). As the dorsal side of rice grain contains a single aleurone layer that is rich in phosphorus (P, primarily in the form of phytic acid) while endosperm contains little P, 1-50 μm was assigned to the aleurone layer, 51-90 μm to the sub-aleurone layer and 91-135 μm to the endosperm.

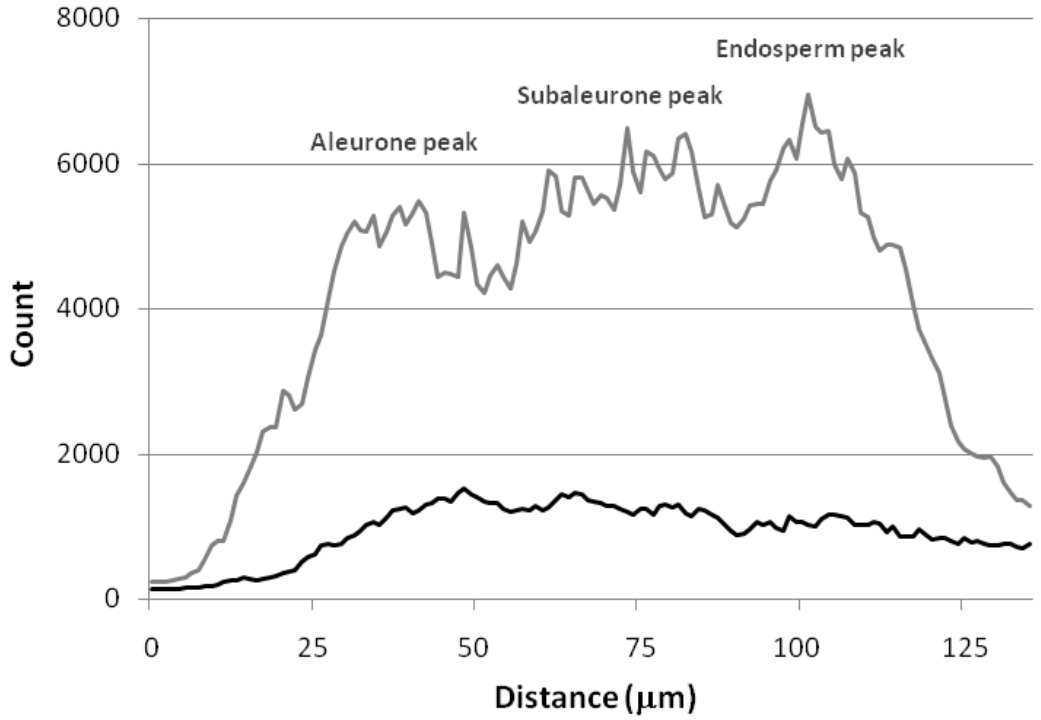

Figure 6. Line scans for Fe in WT and OE-*OsNAS2A* grain. Line scans begin on the ventral side of grain and continue 135 μm towards the endosperm; average WT counts indicated by the black line and average OE-*OsNAS2* counts indicated by the gray line (n = 23). The location of the successively higher Fe peaks in aleurone, sub-aleurone and endosperm regions of OE-*OsNAS2A* grain is indicated on the figure.

Tables

Table 1. Concentrations of Fe and Zn in unpolished and polished rice of WT, one transgenic line overexpressing *OsNAS1* (OE-*OsNAS1S*), two independent transgenic lines overexpressing *OsNAS2* (OE-*OsNAS2B* and OE-*OsNAS2J*) and one line transgenic line overexpressing *OsNAS3* (OE-*OsNAS3B*). The percentages of Fe and Zn retention in the polished grain are presented in the last two columns of the table.

Genotype	**Unpolished (μg g^{-1})**		**Polished (μg g^{-1})**		**% Fe retention**	**% Zn retention**
	Fe	Zn	Fe	Zn		
WT	22	42	4.5	34	21	81
OE-*OsNAS1S*	47	63	9.7	48	21	76
OE-*OsNAS2B*	64	91	19	76	30	84
OE-*OsNAS2J*	54	68	14	52	26	77
OE-*OsNAS3B*	51	65	9.9	49	19	75

Table 2. Average counts of Fe and Zn in aleurone (1-50 μm), sub-aleurone (51-90 μm) and endosperm (91-135 μm) layers of WT and OE-*OsNAS2A* grain as determined by X-ray fluorescence spectroscopy. The Fe:Zn ratio is calculated for each of the three layers.

Genotype	**Aleurone**			**Sub-aleurone**			**Endosperm**		
	Fe	**Zn**	**Ratio**	**Fe**	**Zn**	**Ratio**	**Fe**	**Zn**	**Ratio**
WT	715	1055	0.68	1252	1779	0.70	935	2236	0.42
OE-*OsNAS2B*	3194	1460	2.19	5472	3512	1.56	4268	4757	0.90

Supplementary Table 1. Average concentrations of Fe, Zn, Mn, Cu and Ni in unpolished grain of 3 WT, 30 OE-*OsNAS1*, 39 *OE-OsNAS2* and 24 *OE-OsNAS3* lines as determined by ICP-AES. Samples consisted of 25 unpolished grains per line. Average values for each group of plants are presented as means ± standard error (S.E.) of the mean.

Genotype	Fe	Zn	Mn	Cu	Ni
WT	23 ± 0.5	38 ± 0.3	14 ± 2.4	7 ± 1.5	2 ± 0.5
OE-*OsNAS1*	39 ± 1.3	54 ± 1.5	12 ± 0.3	8 ± 0.2	3 ± 0.1
OE-*OsNAS2*	43 ± 2.2	57 ± 2.7	16 ± 0.3	9 ± 0.3	2 ± 0.1
OE-*OsNAS3*	56 ± 2.4	49 ± 2.9	11 ± 0.4	8 ± 0.2	2 ± 0.1

Appendix Two

gene	primer	primer sequence	expected amplified region
OsNAS1	forward	ATGGAGGCTCAGAACCAAGAGGTCG	1000 bp
	reverse	GTTAGACGGACAGCTCCTTGTTGGC	
OsNAS2	forward	ATGGAGGCTCAGAACCAAGAGGTCG	991 bp
	reverse	ATGCACGCACTCAGACGGATAGCCT	
OsNAS3	forward	ATGACGGTGGAAGTGGAGGCGGTGA	1072 bp
	reverse	GGTGAGGTAGCAAGCGATGGAAGCA	
NPTII	forward	GAAGAACTCGTCAAGAAGGCG	796 bp
	reverse	CATGGGGATTGAACAAGATGG	
OsVIT1	forward	CACCATGGCCGCTGCGACCGATGG	759 bp
	reverse	TTACCGGGTTTGTACCGCCTTC	

* Primers for *OsVIT1* were designed but not utilised

Appendix Three

Number of T0 transgenic rice plants grown after second transformation event.

Cell-Type Specific Expression	Gene of Interest	Number of Transformants (T0)
root: stele	*OsNAS1*	6
	OsNAS2	9
	OsNAS3	12
root: cortex	*OsNAS1*	21
	OsNAS2	12
	OsNAS3	21
developing flower: lodicule	*OsNAS1*	13
	OsNAS2	14
	OsNAS3	18
developing flower: vascular bundle & leaf: collar	*OsNAS1*	10
	OsNAS2	6
	OsNAS3	5
developing flower: ovary & leaf: collar	*OsNAS1*	13
	OsNAS2	6
	OsNAS3	12
35S	*OsNAS1*	20
	OsNAS2	11
	OsNAS3	5

Appendix Four

Os04g0463400 matches the genetic sequence obtained from DNA2.0 for the synthesis of OsVIT1

aaataaaccacctcttcaaacgtgcgtcgcctgaccgcttccatccatccaccagtctcgcttcttcg

tgtctacggtctacctcggcgagtcggcggcggcgatggcggcggcgacggacggcgggggggctgccg

ctgctggcggacaaggcggcgagccacagccaccaccaccacccggagcggcacttcacgtcgggggga

ggtggtccgcgacgtcatcatgggcgtctccgacggcctcaccgtgcccttcgccctcgccgcggggc

tctccggcgccagcgcgccatcctcgctcgtgctcaccgccggcctcgccgaggtcgccgccggcgcc

atctccatgggcctcggagggtatctcgcggccaagagcgaggcagaccattaccagcgggagatgaa

aagggagcaggaggagatcatcgccgtcccggacactgaggctgctgagattggcgagatcatgtcgc

agtacgggctcgaaccgcatgagtatggccctgtcgtggacgggctccgtaggaatcctcaagcttgg

ctcgacttcatgatgaggtttgagctgggattggagaaaccagaccctaaaagagctatacagagcgc

tttaacaattgcgctatcttatgtcattggtggactggtccctctccttccctacatgtttatctcca

cagcacagaacgccatgctcacatctgtcggtgtcacgctggttgcactacttttctttggatacatc

aagggtcgctttactggaaaccgtccattcctcagcgctgtccaaactgctattatcggtgcgcttgc

ttctgctgcggcatatggaatggccaaggccgtgcaaactagatgatttgaaccctcatgtgttcctg

tctgaagtttcagtaggcagaactgaatccaacgaagctgcaatgaatcacaatctcatattaagaat

atgtattttacctttcatgtaacaaggaataaattttgggaaacatgaaataaaagcatgctatttta

agttct

Appendix Five

Agrobacterium mediated transformation of rice grain- detailed procedure

Seed sterilisation	Immersed dehusked rice seeds in 70% ethanol for 1 minute, after which ethanol was removed
	Washed seeds in 30% bleach (v/v) and 1% Tween 20 (v/v) for 30 minutes, with agitation and removed bleach
	Rinsed seeds three times with sterile water on shaking plate for 15 minutes
Seed callus induction	Placed 10 seeds NB medium using sterile forceps
	Once dry, plates were incubated at 28°C, no light, for one month
	To multiply calli, embryonic units were replated onto fresh NB medium and incubated at 28°C, no light for a further 14 days
***Agrobacterium* preparation**	Prepared overnight culture of the *Agrobacterium* lines in 5ml LB/ Rif 50/ Kan 50 medium, at 28°C
	Spread plated 150 µl onto LB/ Rif 50/ Kan 50, dried and incubated inverted plates at 28°C for 3 days
	When dry, loosely parafilm and incubate inverted at 28°C for 3 days
Calli Transformation	*Agrobacterium* colonies were added to 30 ml R2-CL liquid medium and introduced to calli for 15 minutes with gentle agitation
	Calli removed from solution were then placed onto Petri dishes containing R2-CS medium and incubated at 25°C, no light for 3 days
Selection phase	Transformed calli were transferred to Petri dishes containing R2-S medium, dried and incubated without light at 28°C for 2 weeks
Proliferation phase	To promote proliferation of vegetative tissue, calli were transferred onto NBS medium plates, dried and incubated without light 28°C for 3 weeks
Maturation	Healthy, yellow-white calli were transferred onto PR-AG

phase	medium plates and incubated without light at 28°C for 1 week
Regeneration phase	Matured calli were plated onto RN medium and incubated without light at 28°C for 2 days
	Plates were introduced to light (110-130 mm/mpar, cycle of 12h light/dark) for 4 weeks
Rooting of regenerated shoots	Individual shootlets were removed from calli and placed on P medium and incubated at 28°C for 3-4 weeks with light (110-130 mm/mpar, cycle of 12h light/dark)
Growth of plants in greenhouse	Acclimatised plantlets in Jiffy pots in mini-greenhouse for 15 days
	Transplanted larger plant to 1 L UC Davis soils and maintained plants in greenhouse until destruction at weeks

Appendix Six

Agrobacterium mediated transformation of rice grain- detailed media contents

NB medium	**final volume 250ml**	**PR-AG medium**	**final volume 250ml**
N6 Macroelements	12.5 ml	N6 Macroelements	12.5 ml
FeEDTA (Base NB)	2.5 ml	FeEDTA (Base NB)	2.5 ml
B5 Microelements	2.5 ml	B5 Microelements	2.5 ml
B5 vitamins	2.5 ml	B5 vitamins	2.5 ml
myo-inositol	25 g	myo-inositol	25 ml
proline	125 g	proline	125 mg
glutamine	125 g	glutamine	125 mg
casein hydrosylate	75 g	casein hydrosylate	75 mg
sucrose	7.5 g	sucrose	7.5 g
2, 4-D	0.625 mg	ABA	1.25 mg
phytagel	0.65 g	BAP	0.5 mg
pH	5.8	NAA	0.25 mg
R2-CS solid medium	**final volume 250ml**	cefotaxime	25 mg
macroelements R2-I	25 ml	vancomycin	25 mg
macroelements R2-II	25 ml	geneticin (G418)	50 mg
FeEDTA (base R2)	2.5 ml	agarose type 1: low EEO	1.75 g
microelements R2	0.25 ml	pH	5.8
vitamins R2	6.25 ml	**R2-CL liquid medium**	**final volume 250ml**
Glucose (d-glucose monohydrate)	2.5 g	macroelements R2-I	25 ml
2, 4-D	0.625 mg	macroelements R2-II	25 ml
acetosyringone	25 µl	FeEDTA (base R2)	2.5 ml
agarose type 1: low EEO	1.75 g	microelements R2	0.25 ml
pH	5.2	vitamins R2	6.25 ml
NBS medium	**final volume 250ml**	Glucose	2.5 g
N6 macroelements	12.5 ml	2, 4-D	0.625 mg
FeEDTA (base NB)	2.5 ml	acetosyringone	25 µl
B5 Microelements	2.5 ml	pH	5.2
B5 vitamins	2.5 ml	**R2-S medium**	**final volume 250ml**
myo-inositol	25 mg	macroelements R2-I	25 ml
proline	125 mg	macroelements R2-II	25 ml
glutamine	125 mg	FeEDTA (base R2)	2.5 ml
casein hydrosylate	75 mg	microelements R2	0.25 ml

sucrose	7.5 g	vitamins R2	6.25 ml
2, 4-D	0.625 mg	sucrose	7.5 g
cefotaxime	100 mg	2, 4-D	0.625 mg
vancomycin	25 mg	cefotaxime	100 mg
geneticin (G418)	50 mg	vancomycin	25 mg
agarose type 1: low EEO	1.75	geneticin (G418)	50 mg
pH	6	agarose type 1: low EEO	1.75 g
RN medium	**final volume 250ml**	pH	6
N6 Macroelements	12.5 ml	**P medium**	**final volume 250ml**
FeEDTA (Base NB)	2.5 ml	MS basal with vitamins	1.11
B5 Microelements	2.5 ml	sucrose	12.5
B5 vitamins	2.5 ml	phytagel	0.65
myo-inositol	25 mg	pH	5.8
proline	125 mg		
glutamine	125 mg		
casein hydrosylate	75 mg		
sucrose	7.5 g		
BAP	0.75 mg		
NAA	0.125 mg		
phytagel	0.875 g		
pH	5.8		

References

ANDEREGG, G. & RIPPERGER, H. 1989. Correlation between metal complex formation and biological activity of nicotianamine analogues. *Journal of the Chemical Society, Chemical Communications***,** 647-650.

ANZECC/NHMRC 1992. Australian and New Zealand Guidelines for the Assessment and Management of Contaminated sites.

AOYAMA, T., KOBAYASHI, T., TAKAHASHI, M., NAGASAKA, S., USUDA, K., KAKEI, Y., ISHIMARU, Y., NAKANISHI, H., MORI, S. & NISHIZAWA, N. K. 2009. OsYSL18 is a rice iron (III) deoxymugineic acid transporter specifically expressed in reproductive organs and phloem of lamina joints. *Plant Molecular Biology,* 70**,** 681-692.

ARAO, T. & AE, N. 2003. Genotypic variations in cadmium levels of rice grain. *Soil Science and Plant Nutrition,* 49**,** 473-479.

ARAO, T. & ISHIKAWA, S. 2006. Genotypic Differences in Cadmium Concentration and Distribution of Soybean and Rice. *Japan Agricultural Research Quarterly,* 40**,** 21*30.

ASOBAYIRE, F. S., ADOU, P., DAVIDSSON, L., COOK, J. D. & HURRELL, R. F. 2001. Prevalence of iron deficiency with and without concurrent anemia in population groups with high prevalences of malaria and other infections: a study in CÃ´te dâ€˜Ivoire. *The American Journal of Clinical Nutrition,* 74**,** 776-782.

ASSUNCAO, A. G. L., PERSSON, D. L. P., HUSTED, S., SCHJORRING, J. K., ALEXANDER, R. D. & AARTS, M. G. M. 2013. Model of how plants sense zinc deficiency. *Metallomics*.

AYYADURAI, N., KIRUBAKARAN, S., SRISHA, S. & SAKTHIVEL, N. 2005. Biological and Molecular Variability of Sarocladium oryzae, the Sheath Rot Pathogen of Rice (Oryza sativa L.). *Current Microbiology,* 50**,** 319-323.

BACIC, A. & STONE, B. 1981. Chemistry and organization of aleurone cell wall components from wheat and barley. *Functional Plant Biology,* 8**,** 475-495.

BAJAJ, S. & MOHANTY, A. 2005. Recent advances in rice biotechnology—towards genetically superior transgenic rice. *Plant Biotechnology Journal* 3**,** 275–307.

BECHTEL, D. B. & JULIANO, B. O. 1980. Formation of protein bodies in the starchy endosperm of rice (Oryza sativa L.): a re-investigation. *Annals of Botany,* 45**,** 503-509.

BECHTEL, D. B. & POMERANZ, Y. 1977. Ultrastructure of the mature ungerminated rice (Oryza sativa) caryopsis. The caryopsis coat and the aleurone cells. *American Journal of Botany***,** 966-973.

BERECZKY, Z., WANG, H.-Y., SCHUBERT, V., GANAL, M. & BAUER, P. 2003. Differential Regulation of nramp and irt Metal Transporter Genes in Wild Type and Iron Uptake Mutants of Tomato. *THE JOURNAL OF BIOLOGICAL CHEMISTRY,* 278**,** 24697–24704.

BERNARDS, M. L., JOLLEY, V. D., STEVENS, W. B. & HERGERT, G. W. 2002. Phytosiderophore release from nodal, primary, and complete root systems in maize. *Plant and Soil,* 241**,** 105-113.

BOUIS, H. E., CHASSY, B. M. & OCHANDA, J. O. 2003. Genetically modified food crops and their contribution to human nutrition and food quality. *Trends in Food Science & Technology* 14**,** 191-209.

BOUIS, H. E., GRAHAM, R. D. & WELCH, R. M. 2000. The Consultative Group on International Agricultural Research (CGIAR) micronutrients project: justification and objectives. *Food & Nutrition Bulletin,* 21**,** 374-381.

BRIAT, J., CURIE, C. & GAYMARD, F. 2007. Iron utilization and metabolism in plants. *Current Opinion in Plant Biology,* 10**,** 276-282.

BRIAT, J., FOBIS-LOISY, I., GRIGNON, N., LOBRÉAUX, S., PASCAL, N., SAVINO, G., THOIRON, S., VON WIRÉN, N. & VAN WUYTSWINKEL, O. 1995. Cellular and molecular aspects of iron metabolism in plants. *Biology of the Cell,* 84**,** 69-81.

BRIDGE, P. D., HAWKSWORTH, D. L., KAVISHE, D. F. & FARNELL, P. A. 1989. A revision of the species concept in Sarocladium, the causal agent of sheath-rot in rice and bamboo blight, based on biochemical and morphometric analyses. *Plant Pathology,* 38**,** 239-245.

BRINCH-PEDERSEN, H., BORG, S., TAURIS, B. & HOLM, P. B. 2007. Molecular genetic approaches to increasing mineral availability and vitamin content of cereals. *Journal of Cereal Science,* 46**,** 308-326.

BUGHIO, N., YAMAGUCHI, H., NISHIZAWA, N. K., NAKANISHI, H. & MORI, S. 2002. Cloning an iron-regulated metal transporter from rice. *J Exp Bot,* 53**,** 1677-82.

BUSCH, A., RIMBAULD, B., NAUMANN, B., RENSCH, S. & HIPPLER, M. 2008. Ferritin is required for rapid remodeling of the photosynthetic apparatus and minimizes photo-oxidative stress in response to iron availability in Chlamydomonas reinhardtii. *The Plant Journal,* 55**,** 201-211.

CALLAHAN, D. L., KOLEV, S. D., O'HAIR, R. A. J., SALT, D. E. & BAKER, A. J. M. 2007. Relationships of nicotianamine and other amino acids with nickel, zinc and iron in Thlaspi hyperaccumulators. *New Phytologist,* 176**,** 836–848.

CAMPOS-BOWERS, M. H. & WITTENMYER, B. F. 2007. Biofortification in China: policy and practice. *Health Research Policy and Systems,* 5**,** 10-17.

CAYTON, M. 1985. *Boron toxicity in rice,* International Rice Research Institute Los Banos,, Philippines.

CHEN, F., WANG, F., ZHANG, G. & WU, F. 2008. Identification of barley varieties tolerant to cadmium toxicity. *Biological trace element research,* 121**,** 171-179.

CHEN, Z.-S. 1992. Metal contamination of flooded soils, rice plants, and surface waters in Asia.

CHENG, L., WANG, F., SHOU, H., HUANG, F., ZHENG, L., HE, F., LI, J., ZHAO, F.-J., UENO, D., MA, J. F. & WU, P. 2007. Mutation in Nicotianamine Aminotransferase Stimulated the Fe(II) Acquisition System and Led to Iron Accumulation in Rice. *Plant Physiology,* 145**,** 1647–1657.

CHHUNEJA, P., DHALIWAL, H. S., BAINS, N. S. & SINGH, K. 2006. Aegilops kotschyi and Aegilops tauschii as sources for higher levels of grain Iron and Zinc. *Plant Breeding,* 125**,** 529—531.

CHOI, E. Y., GRAHAM, R. D. & STANGOULIS, J. 2007. Semi-quantitative analysis for selecting Fe- and Zn-dense genotypes of staple food crops. *Journal of Food Composition and Analysis,* 20**,** 496-505.

CLARK, R. B. 1983. Plant genotype differences in the uptake, transiocation, accumulation,

and use of mineral elements required for plant growth. *Plant and Soil,* 72**,** 175-196.

CLEMENS, S. 2001. Molecular mechanisms of plant metal tolerance and homeostasis. *planta,* 212**,** 475-486.

CLEMENS, S., PALMGREN, M. G. & KRÄMER, U. 2002. A long way ahead: understanding and engineering plant metal accumulation. *TRENDS in Plant Science,* 7**,** 309-315.

CLIMATE DATA ONLINE, B. O. M. 2013. *Climate Data Online, Bureau of Meteorology* [Online]. Available: http://www.bom.gov.au/climate/data.

CLODE, P. L., KILBURN, M. R., JONES, D. L., STOCKDALE, E. A., CLIFF, J. B., HERRMANN, A. M. & MURPHY, D. V. 2009. In situ mapping of nutrient uptake in the rhizosphere using nanoscale secondary ion mass spectrometry. *Plant Physiology,* 151**,** 1751-1757.

COLANGELO, E. P. & GUERINOT, M. L. 2004. The Essential Basic Helix-Loop-Helix Protein FIT1 Is Required

for the Iron Deficiency Response. *The Plant Cell,* 16**,** 3400–3412.

COMMISSION, C. A. & COMMISSION, C. A. 2011. Joint FAO/WHO food standards programme. *Rome: FAO/WHO,* 122.

CONWAY, G. 1997. *The Doubly Green Revolution: Food for All in the Twenty-First Century,* Comstock Pub. Associates.

CURIE, C. & BRIAT, J. 2003. Iron Transport and Signaling in Plants. *Annu. Rev. Plant Biol.,* 54**,** 183-206.

CURIE, C., PANAVIENE, Z., LOULERGUE, C., DELLAPORTA, S. L., BRIAT, J. & WALKER, E. L. 2001. Maize yellow stripe1 encodes a membrane protein directly involved in Fe(III) uptake. *Nature,* 409**,** 346-349.

CURTIS, M. D. & GROSSNIKLAUS, U. 2003. A gateway cloning vector set for high-throughput functional analysis of genes in planta. *Plant Physiology,* 133**,** 462-469.

DALLMAN, P. R. 1986. Biochemical basis for the manifestations of iron deficiency. *Annu Rev Nutr,* 6**,** 13-40.

DOUCHKOV, D., GRYCZKA, C., STEPHAN, U. W., HELL, R. & BAUMLEIN, H. 2005. Ectopic expression of nicotianamine synthase genes results in improved iron accumulation and increased nickel tolerance in transgenic tobacco. *Plant, Cell and Environment,* 28**,** 365-374.

DRAKAKAKI, G., CHRISTOU, P. & STÖGER, E. 2000. Constitutive expression of soybean ferritin cDNA intransgenic wheat and rice results in increased iron levels in vegetative tissues but not in seeds. *Transgenic Research,* 9**,** 445-452.

DUFNER-BEATTIE, J., WEAVER, B. P., GEISER, J., BILGEN, M., LARSON, M., XU, W. & ANDREWS, G. K. 2007. The mouse acrodermatitis enteropathica gene Slc39a4 (Zip4) is essential for early development and heterozygosity causes hypersensitivity to zinc deficiency. *Human molecular genetics,* 16**,** 1391-1399.

EIDE, D., BRODERIUS, M., FETT, J. & GUERINOT, M. L. 1996. A novel iron-regulated metal transporter from plants identified by functional expression in yeast. *Proceedings of the National Academy of Sciences,* 93**,** 5624-5628.

FECHNER, P., DAMDIMOPOULOU, P. & GAUGLITZ, G. 2011. Biosensors Paving the Way to Understanding the Interaction between Cadmium and the Estrogen Receptor Alpha. *PLoS ONE,* 6**,** e23048.

FOX, C. & GUERINOT, M. L. 1998. MOLECULAR BIOLOGY OF CATION TRANSPORT IN PLANTS. *Annu. Rev. Plant Physiol. Plant Mol. Biol.,* 49**,** 669-96.

FOY, C. D., CHANEY, R. L. & WHITE, M. C. 1978. The physiology of metal toxicity in plants. *Annual Review of Plant Physiology,* 29**,** 511-566.

FULCHER, R., O'BRIEN, T. & LEE, J. 1972. Studies on the aleurone layer I. Oonventional and fluorescence microscopy of the cell wall with emphasis on phenol-carbohydrate complexes in wheat. *Australian Journal of Biological Sciences,* 25**,** 23-34.

GLAHN, R. P., WIEN, E. M., VAN CAMPEN, D. R. & MILLER, D. D. 1996. Caco-2 cell iron uptake from meat and casein digests parallels in vivo studies: use of a novel in vitro method for rapid estimation of iron bioavailability. *The Journal of nutrition,* 126**,** 332-339.

GOPALAKRISHNAN, C., KAMALAKANNAN, A. & VALLUVAPARIDASAN, V. 2010. Effect of Seed-Borne Sarocladium Oryzae, the Incitant of Rice Sheath Rot on Rice Seed Quality. *Journal of Plant Protection Research.*

GOTO, F., YOSHIHARA, T., SHIGEMOTO, N., TOKI, S. & TAKAIWA, F. 1999. Iron fortification of rice seed by the soybean ferritin gene. *Nature Biotechnology,* 17**,** 282-286.

GRAHAM, R. D., KNEZ, M. & WELCH, R. M. 2012. 1 How Much Nutritional Iron Deficiency in Humans Globally Is due to an Underlying Zinc Deficiency? *Advances in Agronomy,* 115**,** 1.

GUERINOT, M. L. 2001. Improving rice yields—ironing out the details. *Nat Biotech,* 19**,** 417-418.

GUNSHIN, H., MACKENZIE, B., BERGER, U. V., GUNSHIN, Y., ROMERO, M. F., BORON, W. F., NUSSBERGER, S., GOLLAN, J. L. & HEDIGER, M. A. 1997. Cloning and characterization of a mammalian proton-coupled metal-ion transporter. *Nature,* 388**,** 482-8.

HAAS, J. D., BEARD, J. L., MURRAY-KOLB, L. E., DEL MUNDO, A. M., FELIX, A. & GREGORIO, G. B. 2005. Iron-Biofortified Rice Improves the Iron Stores of Nonanemic Filipino Women. *Journal of Nutrition,* 135**,** 2823–2830.

HAMON, R. E., MCLAUGHLIN, M. J., NAIDU, R. & CORRELL, R. 1998. Long-term changes in cadmium bioavailability in soil. *Environmental science & technology,* 32**,** 3699-3703.

HANSEN, T. H., LOMBI, E., FITZGERALD, M. A., LAURSEN, K. H., FRYDENVANG, J., HUSTED, S., BOUALAPHANH, C., RESURRECCION, A., HOWARD, D. L., DE JONGE, M. D., PATERSON, D. & SCHJOERRING, J. K. 2012. Losses of essential mineral nutrients by polishing of rice differ among genotypes due to contrasting grain hardness and mineral distribution. *Journal of Cereal Science,* 56**,** 307-315.

HARRIS, N. & JULIANO, B. 1977. Ultrastructure of endosperm protein bodies in developing rice grains differing in protein content. *Annals of Botany,* 41**,** 1-5.

HE, J., ZHU, C., REN, Y., YAN, Y. & JIANG, D. 2006. Genotypic variation in grain cadmium concentration of lowland rice. *Journal of Plant Nutrition and Soil Science,* 169**,** 711-716.

HEARD, P. J., FEENEY, K. A., ALLEN, G. C. & SHEWRY, P. R. 2002. Determination of the elemental composition of mature wheat grain using a modified secondary ion mass spectrometer (SIMS). *Plant Journal,* 30**,** 237-245.

HELL, R. & STEPHAN, U. W. 2003. Iron uptake, trafficking and homeostasis in plants. *planta,* 216**,** 541-551.

HERMAN, E. M. & LARKINS, B. A. 1999. Protein storage bodies and vacuoles. *The Plant Cell Online,* 11**,** 601-613.

HIGUCHI, K., NISHIZAWA, N. K., YAMAGUCHI, H., ROMHELD, V., MARSCHNER, H. & MORI, S. 1995. Response of nicotianamine synthase activity to Fe-deficiency in tobacco plants as compared with barley. *Journal of Experimental Botany,* 46**,** 1061-1063.

HIMENO, S., YANAGIYA, T. & FUJISHIRO, H. 2009. The role of zinc transporters in cadmium and manganese transport in mammalian cells. *Biochimie,* 91**,** 1218-1222.

HOAGLAND, D. R. & ARNON, D. I. 1950. The water-culture method for growing plants without soil. *Circular. California Agricultural Experiment Station,* 347.

HOHL, I., ROBINSON, D. G., CHRISPEELS, M. J. & HINZ, G. 1996. Transport of storage proteins to the vacuole is mediated by vesicles without a clathrin coat. *Journal of Cell Science,* 109**,** 2539-2550.

HOSHIKAWA, K. 1989. The growing rice plant. *Tokyo.: An anatomical monograph. Nobunkyo*.

HOTZ, C. & MCCLAFFERTY, B. 2007. From harvest to health: challenges for developing biofortified staple foods and determining their impact on micronutrient status. *Food & Nutrition Bulletin,* 28**,** 271S-279S.

HSEU, Z.-Y., SU, S.-W., LAI, H.-Y., GUO, H.-Y., CHEN, T.-C. & CHEN, Z.-S. 2010. Remediation techniques and heavy metal uptake by different rice varieties in metal-contaminated soils of Taiwan: new aspects for food safety regulation and sustainable agriculture. *Soil Science & Plant Nutrition,* 56**,** 31-52.

HUNT, J. M. 2002. Reversing Productivity Losses from Iron Deficiency: The Economic Case. *J. Nutr.,* 132**,** 794S-801.

HURRELL, R. F. 2003. Influence of vegetable protein sources on trace element and mineral bioavailability. *The Journal of nutrition,* 133**,** 2973S-2977S.

HUSTED, S., PERSSON, D. P., LAURSEN, K. H., HANSEN, T. H., PEDAS, P., SCHILLER, M., HEGELUND, J. N. & SCHJOERRING, J. K. 2011. Review: The role of atomic spectrometry in plant science. *Journal of Analytical Atomic Spectrometry,* 26**,** 52-79.

IBARAKI, T., KUROYANAGI, N. & MURAKAMI, M. 2009. Practical phytoextraction in cadmium-polluted paddy fields using a high cadmium accumulating rice plant cultured by early drainage of irrigation water. *Soil Science and Plant Nutrition,* 55**,** 421-427.

INGOLD, E., SUGIYAMA, M. & KOMAMINE, A. 1988. Secondary cell wall formation: changes in cell wall constituents during the differentiation of isolated mesophyll cells of Zinnia elegans to tracheary elements. *Plant and cell physiology,* 29**,** 295-303.

INOUE, H., HIGUCHI, K., TAKAHASHI, M., NAKANISHI, H., MORI, S. & NISHIZAWA, N. K. 2003. Three rice nicotianamine synthase genes, OsNAS1, OsNAS2 and OsNAS3 are expressed in cells involved in long-distance transport of Iron and differentially regulated by iron. *The Plant Journal,* 36**,** 366-381.

INOUE, H., KOBAYASHI, T., NOZOYE, T., TAKAHASHI, M., KAKEI, Y., SUZUKI, K., NAKAZONO, M., NAKANISHI, H., MORI, S. & NISHIZAWA, N. K. 2009. Rice OsYSL15 is an iron-regulated iron (III)-deoxymugineic acid transporter expressed in the roots and is essential for iron uptake in early growth of the seedlings. *Journal of Biological Chemistry,* 284**,** 3470-3479.

ISHIMARU, Y., BASHIR, K., NAKANISHI, H. & NISHIZAWA, N. K. 2012. OsNRAMP5, a major player for constitutive iron and manganese uptake in rice. *Plant Signaling & Behavior,* 7**,** 763-766.

ISHIMARU, Y., SUZUKI, M., TSUKAMOTO, T., SUZUKI, K., NAKAZONO, M., KOBAYASHI, T., WADA, Y., WATANABE, S., MATSUHASHI, S., TAKAHASHI, M., NAKANISHI, H., MORI, S. & NISHIZAWA, N. K. 2006. Rice plants take up iron as an Fe3-phytosiderophore and as Fe2. *The Plant Journal,* 45**,** 335-346.

JARUP, L. & AKESSON, A. 2009. Current status of cadmium as an environmental health problem. *Toxicology and Applied Pharmacology,* 238**,** 201-208.

JIANG, L., PHILLIPS, T. E., HAMM, C. A., DROZDOWICZ, Y. M., REA, P. A., MAESHIMA, M., ROGERS, S. W. & ROGERS, J. C. 2001. The protein storage vacuole a unique compound organelle. *The Journal of cell biology,* 155**,** 991-1002.

JOHNSON, A. A., HIBBERD, J. M., GAY, C., ESSAH, P. A., HASELOFF, J., TESTER, M. & GUIDERDONI, E. 2005. Spatial control of transgene expression in rice (Oryza sativa L.) using the GAL4 enhancer trapping system. *The Plant Journal,* 41**,** 779-789.

JOHNSON, A. A., KYRIACOU, B., CALLAHAN, D. L., CARRUTHERS, L., STANGOULIS, J., LOMBI, E. & TESTER, M. 2011. Constitutive overexpression of the OsNAS gene family reveals single-gene strategies for effective iron-and zinc-biofortification of rice endosperm. *PLoS One,* 6**,** e24476.

JOHNSON, K. D., HÖFTE, H. & CHRISPEELS, M. J. 1990. An intrinsic tonoplast protein of protein storage vacuoles in seeds is structurally related to a bacterial solute transporter (GIpF). *The Plant Cell Online,* 2**,** 525-532.

JULIANO, B. 2000. Comments on possible contributions of the Philippine agricultural research system to improving human nutrition. *Food & Nutrition Bulletin,* 21**,** 529-531.

KAKEI, Y., ISHIMARU, Y., KOBAYASHI, T., YAMAKAWA, T., NAKANISHI, H. & NISHIZAWA, N. 2012. OsYSL16 plays a role in the allocation of iron. *Plant Molecular Biology,* 79**,** 583-594.

KATO, M., ISHIKAWA, S., INAGAKI, K., CHIBA, K., HAYASHI, H., YANAGISAWA, S. & YONEYAMA, T. 2010. Possible chemical forms of cadmium and varietal differences in cadmium concentrations in the phloem sap of rice plants (Oryza sativa L.). *Soil Science & Plant Nutrition,* 56**,** 839-847.

KAWADA, T. & SUZUKI, S. 1998. A review on the cadmium content of rice, daily cadmium intake, and accumulation in the kidneys. *JOURNAL OF OCCUPATIONAL HEALTH-ENGLISH EDITION-,* 40**,** 264-269.

KIM, S. A., PUNSHON, T., LANZIROTTI, A., LI, L., ALONSO, J. M., ECKER, J. R., KAPLAN, J. & GUERINOT, M. L. 2006. Localization of iron in Arabidopsis seed requires the vacuolar membrane transporter VIT1. *Science,* 314**,** 1295-1298.

KOIKE, S., INOUE, H., MIZUNO, D., TAKAHASHI, M., NAKANISHI, H., MORI, S. & NISHIZAWA, N. K. 2004 OsYSL2 is a rice metal-nicotianamine transporter that is

regulated by iron and expressed in the phloem. *The Plant Journal*, 39**,** 415-424.

KORSHUNOVA, Y. O., EIDE, D., CLARK, W. G., GUERINOT, M. L. & PAKRASI, H. B. 1999. The IRT1 protein from Arabidopsis thaliana is a metal transporter with a broad substrate range. *Plant molecular biology,* 40**,** 37-44.

KOVALCHUK, N., SMITH, J., PALLOTTA, M., SINGH, R., ISMAGUL, A., ELIBY, S., BAZANOVA, N., MILLIGAN, A. S., HRMOVA, M. & LANGRIDGE, P. 2009. Characterization of the wheat endosperm transfer cell-specific protein TaPR60. *Plant molecular biology,* 71**,** 81-98.

KRAEMER, K. & ZIMMERMANN, M. B. 2007. *Nutritional anemia*, Sight and Life Press Basel.

LANQUAR, V., LELIÈVRE, F., BOLTE, S., HAMÈS, C., ALCON, C., NEUMANN, D., VANSUYT, G., CURIE, C., SCHRÖDER, A. & KRÄMER, U. 2005. Mobilization of vacuolar iron by AtNRAMP3 and AtNRAMP4 is essential for seed germination on low iron. *The EMBO journal,* 24**,** 4041-4051.

LE JEAN, M., SCHIKORA, A., MARI, S., BRIAT, J. F. & CURIE, C. 2005. A loss-of-function mutation in AtYSL1 reveals its role in iron and nicotianamine seed loading. *Plant J,* 44**,** 769-82.

LEE, S. & AN, G. 2009. Over-expression of OsIRT1 leads to increased iron and zinc accumulations in rice. *Plant, cell & environment,* 32**,** 408-416.

LEE, S., KIM, Y.-S., JEON, U. S., KIM, Y.-K., SCHJOERRING, J. K. & AN, G. 2012. Activation of Rice nicotianamine synthase 2 (OsNAS2) enhances iron availability for biofortification. *Molecules and cells,* 33**,** 269-275.

LEUNG, K., GVRITISHVILI, A., LIU, Y. & TOMBRAN-TINK, J. 2012. ZIP2 and ZIP4 Mediate Age-Related Zinc Fluxes Across the Retinal Pigment Epithelium. *Journal of Molecular Neuroscience,* 46**,** 122-137.

LEVI-SETTI, R. 1988. Structural and microanalytical imaging of biological materials by scanning microscopy with heavy-ion probes. *Annual review of biophysics and biophysical chemistry,* 17**,** 325-347.

LI, L., CHEN, O. S., WARD, D. M. & KAPLAN, J. 2001. CCC1 is a transporter that mediates vacuolar iron storage in yeast. *Journal of Biological Chemistry,* 276**,** 29515-29519.

LI, P., WANG, X., ZHANG, T., ZHOU, D. & HE, Y. 2008. Effects of several amendments on rice growth and uptake of copper and cadmium from a contaminated soil. *Journal of Environmental Sciences,* 20**,** 449-455.

LING, H.-Q., KOCH, G., BÄUMLEIN, H. & GANAL, M. W. 1999. Map-based cloning of chloronerva, a gene involved in iron uptake of higher plants

encoding nicotianamine synthase. *Proceedings of the National Academy of Sciences,* 96**,** 7098-7103.

LIU, D. H., ADLER, K. & STEPHAN, U. W. 1998. Iron-containing particles accumulate in organelles and vacuoles of leaf and root cells in the nicotianamine-free tomato mutantchloronerva. *Protoplasma,* 201**,** 213-220.

LOMBI, E., HETTIARACHCHI, G. M. & SCHECKEL, K. G. 2011. Advanced in situ spectroscopic techniques and their applications in Environmental Biogeochemistry: Introduction to the special section. *Journal of Environmental Quality,* 40**,** 659-666.

LOMBI, E., SCHECKEL, K., PALLON, J., CAREY, A., ZHU, Y.-G. & MEHARG, A. A. 2009. Speciation and distribution of arsenic and localization of nutrients in rice grains. *New Phytologist,* 184**,** 193-201.

LOTT, J. N. & SPITZER, E. 1980. X-ray analysis studies of elements stored in protein body globoid crystals of Triticum grains. *Plant Physiology,* 66**,** 494-499.

LUCCA, P., HURRELL, R. & POTRYKUS, I. 2002. Fighting iron deficiency anemia with iron-rich rice. *Journal of the American College of Nutrition,* 21**,** 184S-190S.

MARI, S., GENDRE, D., PIANELLI, K., OUERDANE, L., LOBINSKI, R., BRIAT, J., LEBRUN, M. & CZERNIC, P. 2006. Root-to-shoot long-distance circulation of nicotianamine and nicotianamineâ€“nickel chelates in the metal hyperaccumulator Thlaspi caerulescens. *Journal of Experimental Botany,* 57**,** 4111-4122.

MASUDA, H., KOBAYASHI, T., ISHIMARU, Y., TAKAHASHI, M., AUNG, M. S., NAKANISHI, H., MORI, S. & NISHIZAWA, N. K. 2013. Iron-biofortification in rice by the introduction of three barley genes participated in mugineic acid biosynthesis with soybean ferritin gene. *Frontiers in plant science,* 4.

MCLAUGHLIN, M. J., MAIER, N., FREEMAN, K., TILLER, K., WILLIAMS, C. & SMART, M. 1995. Effect of potassic and phosphatic fertilizer type, fertilizer Cd concentration and zinc rate on cadmium uptake by potatoes. *Fertilizer Research,* 40**,** 63-70.

MEDA, A. R., SCHEUERMANN, E. B., PRECHSL, U. E., ERENOGLU, B., SCHAAF, G., HAYEN, H., WEBER, G. & VON WIRÉN, N. 2007. Iron acquisition by phytosiderophores contributes to cadmium tolerance. *Plant physiology,* 143**,** 1761-1773.

MEERS, E., SAMSON, R., TACK, F., RUTTENS, A., VANDEGEHUCHTE, M., VANGRONSVELD, J. & VERLOO, M. 2007. Phytoavailability assessment of heavy metals in soils by single extractions and accumulation by< i> Phaseolus vulgaris</i>. *Environmental and Experimental Botany,* 60**,** 385-396.

MEHARG, A. A., LOMBI, E., WILLIAMS, P. N., SCHECKEL, K. G., FELDMANN, J., RAAB, A., ZHU, Y. & ISLAM, R. 2008. Speciation and

localization of arsenic in white and brown rice grains. *Environmental Science & Technology,* 42**,** 1051-1057.

MOORE, K. L., SCHRODER, M., LOMBI, E., ZHAO, F. J., MCGRATH, S. P., HAWKESFORD, M. J., SHEWRY, P. R. & GROVENOR, C. R. M. 2010. NanoSIMS analysis of arsenic and selenium in cereal grain. *New Phytologist,* 185**,** 434-445.

MOORE, K. L., SCHRÖDER, M., WU, Z., MARTIN, B. G., HAWES, C. R., MCGRATH, S. P., HAWKESFORD, M. J., MA, J. F., ZHAO, F.-J. & GROVENOR, C. R. 2011. High-resolution secondary ion mass spectrometry reveals the contrasting subcellular distribution of arsenic and silicon in rice roots. *Plant physiology,* 156**,** 913-924.

MURAKAMI, M., NAKAGAWA, F., AE, N., ITO, M. & ARAO, T. 2009. Phytoextraction by rice capable of accumulating Cd at high levels: reduction of Cd content of rice grain. *Environmental science & technology,* 43**,** 5878-5883.

MURATA, Y., MA, J. F., YAMAJI, N., UENO, D., NOMOTO, K. & IWASHITA, T. 2006. A specific transporter for iron (III)â€“phytosiderophore in barley roots. *The Plant Journal,* 46**,** 563-572.

NABLE, R. O., BANUELOS, G. S. & PAULL, J. G. 1997. Boron toxicity. *Plant and Soil,* 193**,** 181-198.

NAKANISHI, H., OGAWA, I., ISHIMARU, Y., MORI, S. & NISHIZAWA, N. K. 2006. Iron deficiency enhances cadmium uptake and translocation mediated by the Fe2+ transporters OsIRT1 and OsIRT2 in rice. *Soil Science and Plant Nutrition,* 52**,** 464-469.

NESTEL, P., BOUIS, H. E., MEENAKSHI, J. & PFEIFFER, W. 2006. Biofortification of staple food crops. *The Journal of nutrition,* 136**,** 1064-1067.

NORMILE, D. 2008. Reinventing Rice to Feed the World. *Science,* 321**,** 330-333.

NOZOYE, T., INOUE, H., TAKAHASHI, M., ISHIMARU, Y., NAKANISHI, H., MORI, S. & NISHIZAWA, N. K. 2007. The expression of iron homeostasis-related genes during rice germination. *Plant molecular biology,* 64**,** 35-47.

NOZOYE, T., NAGASAKA, S., KOBAYASHI, T., TAKAHASHI, M., SATO, Y., SATO, Y., UOZUMI, N., NAKANISHI, H. & NISHIZAWA, N. K. 2011. Phytosiderophore Efflux Transporters Are Crucial for Iron Acquisition in Graminaceous Plants. *Journal of Biological Chemistry,* 286**,** 5446-5454.

OCKENDEN, I., DORSCH, J. A., REID, M. M., LIN, L., GRANT, L. K., RABOY, V. & LOTT, J. N. 2004. Characterization of the storage of phosphorus, inositol phosphate and cations in grain tissues of four barley (< i> Hordeum vulgare</i> L.)< i> low phytic acid</i> genotypes. *Plant Science,* 167**,** 1131-1142.

OGAWA, I., NAKANISHI, H., MORI, S. & NISHIZAWA, N. K. 2009. Time course analysis of gene regulation under cadmium stress in rice. *Plant and soil,* 325**,** 97-108.

OGAWA, Y., KUENSTING, H., SUGIYAMA, J., OHTANI, T., LIU, X. Q., KOKUBO, M., KUDOH, K. & HIGUCHI, T. 2002. Structure of a Rice Grain Represented by a New Three-Dimensional Visualisation Technique. *Journal of Cereal Science,* 36**,** 1-7.

OTEGUI, M. S., CAPP, R. & STAEHELIN, L. A. 2002. Developing seeds of Arabidopsis store different minerals in two types of vacuoles and in the endoplasmic reticulum. *The Plant Cell Online,* 14**,** 1311-1327.

OZTURK, L., YAZICI, M. A., YUCEL, C., TORUN, A., CEKIC, C., BAGCI, A., OZKAN, H., BRAUN, H. J., SAYERS, Z. & CAKMAK, I. 2006. Concentration and localization of zinc during seed development and germination in wheat. *Physiologia Plantarum,* 128**,** 144-152.

PALMER, L. T. 2013. *RE: Personal Communication.*

PALMGREN, M. G., CLEMENS, S., WILLIAMS, L. E., KRÄMER, U., BORG, S., SCHJØRRING, J. K. & SANDERS, D. 2008. Zinc biofortification of cereals: problems and solutions. *Trends in plant science,* 13**,** 464-473.

PICH, A., HILLMER, S., MANTEUFFEL, R. & SCHOLZ, G. 1997. First immunohistochemical localization of the endogenous Fe2+-chelator nicotianamine. *Journal of Experimental Botany,* 48**,** 759-767.

PICH, A., SCHOLZ, G. & STEPHAN, U. W. 1994. Iron-dependent changes of heavy metals, nicotianamine, and citrate in different plant organs and in the xylem exudate of two tomato genotypes. Nicotianamine as possible copper translocator. *Plant and Soil,* 165**,** 189-196.

PICKERING, I. J., WRIGHT, C., BUBNER, B., ELLIS, D., PERSANS, M. W., EILEEN, Y. Y., GEORGE, G. N., PRINCE, R. C. & SALT, D. E. 2003. Chemical form and distribution of selenium and sulfur in the selenium hyperaccumulator Astragalus bisulcatus. *Plant Physiology,* 131**,** 1460-1467.

PROM-U-THAI, C., BERNIE, D., THOMSON, G. & BENJAVAN, R. 2003. Easy and rapid detection of iron in rice grain. *ScienceAsia,* 29**,** 203-207.

PROM-U-THAI, C., FUKAI, S., GODWIN, I. D., RERKASEM, B. & HUANG, L. 2008. Iron-fortified parboiled rice - A novel solution to high iron density in rice-based diets. *Food Chemistry,* 110**,** 390-398.

PUNSHON, T., GUERINOT, M. L. & LANZIROTTI, A. 2009. Using synchrotron X-ray fluorescence microprobes in the study of metal homeostasis in plants. *Annals of botany,* 103**,** 665-672.

RAHMAN, M. A., HASEGAWA, H., RAHMAN, M. M., RAHMAN, M. A. & MIAH, M. 2007. Accumulation of arsenic in tissues of rice plant (< i> Oryza sativa</i> L.) and its distribution in fractions of rice grain. *Chemosphere,* 69**,** 942-948.

RICE GENOME ANNOTATION PROJECT, N. 2013. Available: http://www.ncbi.nlm.nih.gov/nuccore.

ROSCHZTTARDTZ, H., CONÉJÉRO, G., CURIE, C. & MARI, S. 2009. Identification of the endodermal vacuole as the iron storage compartment in the Arabidopsis embryo. *Plant physiology,* 151**,** 1329-1338.

ROSCHZTTARDTZ, H., CONÉJÉRO, G., CURIE, C. & MARI, S. 2010. Straightforward histochemical staining of Fe by the adaptation of an old-school technique: Identification of the endodermal vacuole as the site of Fe storage in Arabidopsis embryos. *Plant signaling & behavior,* 5**,** 56-57.

RYAN, C. 2000. Quantitative trace element imaging using PIXE and the nuclear microprobe. *International Journal of Imaging Systems and Technology,* 11**,** 219-230.

RYAN, C. & JAMIESON, D. 1993. Dynamic analysis: on-line quantitative PIXE microanalysis and its use in overlap-resolved elemental mapping. *Nuclear Instruments and Methods in Physics Research Section B: Beam Interactions with Materials and Atoms,* 77**,** 203-214.

SALLAUD, C., MEYNARD, D., VAN BOXTEL, J., GAY, C., BES, M., BRIZARD, J., LARMANDE, P., ORTEGA, D., RAYNAL, M. & PORTEFAIX, M. 2003. Highly efficient production and characterization of T-DNA plants for rice (Oryza sativa L.) functional genomics. *Theoretical and Applied Genetics,* 106**,** 1396-1408.

SANITA DI TOPPI, L. & GABBRIELLI, R. 1999. Response to cadmium in higher plants. *Environmental and Experimental Botany,* 41**,** 105-130.

SATARUG, S., BAKER, J. R., URBENJAPOL, S., HASWELL-ELKINS, M., REILLY, P. E., WILLIAMS, D. J. & MOORE, M. R. 2003. A global perspective on cadmium pollution and toxicity in non-occupationally exposed population. *Toxicology letters,* 137**,** 65-83.

SATARUG, S. & MOORE, M. R. 2004. Adverse health effects of chronic exposure to low-level cadmium in foodstuffs and cigarette smoke. *Environmental health perspectives,* 112**,** 1099.

SCHAAF, G., SCHIKORA, A., HÄBERLE, J., VERT, G., LUDEWIG, U., BRIAT, J.-F., CURIE, C. & VON WIRÉN, N. 2005. A putative function for the Arabidopsis Fe–phytosiderophore transporter homolog AtYSL2 in Fe and Zn homeostasis. *Plant and Cell Physiology,* 46**,** 762-774.

SHERWIN, J. C., REACHER, M. H., DEAN, W. H. & NGONDI, J. 2012. Epidemiology of vitamin A deficiency and xerophthalmia in at-risk populations. *Transactions of the Royal Society of Tropical Medicine and Hygiene,* 106**,** 205-214.

SMART, K. E., SMITH, J. A. C., KILBURN, M. R., MARTIN, B. G. H., HAWES, C. & GROVENOR, C. R. M. 2010. High-resolution elemental localization in vacuolate plant cells by nanoscale secondary ion mass spectrometry. *The Plant Journal,* 63**,** 870-879.

SMITH, I. F. 2000. Micronutrient interventions: options for Africa. *Food & Nutrition Bulletin,* 21**,** 532-537.

SPEROTTO, R. A., BOFF, T., DUARTE, G. L., SANTOS, L. S., GRUSAK, M. A. & FETT, J. P. 2010. Identification of putative target genes to manipulate Fe and Zn concentrations in rice grains. *Journal of plant physiology,* 167**,** 1500-1506.

STANGOULIS, J. Technical aspects of zinc and iron analysis in biofortification of the staple food crops, wheat and rice. 19th World Congress of Soil Science, 2010.

STILLMAN, M. J., CAI, W. & ZELAZOWSKI, A. J. 1987. Cadmium binding to metallothioneins. Domain specificity in reactions of alpha and beta fragments, apometallothionein, and zinc metallothionein with Cd2+. *Journal of Biological Chemistry,* 262**,** 4538-4548.

TAIWAN, E. 2009. Toxicity characteristics leaching procedure (TCLP). *NIEA R201. C,* 14.

TAIZ, L. & ZEIGER, E. 2002. Plant Physiology *Massachusetts: Sinauer Associates Inc. Publishers*.

TAKAHASHI, H., SAITO, Y., KITAGAWA, T., MORITA, S., MASUMURA, T. & TANAKA, K. 2005. A novel vesicle derived directly from endoplasmic reticulum is involved in the transport of vacuolar storage proteins in rice endosperm. *Plant and cell physiology,* 46**,** 245-249.

TAKAHASHI, M., INOUE, H., ISHIMARU, Y., NAKANISHI, H., MORI, S. & NISHIZAWA, N. K. 2006. The role of nicotianamine and mugineic acid in metal transport at reproductive stage. *Plant Cell Physiol,* 47**,** s230.

TAKAHASHI, M., TERADA, Y., NAKAI, I., NAKANISHI, H., YOSHIMURA, E., MORI, S. & NISHIZAWA, N. K. 2003. Role of nicotianamine in the intracellular delivery of metals and plant reproductive development. *The Plant Cell Online,* 15**,** 1263-1280.

TAKAHASHI, R., ISHIMARU, Y., SENOURA, T., SHIMO, H., ISHIKAWA, S., ARAO, T., NAKANISHI, H. & NISHIZAWA, N. K. 2011. The OsNRAMP1 iron transporter is involved in Cd accumulation in rice. *Journal of Experimental Botany,* 62**,** 4843-4850.

TANAKA, K., YOSHIDA, T., KOZI, A. & ZENZABURO, K. 1973. Subcellular particles isolated from aleurone layer of rice seeds. *Archives of Biochemistry and Biophysics,* 155**,** 136-143.

TOSI, P., PARKER, M., GRITSCH, C. S., CARZANIGA, R., MARTIN, B. & SHEWRY, P. R. 2009. Trafficking of storage proteins in developing grain of wheat. *J. Exp. Bot.,* 60**,** 979-991.

VERT, G., GROTZ, N., DÉDALDÉCHAMP, F., GAYMARD, F., GUERINOT, M. L., BRIAT, J.-F. & CURIE, C. 2002. IRT1, an Arabidopsis transporter essential for iron uptake from the soil and for plant growth. *The Plant Cell Online,* 14**,** 1223-1233.

VOGT, S. MAPS: A set of software tools for analysis and visualization of 3D X-ray fluorescence data sets. Journal de Physique IV (Proceedings), 2003. EDP sciences, 635-638.

VON WIREN, N., KLAIR, S., BANSAL, S., BRIAT, J.-F., KHODR, H., SHIOIRI, T., LEIGH, R. A. & HIDER, R. C. 1999. Nicotianamine chelates both FeIII and FeII. Implications for metal transport in plants. *Plant Physiology,* 119**,** 1107-1114.

WADA, T. & LOTT, J. N. A. 1997. Light and electron microscopic and energy dispersive X-ray microanalysis studies of globoids in protein bodies of embryo tissues and the aleurone layer of rice (Otyza sativa L.) grains. *Canadian journal of botany,* 75**,** 1137-1147.

WEBER, E. & NEUMANN, D. 1980. Protein bodies, storage organelles in plant seeds. *Biochemie und Physiologie der Pflanzen,* 175**,** 279-306.

WELCH, R. M. & GRAHAM, R. D. 2000. A new paradigm for world agriculture: productive, sustainable, nutritious, healthful food systems. *Food & Nutrition Bulletin,* 21**,** 361-366.

WELCH, R. M. & GRAHAM, R. D. 2004. Breeding for micronutrients in staple food crops from a human nutrition perspective. *Journal of Experimental Botany,* 55**,** 353-364.

WHEAL, M. S., FOWLES, T. O. & PALMER, L. T. 2011. A cost-effective acid digestion method using closed polypropylene tubes for inductively coupled plasma optical emission spectrometry (ICP-OES) analysis of plant essential elements. *Analytical Methods,* 3**,** 2854-2863.

YAMAGUCHI, N., ISHIKAWA, S., ABE, T., BABA, K., ARAO, T. & TERADA, Y. 2012. Role of the node in controlling traffic of cadmium, zinc, and manganese in rice. *Journal of Experimental Botany,* 63**,** 2729-2737.

YI, Y. & GUERINOT, M. L. 1996. Genetic evidence that induction of root Fe (III) chelate reductase activity is necessary for iron uptake under iron deficiency†. *The Plant Journal,* 10**,** 835-844.

YOKOSHO, K., YAMAJI, N., UENO, D., MITANI, N. & MA, J. F. 2009. OsFRDL1 Is a Citrate Transporter Required for Efficient Translocation of Iron in Rice. *Plant Physiology,* 149**,** 297-305.

YOSHIDA, K. T., WADA, T., KOYAMA, H., MIZOBUCHI-FUKUOKA, R. & NAITO, S. 1999. Temporal and spatial patterns of accumulation of the transcript of myo-inositol-1-phosphate synthase and phytin-containing particles during seed development in rice. *Plant Physiology,* 119**,** 65-72.

YOSHIHARA, T., OOYAMA, A., GOTO, F. & TAKAIWA, F. 2005. Iron accumulation does not parallel the high expression level of ferritin in transgenic rice seeds. *Planta,* 222**,** 225-233.

ZHANG, Y., XU, Y. H., YI, H. Y. & GONG, J. M. 2012. Vacuolar membrane transporters OsVIT1 and OsVIT2 modulate iron translocation between flag leaves and seeds in rice. *The Plant Journal,* 72**,** 400-410.

ZHENG, L., HUANG, F., NARSAI, R., WU, J., GIRAUD, E., HE, F., CHENG, L., WANG, F., WU, P. & WHELAN, J. 2009. Physiological and transcriptome analysis of iron and phosphorus interaction in rice seedlings. *Plant Physiology,* 151**,** 262-274.